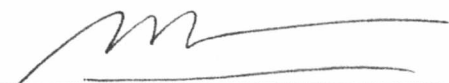


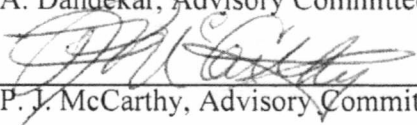
PETROPHYSICAL PROPERTY MODELING OF UMIAT FIELD, A FROZEN OIL
RESERVOIR

By

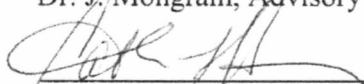
Levi-johnson I. Obioma

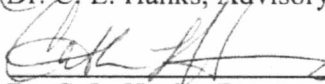
RECOMMENDED:


Dr. A. Dandekar, Advisory Committee Member


Dr. P. J. McCarthy, Advisory Committee Member



Dr. J. Mongrain, Advisory Committee Co-Chair


Dr. C. L. Hanks, Advisory Committee Co-Chair


Dr. C. L. Hanks, Department Chair, Petroleum Engineering

APPROVED:


Dr. Douglas Goering, Dean, College of Engineering and Mines


Dr. Lawrence Duffy, Dean of the Graduate School

Date

Aug 12, 2010

Levi-Johnson, Obioma I.

PETROPHYSICAL PROPERTY MODELING OF UMIAT FIELD, A FROZEN OIL
RESERVOIR

A
THESIS

Presented to the faculty of the University of Alaska, Fairbanks

in Partial Fulfillment of the Requirements

For the Degree of

MASTER OF SCIENCE

By

Levi-johnson I. Obioma, B.Tech.

Fairbanks, Alaska

August 2010

ALASKA
TN
870.57
L485
2010

ABSTRACT

Umiat field, a frozen oil reservoir, is situated in the folded and thrust-faulted Cretaceous sedimentary rocks at the leading edge of the Brooks Range foothills of northern Alaska. The main oil reservoirs are between 500-1400 feet deep and in permafrost. The main oil-producing zones in the Umiat field are the Grandstand shoreface sandstones.

Statistical analyses of the porosity and permeability of the Upper and Lower sands indicate that the sands have distinct petrophysical characteristics. A plot of cumulative flow capacity versus cumulative storage capacity (i.e. Modified Lorenz Plot) defined the flow structures of the Upper and Lower sands in Umiat well # 9. The observed heterogeneities can be correlated with very fine-grained sediments observed in the conventional core of the interval.

A petrophysical property model of Umiat field was built consistent with the existing data and geologic knowledge about the reservoir. This model will be used in the future to test various production strategies for Umiat field. Based on this model, the estimated oil in place is 1.2 billion stock tank barrels and the associated gas is 84 billion standard cubic feet.

Table of Contents

	Page
Signature Page.....	i
Title Page.....	ii
Abstract.....	iii
Table of Contents.....	iv
List of Figures.....	vii
List of Tables.....	xi
List of Appendices.....	xiii
Acknowledgements.....	xiv
Disclaimer.....	xv
Chapter 1 Introduction	1
1.1 Location of Umiat field.....	1
1.2 Limitations in the development of Umiat field.....	2
1.3 Production strategies of Umiat field.....	3
1.4 Objectives of study.....	3
1.5 Source of data.....	4
Chapter 2 Geologic setting of Umiat field.....	5
2.1 Nanushuk Formation.....	9
2.11 The Grandstand sands.....	10
2.12 The Chandler sand.....	11
2.2 Umiat field structure.....	11

2.3 Oil source and petroleum system of Umiat field.....	14
Chapter 3 Development history of Umiat field.....	15
3.1 Reservoir characteristics of the Nanushuk Formation.....	15
3.2 Productivity of the Umiat test wells.....	15
Chapter 4 Statistical analyses of the Grandstand sands.....	19
4.1 Summary statistics.....	19
4.2 Comparison of the Lower and Upper sands based on cross plots.....	21
4.3 Histograms.....	24
4.4 Box plots	28
4.5 T-tests.....	33
4.6 Comparison of the Upper and Lower sands based on porosity and permeability cut-offs	36
4.7 Modified Lorenz plot.....	38
Chapter 5 Petrophysical property modeling of Umiat field.....	43
5.1 Step by step procedure of building Umiat petrophysical property model.....	45
5.11 Setting up the Coordinate system and units.....	45
5.12 Defining the stratigraphic framework.....	45
5.13 Importing horizon and fault data.....	46
5.14 Fault modeling.....	46
5.15 Creating the model boundary.....	48
5.16 Horizon modeling.....	48
5.17 Importing well data.....	49

5.18 Creating the Lithofacies logs.....	50
5.19 Creating the zone logs.....	50
5.2 Grid generation.....	52
5.21 Gridding parameters.....	52
5.3 Creating the blocked wells.....	56
5.4 Indicator grid modeling.....	57
5.5 Petrophysical property modeling.....	63
Chapter 6 Volumetric calculation.....	80
6.1 Estimation of stock tank oil initially in place and associated gas.....	80
6.11 Previous estimates.....	80
6.12 Estimates from this study.....	81
6.2 Results.....	84
Chapter 7 Results and discussion.....	87
7.1 Statistical analyses.....	87
7.2 Petrophysical property modeling.....	89
7.3 Uncertainties in the petrophysical property modeling and OOIP calculation.....	90
Chapter 8 Conclusion and Recommendations.....	91
8.1 Conclusion.....	91
8.2 Recommendations.....	93
References.....	94
Appendix A.....	98
Appendix B.....	129

List of Figures

	Page
Figure1: Location of Umiat field. Modified from Kumar et al. (2002).....	1
Figure 2: Locations of oil and gas accumulations on the North Slope of Alaska. Modified from Kumar et al. (2002).....	6
Figure 3: Generalized stratigraphic column for Northern Alaska. Modified from Kornbrath et al.(1997).....	7
Figure 4: Stratigraphic columns of the reservoir interval at Umiat field. Modified from Huckabay (2010).....	8
Figure 5: Map of Umiat field showing the two seismic lines U8-78 and 72-77 run in 1946 (diagram after Kumar, Nelson, et al. 2002).....	8
Figure 6 : Seismic section of Umiat field from Kumar et al. (2002).....	9
Figure 7 : Map showing geologic trends and wells in the NPRA. Modified from Kornbrath et al. (1997).....	13
Figure 8: Cross plot of the Upper and Lower sands in Umiat.....	22
Figure 9: Cross plot of the Upper sand in 7 test wells in Umiat.....	23
Figure 10: Cross plot of the Lower sand in 6 test wells in Umiat.....	23
Figure 11: Histogram of the combined Upper and Lower sands porosity.....	25
Figure 12: Histogram of the combined Upper and Lower sands permeability.....	26
Figure 13: Histogram of Upper sand porosity	26
Figure 14: Histogram of Lower sand porosity.....	27
Figure 15: Histogram of Upper sand permeability.....	27
Figure 16: Histogram of Lower sand permeability.....	28
Figure 17: Generic box plot.....	29

Figure 18: Box plots showing the Upper sand porosity in some Umiat wells.....	30
Figure 19: Box plots showing the Upper sand permeability in some Umiat wells.....	31
Figure 20: Box plots showing the Lower sand porosity of some Umiat wells.....	32
Figure 21: Box plots showing the Lower sand permeability in some Umiat wells.....	32
Figure 22: Map of Umiat wells showing the porosity change in the Upper sand. Modified from Kumar et al. (2002).....	35
Figure 23: Map of Umiat wells showing the porosity change in the Lower sand. Modified from Kumar, Nelson et al. (2002).....	36
Figure 24: Modified Lorenz plot of the Upper sand in well 9.....	39
Figure 25: Modified Lorenz plot of the Lower sand in well 9 with the uncored interval.....	39
Figure 26: Modified Lorenz plot of the Lower sand in well 9 with values assigned to the uncored interval.....	40
Figure 27: Flowchart of the entire modeling procedure.....	44
Figure 28: Fault model of Umiat field	48
Figure 29: Horizon model of Umiat field	49
Figure 30: Umiat model box showing the location of the 11 Umiat wells	50
Figure 31: Umiat well #9 showing the lithofacies log and zone log in the log editor	51
Figure 32: Histogram showing the sand thickness interval in the Chandler sand	53
Figure 33: Histogram showing the sand thickness interval in the Upper sand	54
Figure 34: Histogram showing the sand thickness interval of the Shale barrier.....	54
Figure 35: Histogram showing the sand thickness interval in the Lower sand.....	55
Figure 36: Blocked wells of the Umiat field showing the porosity values.....	57

Figure 37: Indicator model after one realization showing the lithofacies distribution of the Chandler sand.....	60
Figure 38: Indicator model after one realization showing the lithofacies distribution of the upper part of the Upper sand.....	61
Figure 39: Indicator model after one realization showing the elongated sand bodies in the lower part of the Upper sand.....	61
Figure 40: Indicator model after one realization of Shale barrier in Umiat field.....	62
Figure 41: Indicator model after one realization of Lower sand in Umiat field.....	63
Figure 42: Flow chart showing the procedures in petrophysical property modeling.....	64
Figure 43: Porosity variogram result of shale in the Upper sand in the X-Y direction (Axes in feet).....	68
Figure 44: Permeability variogram result of sand in the Upper sand in the X-Y direction (Axes in feet).....	68
Figure 45: Permeability variogram result of sand in the Lower sand in the X-Y direction (Axes in feet).....	69
Figure 46: Porosity variogram result of shale in the Upper sand in the X-Z direction (Axes in feet).....	69
Figure 47: Chandler sand permeability distribution from the petrophysical property modeling.....	70
Figure 48: Chandler sand porosity distribution from the petrophysical property modeling.....	70
Figure 49: Histogram showing the porosity input data of shale in the Chandler sand.....	73
Figure 50: Histogram showing the porosity output data of shale in the Chandler sand	73
Figure 51: Histogram showing the porosity input data of sand in the Chandler sand	74
Figure 52: Histogram showing the porosity output data of sand in the Chandler sand	74

Figure 53: Comparison of the indicator and porosity models of the Chandler sand77

Figure 54: Comparison of indicator and permeability models of the Chandler sand
.....78

Figure 55: Umiat model showing the 3 fault blocks and their hydrocarbon pore volume
.....83

List of Tables

	Page
Table 1: Drilling and production data in Umiat field Alaska, 1944-53. Modified from Gates and Caraway 1960	17
Table 2: Summary statistics of the Combined Upper and Lower sands in all wells.....	20
Table 3: Summary statistics of the Upper and Lower sands in all wells	20
Table 4: Summary statistics of the Upper sand by well	21
Table 5: Summary statistics of the Lower sand by well	21
Table 6: T-test results of the Upper and Lower sands porosity in well 9	33
Table 7: T-test results for the Upper sand in wells with available porosity data using well 9 as the parent population	34
Table 8: T-test results for the Lower sand in wells with available porosity data using well 9 as the parent population	34
Table 9: Permeability cut-offs based on petrographic studies of Umiat #1. Modified from Collins (1958)	37
Table 10: Summary of probability results based porosity and permeability cut offs	37
Table 11: Simbox thicknesses of horizons in Umiat field	56
Table 12: Range values in the variogram for the sand bodies in all the zones in Umiat field	66
Table 13: Zone by zone summary results of the porosity modeling job	75
Table 14: Zone by zone summary results of the permeability modeling job	76
Table 15: Assumptions for OOIP estimate after Watt et al. (2010)	80
Table 16: Input parameters for volumetric calculation	83

Table 17: Summary of volumetric results	86
---	----

List of Appendices

	Page
Appendix A	97
Appendix B.....	140

ACKNOWLEDGEMENTS

I would like to thank God almighty for giving me strength and perseverance throughout the course of my studies. I would also like to thank my thesis advisory committee members: Dr. Catherine Hanks, Dr. Joanna Mongrain, Dr. Abhijit Dandekar, and Dr. Paul McCarthy.

My gratitude also goes to the employees of Renaissance Alaska, Roxar Inc., Dr. Godwin Chukwu, faculty members and staff of the Petroleum Engineering Department and all my friends who offered me help in one way or the other to make this work's completion possible.

In addition, I would like to give sincere appreciation to my sisters who have stood by me all these years.

DISCLAIMER

This thesis was prepared as an account of work sponsored by an agency of the United States Government. Neither the United States Government nor any agency thereof, nor any of their employees, makes any warranty, express or implied or assumes any legal liability or responsibility for the accuracy, completeness, or usefulness of any information, apparatus, product, or process disclosed or represents that its use would not infringe privately owned rights. Reference herein to any specific commercial product, process, or service by trade name, trademark, manufacturer, or otherwise does not necessarily constitute or imply its endorsement, recommendation, or favoring by the United States Government or any agency thereof. The views and opinions of authors expressed herein do not necessarily state or reflect those of the United States Government or any agency thereof.

CHAPTER 1

INTRODUCTION

1.1 LOCATION OF UMIAT FIELD

Umiat field is located in the folded and thrust-faulted Cretaceous sedimentary rocks at the leading edge of the Brooks Range foothills. It is close to the eastern boundary of the National Petroleum Reserve Alaska (NPRA) (Figure 1) on the Arctic Coastal Plain, about 180 miles southeast of Point Barrow (Figure 2). It is 10 miles long and 3 miles wide, with an axis that trends east-west (Gates and Caraway 1960). The Umiat oil field covers an area of about 327 million square feet. The main oil-producing zones in this field are the Grandstand marine sandstones in the Nanushuk Formation of the Cretaceous age (Baptist 1960).

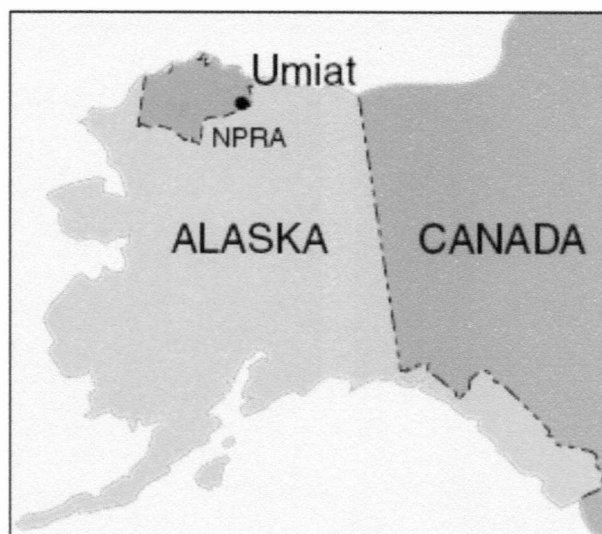


Figure1: Location of Umiat field. Modified from Kumar et al. (2002)

1.2 LIMITATIONS IN THE DEVELOPMENT OF UMIAT FIELD

The Umiat reservoir lies within the zone of continuous permafrost (a soil/rock which has remained frozen for two or more consecutive years) which is approximately 770-1050 feet thick. The presence of permafrost and the shallow nature of the accumulation made it almost impossible to produce oil from this reservoir in the past. This is because the fresh water drilling mud froze when it came in contact with the reservoir blocking the pores and consequently resulting in reduced permeability.

There is little or no information on the production methods for a rock/light oil/ice system at low pressures such as exists at Umiat field. The reservoir is possibly an undersaturated reservoir so solution gas drive for primary production as proposed by Baptist (1960) may be limited though all the gas is in solution. This is because the low pressure of the reservoir will serve as a source of energy for only a short period of time. A secondary recovery mechanism will therefore have to be introduced to maintain pressure for optimal production.

Although the oil is light with API gravity of about 36°, it may behave like viscous oil in a frozen reservoir. Viscous oil production techniques involving steam or water injection will be inappropriate because injected water would freeze in the reservoir, clog pores and decrease permeability. On the other hand, injecting steam would melt the permafrost and be prone to cause damage to the wellbore.

1.3 PRODUCTION STRATEGIES FOR UMIAT FIELD

Possible production strategies for the Umiat field could include, but are not limited to: Cold gas injection so as to maintain reservoir pressure or the injection of a fluid with a low freezing point which will not alter the reservoir temperature and also serve to improve production.

Horizontal and multilateral drilling methods will speculatively be most suitable for Umiat field. Horizontal drilling techniques have been demonstrated in recent years to be more profitable than alternative conventional vertical drilling. This is because horizontal drilling exposes significantly more reservoir rock to the well bore thereby improving sweep efficiency. According to Broman et al. (1992), horizontal well performance information at Prudhoe Bay has revealed an increase in oil production rate and an increase in recovery from a majority of the wells in contrast to offset vertical wells. If applied to the Umiat field, horizontal drilling could make production economical.

1.4 OBJECTIVES OF STUDY

The main objectives of this study are:

- 1) To establish the similarity between the Upper and Lower sands in terms of porosity and permeability.
- 2) To delineate the change in porosity and permeability properties across Umiat field.

- 3) To identify the flow barriers and flow units within the Grandstand sands.
- 4) To build a petrophysical property model for Umiat field detailing:
 - a) Porosity and permeability distribution
 - b) Lithofacies distribution
- 5) To estimate the oil initially in place and associated gas in Umiat field.

1.5 SOURCE OF DATA

The porosity and permeability data as well as the lithologic description used for the purpose of this work were obtained from Umiat test wells Alaska report (Collins 1958). The horizon and fault input data, well locations and well picks information used for the petrophysical property modeling job were provided by Renaissance Alaska.

CHAPTER 2

GEOLOGIC SETTING OF UMIAT FIELD

The reservoir sediments in Umiat field are Cretaceous in age and were deposited in a foreland basin that developed in advance of the growing Brooks Range orogen (Mull et al. 2003; Houseknecht and Schenk 2004) (Figure 2).

The Grandstand sands and the Chandler sand are the two major reservoir units in Umiat field and they belong to the Nanushuk Formation of the Cretaceous age (Figures 3 and 4). Rocks in the Grandstand and Chandler consist almost entirely of clay shale and sandstone. Generally the stratigraphic sequence in the Umiat area is complexly interbedded delta front and delta plain facies. This is based on lithologic, textural and sedimentary-structural, faunal and floral and regional paleogeographic evidence (Fox et al. 1979).

The reservoir interval in Umiat is between 500-1400 feet and most of it is within permafrost (770-1050 feet). The dominant trapping mechanism is a combination of structural/stratigraphic traps (Figure 5 and 6) and the oil source is believed to be lie beneath the Torok shale and/or Lower Cretaceous pebble shale (Magoon 1994) (Figure 4).The clayshale, claystone and very fine-grained sediments in the reservoir act as seals. Hydrocarbons were produced mainly from the Grandstand sands. Gates and Caraway (1960) however report that a small quantity of oil was produced from the overlying Chandler sand (Figure 4).

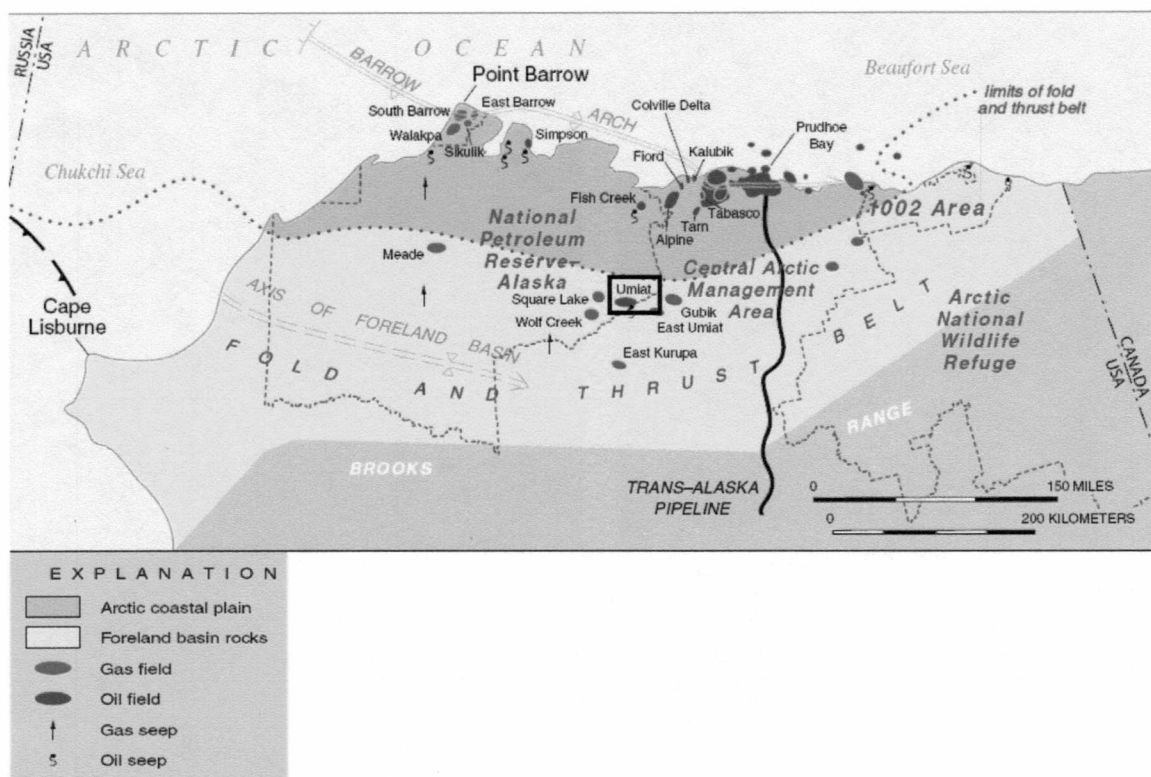


Figure 2: Locations of oil and gas accumulations on the North Slope of Alaska. Modified from Kumar et al. (2002)

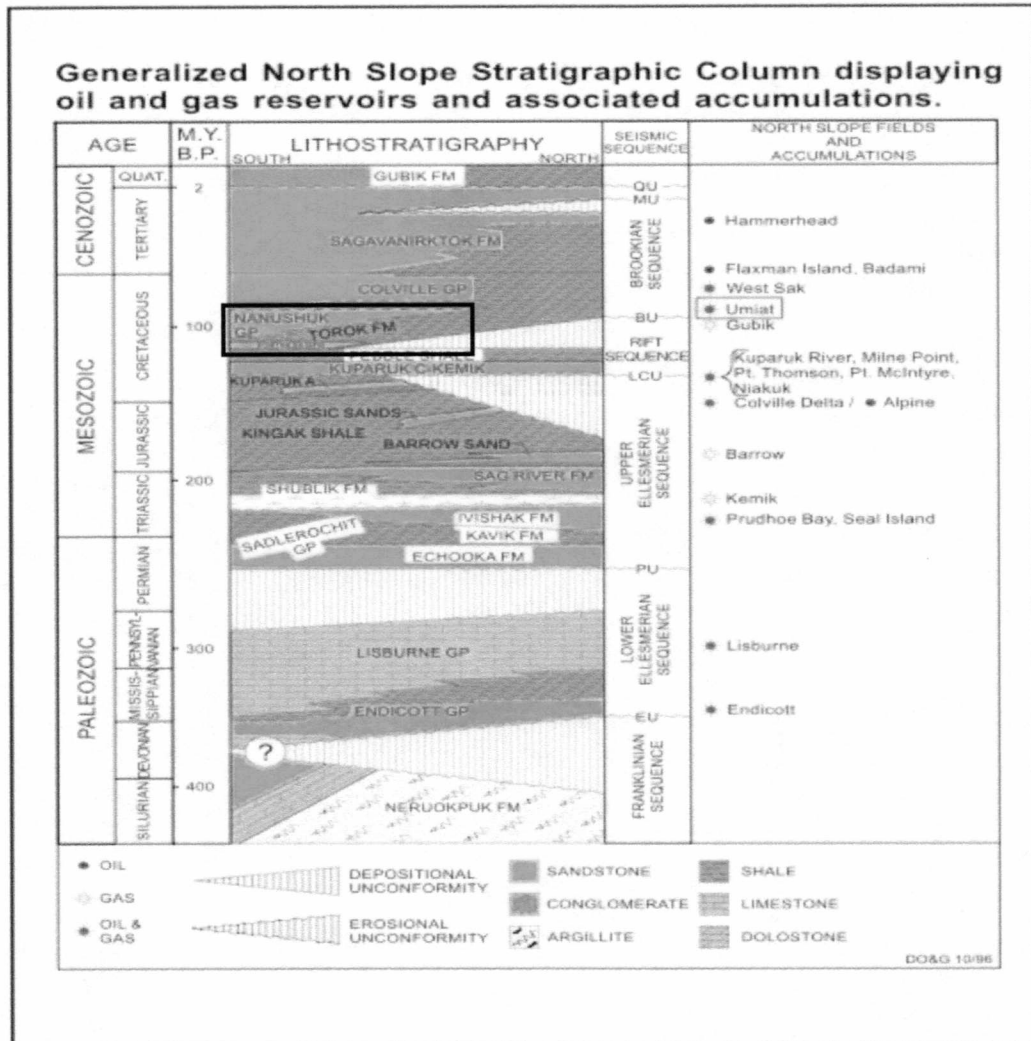


Figure 3: Generalized stratigraphic column for Northern Alaska. Modified from Kornbrath et al. (1997). The black box represents the reservoir interval at Umiat. See Figure 4 for a more detailed representation of the reservoir interval.

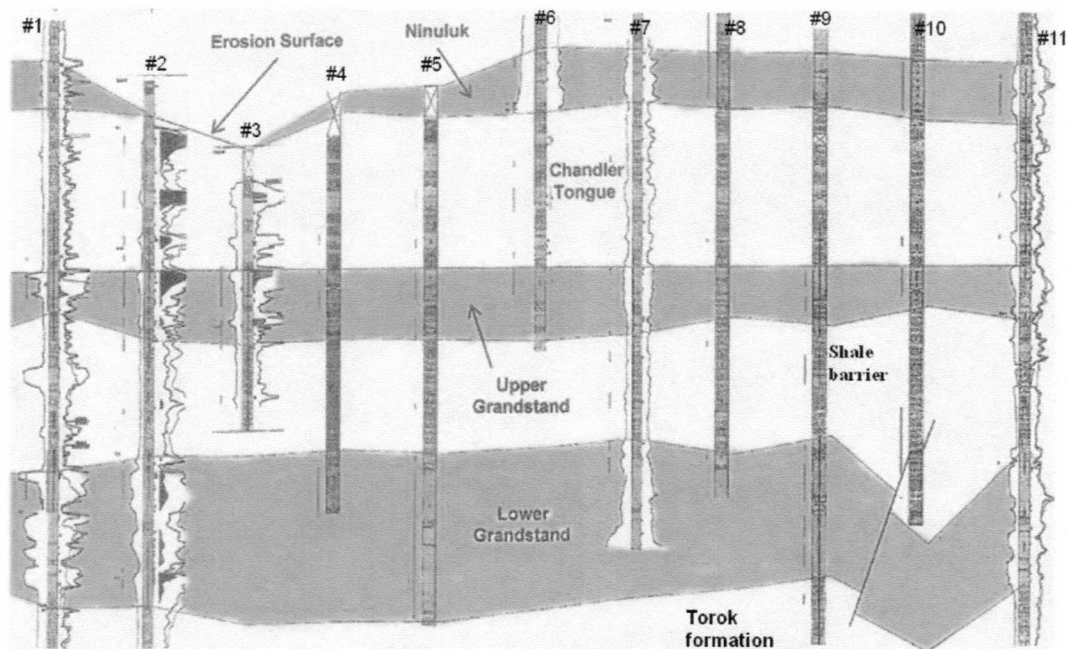


Figure 4: Stratigraphic columns of the reservoir interval at Umiat field. Modified from Huckabay (2010), personal communication.

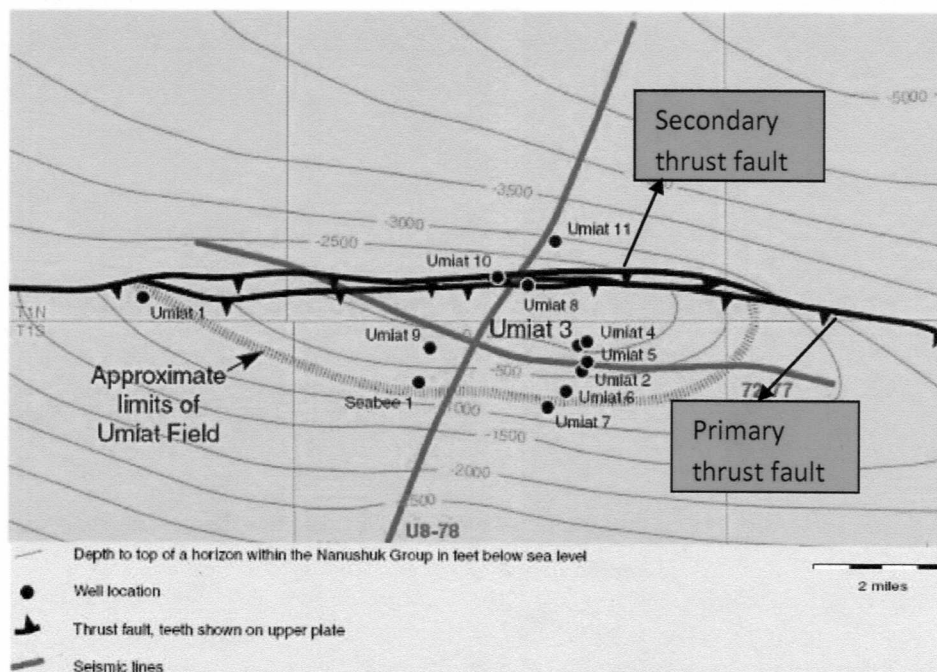


Figure 5: Map of Umiat field showing the two seismic lines U8-78 and 72-77 run in 1946 (diagram after Kumar et al. 2002)

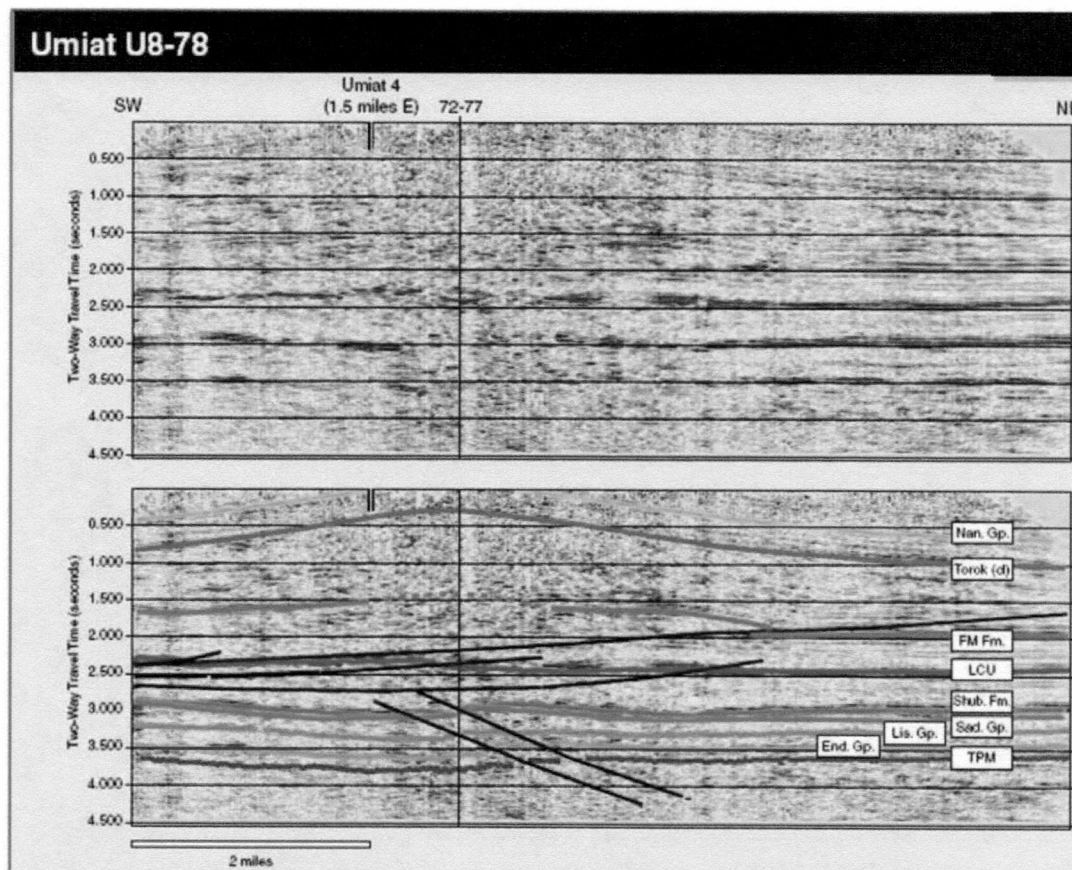


Figure 6 : Seismic section of Umiat field from Kumar et al. (2002)

2.1 NANUSHUK FORMATION

According to work by Mull et al. (2003), the Nanushuk Group has been demoted from a Group to a Formation. This was done to shorten the nomenclature and help in the area understanding of these rocks. The Nanushuk Formation consists of unnamed informal lower and upper units that are dominantly marine and nonmarine, respectively. The

Grandstand Formation, Chandler Formation and the Killik tongue of the Chandler Formation were abandoned. The Nanushuk Formation in this work consists of the Grandstand sands (Upper and Lower) and the Chandler sand. Due to the time when the data was obtained, some of the Figures presented in this work bear the old nomenclature.

2.11 THE GRANDSTAND SANDS

The main oil-producing zones in Umiat field are Grandstand marine sandstones in the Nanushuk Formation of Cretaceous age (Baptist 1960) (Figure 3). They consist almost entirely of sandstone, shale, and little siltstone. The top of the Grandstand is characterized by the abrupt appearance of an arenaceous foraminiferal assemblage containing the *Verneuilinoides borealis* fauna which suggests a shallow water marine environment (Collins 1958). In the Umiat area, the Grandstand sands consist of a complexly inter-bedded delta-front and delta-plain facies called the Umiat Delta which prograded northeasterly with the source terrane southwest of Umiat (Ahlbrandt 1979).

Within the reservoir interval, the uppermost sandstone bed in the Grandstand (also referred to as the Upper sand) has an average thickness of 100 feet with good porosity. The Upper sand is separated from the Lower sandstone bed in the Grandstand (Lower sand) by an average of about 300 feet or more of gray shale referred to as the Shale barrier in this study (Figure 4). The Lower sand has a much thicker average of about 250 feet but only the top 100 feet has good porosity. The depth of the producing sands depends on the surface topography and subsurface structure.

The Grandstand sands at Umiat have less clay than those in the foothills wells to the west. Brosge (1966) believes that the relative cleanness of the sands is as a result of winnowing and reworking of the sediments in a part of the sedimentary basin that subsided quickly.

2.12 THE CHANDLER SAND

The Chandler sand represents a thick progradational sequence of delta front and delta plain marginal marine facies (Fox et al. 1979) (Figure 4). It consists of sandstone, siltstone, shale and coal. It prograded northeasterly and has the same southwest source terrane as the Grandstand sands in the Umiat area. It is primarily a near-shore marine facies as evident by the type of flora and fauna present (Collins 1958).

Within the reservoir interval, the Chandler sand consists of inter-bedded silty sandstone, siltstone, shale, and claystone. The early to late Cretaceous Chandler sand is 260-280 feet thick in the Umiat area.

2.2 UMIAT FIELD STRUCTURE

According to Kornbrath et al.(1997), the trapping structure at Umiat is an east-west trending, thrust-faulted anticline located in the Fold Belt Trend (Figure 7). This Fold Belt Trend consists primarily of younger Cretaceous sandstones of the Brookian Succession Trend (Figure 7) with traps which are commonly broad anticlinal structures, some of which are breached at higher levels.

The trap in Umiat field is a combination of structural and stratigraphic type. As a result of the highly faulted nature of this reservoir, the faults serve as traps while the

fine grained sediments act as both stratigraphic traps and seals. Houseknecht and Schenk (2004) suggest that Umiat oil field could have developed as a stratigraphic trap that was subsequently folded, resulting in a combination of structural/stratigraphic type. The vertical closure on the trap is about 1,000 feet (Molenaar 1982).

Potter and Moore (2003) estimate that about 65 percent of the trap is filled with hydrocarbons based on the height of hydrocarbon column versus height from the top of the trap down to the spill point. If a few relatively thin reservoir intervals are considered to make up the volume of the accumulation, the average trap fill will be relatively high.

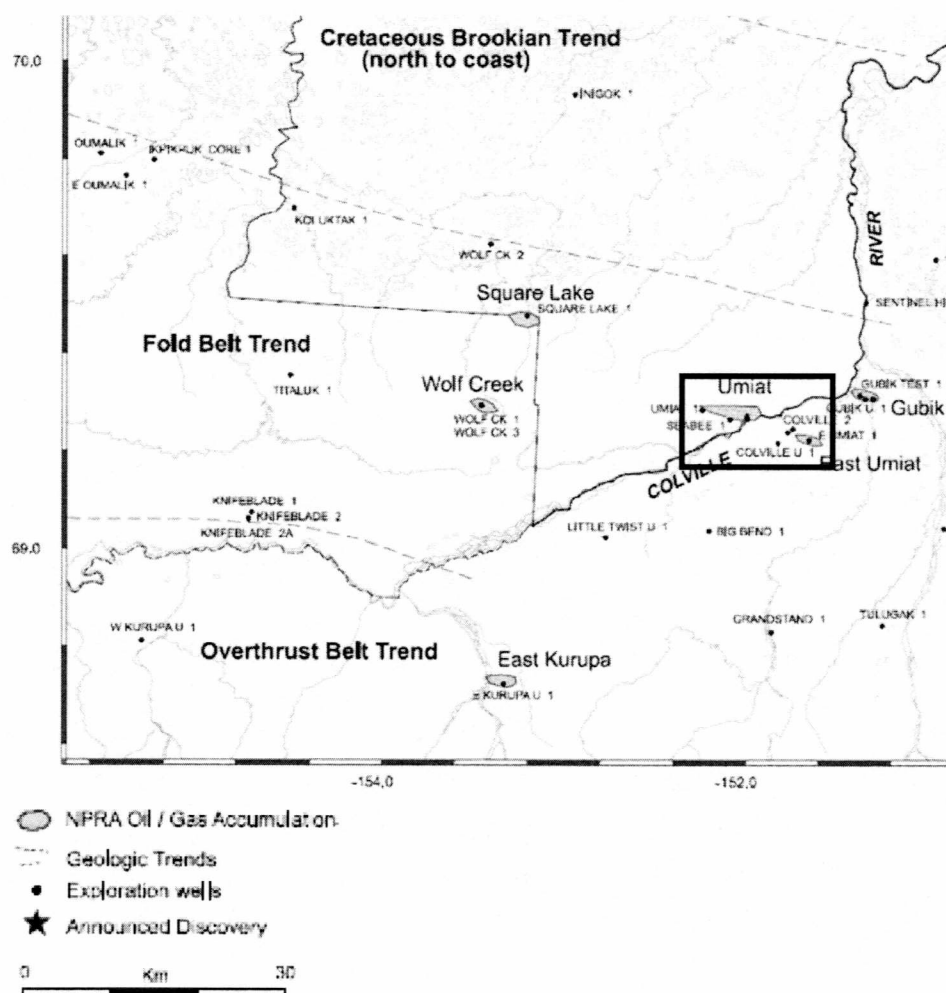


Figure 7 : Map showing geologic trends and wells in the NPR. Modified from Kornbrath et al. (1997)

However if one considers the entire vertical closure on the anticline to make up the trap the average trap fill would be relatively low.

According to Potter and Moore (2003), subsurface data from the Umiat field and other seismic reflection data within the play region show that the Umiat trap and similar structures are compartmentalized by thrust faults (Figure 5 and 6). Thrust faults are

characterized by repeated stratigraphic sections and the thickness of the repeated beds is a measure of the vertical displacement of the faults.

2.3 OIL SOURCE AND PETROLEUM SYSTEM OF UMIAT FIELD

The oil source in Umiat field is believed to lie beneath the Torok Shale and/or Lower Cretaceous Pebble Shale (Magoon 1994) (Figures 3 and 4). Geologic reconstructions and thermal maturity data from the Fold Belt Trend signify that these sandstones were buried to great depths in the Colville Trough during the Late Cretaceous and Paleogene (Cole et al. 1995). The structurally complex Fold Belt Trend holds known gas accumulations and an oil accumulation at Umiat.

Wells drilled within this trend to the east of the NPRA have not been successful though the area has large faults that may present migration pathways for oil to move into structures as seen in Umiat (Kornbrath et al. 1997). The unproductivity of these wells could be as a result of poor reservoir characteristics. The migration path in this field is possibly vertical through the faults in the Umiat anticline.

There are two possible Petroleum systems as proposed by Magoon (1994) to explain the oil at Umiat

- 1) Assumes tertiary generation and migration of Umiat oils
- 2) Assumes Umiat oils were generated during early Cretaceous time and accumulation originated as a stratigraphic trap that has been subsequently folded.

CHAPTER 3

DEVELOPMENT HISTORY OF UMIAT FIELD

3.1 RESERVOIR CHARACTERISTICS OF THE NANUSHUK FORMATION

The characteristics and conditions of the producing sandstones of the Grandstand are mostly massive while some have siltstone and claystone laminae (Baptist 1960). The porous and permeable reservoirs in the Grandstand sands and Chandler sand as suggested by Fox et al. (1979) have sparse amounts of metamorphic rock debris in areas where energy setting at the site of deposition facilitated sorting and winnowing of the sediment. The reservoir is therefore expected to have a higher productivity in these areas. The Grandstand sandstones are light to medium gray and are made up of sub-angular to sub-rounded grains of quartz and dark rock fragments with some mica and carbonaceous material.

It is generally believed that swelling clays have an adverse effect on valuable porosity and permeability of reservoir rocks. However they are not present in the Grandstand sands and Chandler sand. Extensive experiments done by Baptist (1959) on core samples from the Grandstand sands confirm the absence of swelling clays.

3.2 PRODUCTIVITY OF THE UMIAT TEST WELLS

Eleven Umiat test wells were drilled between 1944 and 1953 when the U.S Navy explored the National Petroleum Reserve Alaska (NPRA) to determine its oil potential.

Six of the eleven test wells drilled on the Umiat anticline produced light oil with the main oil reservoirs between 500-1400 feet deep. Initial production rates dropped due to the formation of ice around the well bore when fresh water drilling mud was used.

Umiat #1, the first test well drilled was 6,000 feet deep and is located west of the producing area (Figure 5). The deepest hole of about 6,212 feet was the Umiat #2 which is located structurally high on the anticline. Surprisingly this well did not produce oil. This can be attributed to the fact that it was drilled with fresh water drilling mud which froze when it came in contact with the reservoir, clogged the pores, thereby making it impermeable to oil. The shallowest Upper sand well was Umiat #5 at 248 feet and the deepest Lower sand well was Umiat #9 at 866 ft. Baptist (1959) believes that Umiat #1 and #7 were too structurally low to produce oil. Despite that Umiat#2 and Umiat#5 are 200 feet apart and on about the same elevation. Experiments by Gates and Caraway (1960) showed that Umiat#2 and Umiat#5 had different production rates (Table 1). An estimated 400 bbl/day maximum pump capacity was produced from Umiat#5 drilled with cable tools while Umiat#2 which was drilled with a rotary rig using water-based mud produced a trace amount of oil and was later abandoned. The damage noted in wells drilled with a conventional rotary rig using water-based mud was due to the freezing of the water in the sands around the well bore area and not as a result of the swelling clays as earlier assumed (Baptist 1959).

Table 1: Drilling and production data in Umiat field Alaska, 1944-53. Modified from Gates and Caraway 1960

Well No	Drilling method	Drilling mud	Production rate bbl/day	Production test method	Length of test days	Total depth (ft)
1	Rotary	Clay-water	0	Formation	Less than 1	6005
2	Rotary	Clay-water	Trace	Formation	Less than 1	6212
3	Rotary	Clay-water	24	Pumping	14 approx	572
4	Cable	Brine	100	Pumping	18	840
6	Cable	Brine	80 (wet)	Pumping	1 approx	825
7	Cable	Brine	less than 1	Bailing	1 approx	1384
8	Cable	Brine	60	Pumping	14	1327
10	Cable	Brine	70	Bailing	1	1573
5	Cable	Brine, reamed oil	more than 400	Pumping	93	1077
9	Rotary	Oil-base	more than 300	Pumping	45	1257
11	Rotary	Oil in water emulsion	0	Formation	1	3303

Results from the experiments conducted by Gates and Caraway (1960) show that the use of fresh water drilling mud reduced productivity of some of the eleven test wells drilled. In contrast, wells drilled with sodium chloride and cable tools had intermediate production rates because the brine lowered the freezing temperature below the minimum temperature in the permafrost. Three of the four wells drilled with water-based mud were abandoned and could have been more productive had oil-based mud been used.

Umiat reservoir pressure was between 50 to 350 psi (Baptist 1959). Despite the fact that the reservoir sands in Umiat are in permafrost and the reservoir pressures are low (an estimated 170 psi at 470 feet in the Grandstand sands), Baptist (1959) believes that there will be a significant recovery from the field because the small amount of gas dissolved in the oil aided by gravity drainage will serve as the main source of energy for production. Experiments on cores conducted by Baptist (1959) under simulated permafrost conditions stipulate that oil can be produced by depletion drive with a pressure drop of about 100 psi below the saturation pressure. In addition the results

show that the freezing of formation water has more effect in reducing oil productivity than that due to increased viscosity. For example lowering the temperature from 70° F to 26° F reduced the rate of oil flow by about 54 percent.

CHAPTER 4

STATISTICAL ANALYSES OF THE GRANDSTAND SANDS

The porosity and permeability properties of the Upper sand and Lower sand were statistically analyzed using Microsoft excel in order to understand their distribution. Similarity between the Upper and Lower sands, probability of encountering reservoir quality sands using various cutoff values and the determination of flow properties within the sands were also examined. These analyses provided the information necessary for a more precise forecast of heterogeneities, flow and storage capacities, as well as drainage areas and provided a good foundation for subsequent petrophysical property modeling of the Umiat field.

The statistical analyses were not carried out for the Chandler sand because of insufficient data. Some of the Umiat wells without porosity and permeability data were also not included in these analyses. The summary of the data used are represented in the appendices (A.1 and A.2).

4.1 SUMMARY STATISTICS

The summary statistics were used to review the set of observations in the Grandstand sands. The average porosity and permeability of the combined Upper sand and Lower sand (Table 2) is 14.06 percent and 55.12 millidarcies respectively. In the Upper sand the average porosity value is 12.95 percent while the average permeability value is 42.20 millidarcies (Table 3). The Lower sand has an average porosity value of

14.98 percent and an average permeability value of 70.73 millidarcies (Table 3). On a well-to-well basis (Tables 4 and 5) some of the wells exhibit higher average porosity and permeability values than the observed values in Tables 2 and 3. This confirms the need to scrutinize data in “field scale” as well as in “well scale”. A single porosity or permeability value assumption for all the wells will not represent the reservoir as efficiently as assigning each well with its own porosity or permeability value.

Table 2: Summary statistics of the Combined Upper and Lower sands in all wells

Measures of Central Tendency	Combined Upper and Lower Sands	
	POROSITY(%)	PERMEABILITY(md)
MEDIAN	14.40	19.12
MEAN	14.06	55.12
Lower Quartile	11.60	1.40
Upper Quartile	16.60	70.00
Standard deviation	3.52	84.24
5TH PERCENTILE	8.28	0.10
95TH PERCENTILE	19.02	240.00

Table 3: Summary statistics of the Upper and Lower sands in all wells

Measures of Central Tendency	Upper sand		Lower sand	
	POROSITY(%)	PERMEABILITY(md)	POROSITY(%)	PERMEABILITY(md)
MEDIAN	13.80	11.00	15.25	27.00
MEAN	12.95	42.22	14.98	70.73
Lower Quartile	9.80	0.50	12.63	5.13
Upper Quartile	16.15	46.00	17.38	95.25
Standard deviation	3.72	75.53	3.05	91.91
5TH PERCENTILE	7.74	0.10	10.11	0.41
95TH PERCENTILE	19.03	171.90	18.90	279.00

Table 4: Summary statistics of the Upper sand by well

Measures of Central Tendency	UPPER SAND									
	POROSITY (%)					PERMEABILITY (md)				
	well 1	well 2	well 3	well 9	well 11	well 1	well 2	well 3	well 9	well 11
MEDIAN	14.40	15.00	15.05	11.25	16.50	3.80	39.20	63.50	0.95	81.00
MEAN	13.76	4.23	15.01	12.24	16.58	7.71	73.68	114.74	23.83	96.20
Lower Quartile	10.90	13.01	13.75	9.00	15.00	1.10	16.45	43.25	0.20	27.00
Upper Quartile	15.85	15.78	16.50	14.93	17.60	8.75	69.00	143.75	40.00	120.00
Standard deviation	3.26	3.36	1.63	4.21	1.77	9.82	99.64	141.43	38.36	87.99
5TH PERCENTILE	9.40	9.60	12.76	7.50	14.84	0.75	6.84	9.02	0.10	19.80
95TH PERCENTILE	17.95	17.75	16.82	19.11	18.72	26.50	222.00	348.60	120.00	212.00

Table 5: Summary statistics of the Lower sand by well

Measures of Central Tendency	LOWER SAND							
	POROSITY				PERMEABILITY			
	well 1	well 2	well 9	well 11	well 1	well 2	well 9	well 11
MEDIAN	17.60	14.25	14.80	17.10	14.40	12.80	53.00	158.00
MEAN	17.49	14.65	14.34	16.62	22.29	46.40	77.27	188.06
Lower Quartile	15.60	12.53	12.30	16.40	4.00	4.35	6.40	100.00
Upper Quartile	17.90	17.33	16.50	17.40	35.00	66.63	97.00	280.00
Standard deviation	2.77	2.80	4.21	2.34	21.37	64.80	90.25	155.35
5TH PERCENTILE	14.90	11.29	9.62	13.60	2.32	3.83	0.32	21.84
95TH PERCENTILE	21.84	18.59	18.26	18.92	55.70	174.35	268.00	376.00

4.2 COMPARISON OF THE LOWER AND UPPER SANDS BASED ON CROSS PLOTS

Cross plots are plots of two variables measured at the same location along two axes which can be linear or logarithmic. Porosity and permeability cross plots for Upper and Lower sands (Figures 8, 9 and 10) were used to determine possible relationships and estimate correlation factors between the porosity and permeability values in these two sands. The data used for these analyses are provided in appendices A.1 and A.2.

The R-squared value was also calculated for the various cross plots. R-squared values are numbers which demonstrate the confidence with which one variable can be

predicted from another variable on the cross plot. The closer the R-squared value is to 1 the closer the relationship between the two variables.

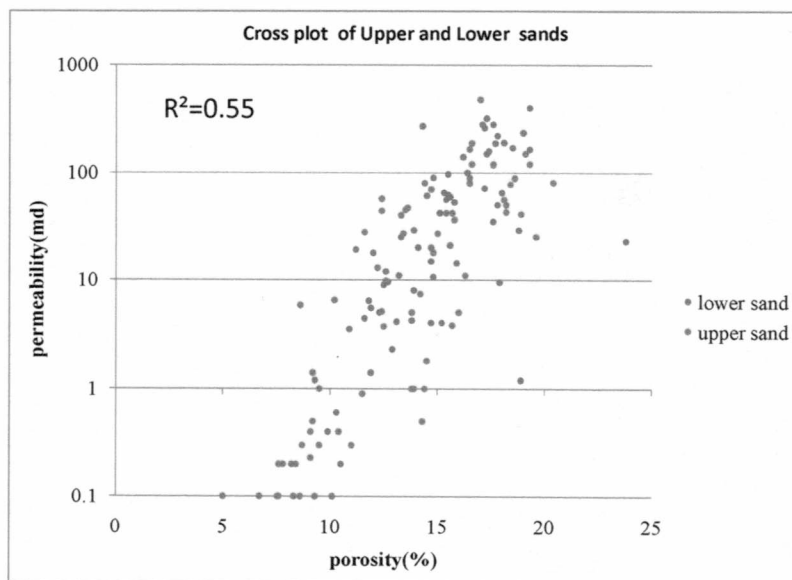


Figure 8: Cross plot of the Upper and Lower sands in Umiat

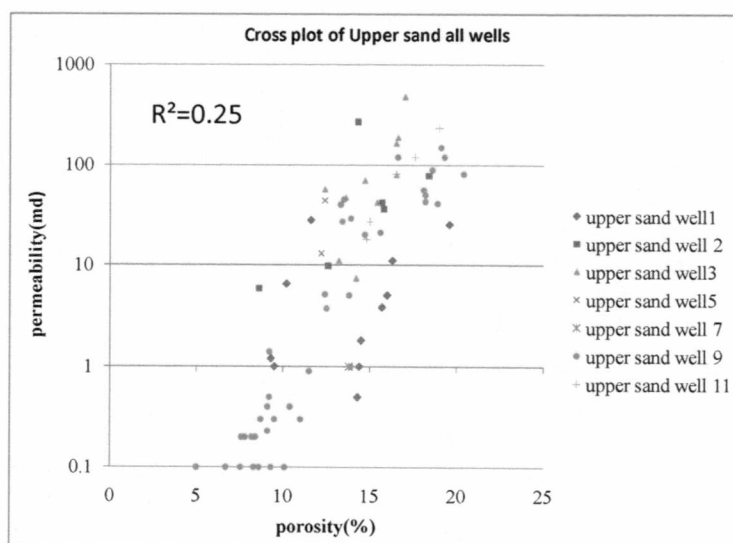


Figure 9: Cross plot of the Upper sand in 7 test wells in Umiat

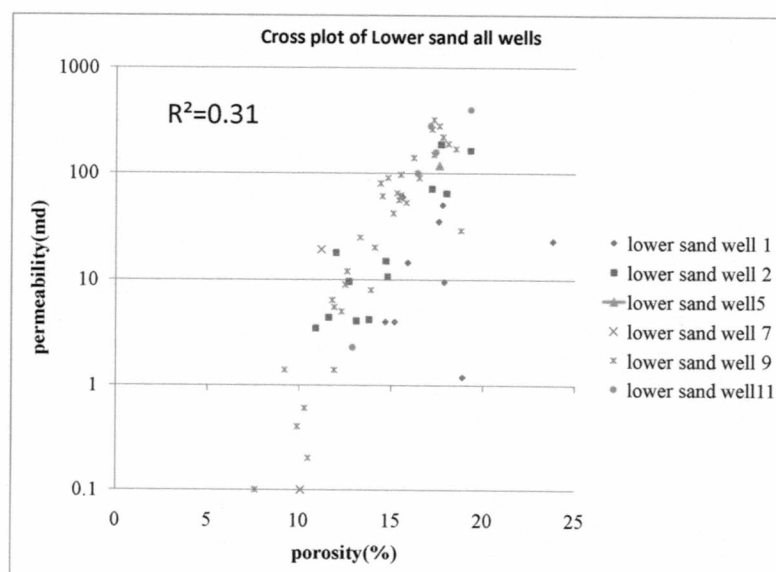


Figure 10: Cross plot of the Lower sand in 6 test wells in Umiat

The R-squared value for the cross plots in all the wells with porosity and permeability data were calculated.

The R-squared value for the Upper and Lower sands combined is 0.55 (Figure 8); the value for the Upper sand is 0.25 (Figure 9) while the value for the Lower sand is 0.31 (Figure 10). This indicates that the relationship between porosity and permeability in the Upper and Lower sands is not particularly strong. Therefore permeability values cannot be predicted with accuracy from porosity values alone. Visual inspection of the well by well cross plots (Figure 9 and 10) show a weak relationship between porosity and permeability in both the Upper and Lower sands.

4.3 HISTOGRAMS

A histogram is a summary chart which illustrates the frequency distribution of a data set falling in different ranges defined by the bin size. It can also be used to examine the nature of the population in a dataset. The porosity and permeability data is represented on the X-axis while their frequency is shown on the Y-axis.

The histograms for the Grandstand sands were constructed using Microsoft excel for the Upper and Lower sands combined (Figures 11 and 12) before they were split into individual data sets (Figures 13, 14, 15 and 16). The combined histogram of porosity suggests that there might be more than one normal population in the data distribution (Figure 11). This is because of the multimodal nature of this distribution.

The most frequent porosity in the Upper and Lower sands combined is between 15-17 percent (Figure 11) while the most frequent permeability values in the combined Upper and Lower sands is less than 15.1 millidarcies (Figure 12).

Most of the porosity values in the Upper sand fall between 15 percent and 17 percent (Figure 13) while the most frequent porosities in the Lower sand are between 19 percent and 21 percent (Figure 14). The permeability values in the Upper and Lower sands separated are mostly below 15.1 millidarcies (Figure 15 and 16). This shows that most of the permeability values fall at the lower end of the permeability range.

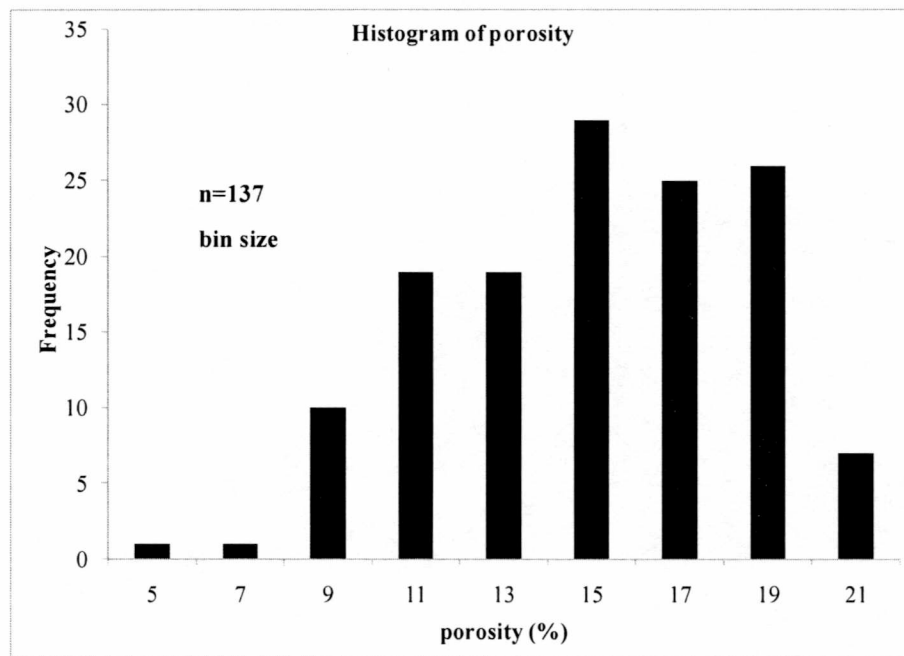


Figure 11: Histogram of the combined Upper and Lower sands porosity

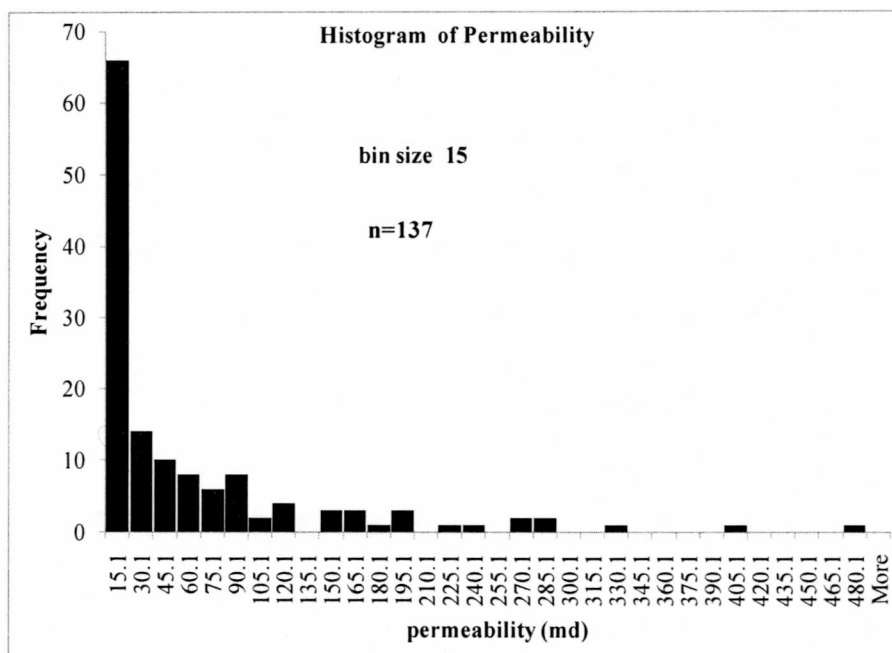


Figure 12: Histogram of the combined Upper and Lower sands permeability

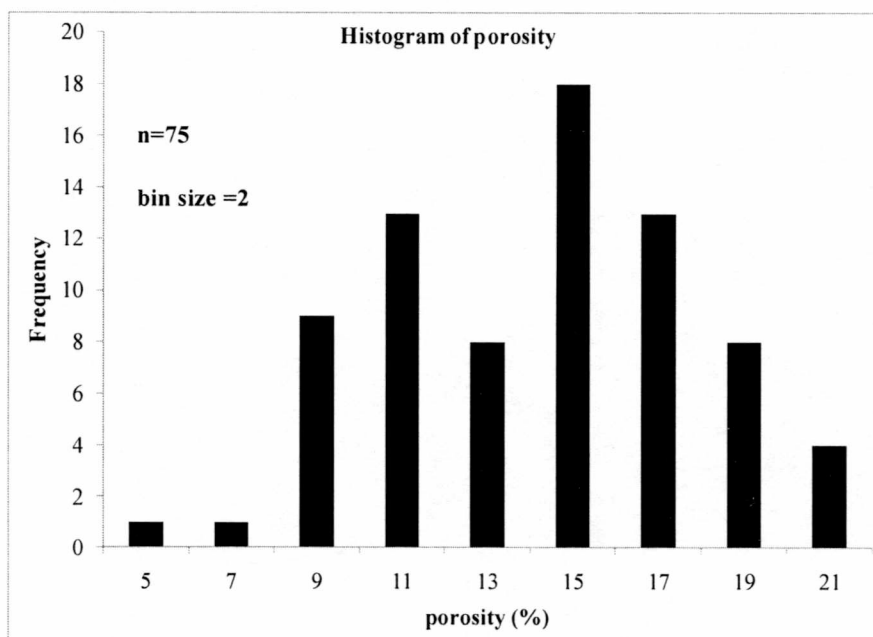


Figure 13: Histogram of Upper sand porosity

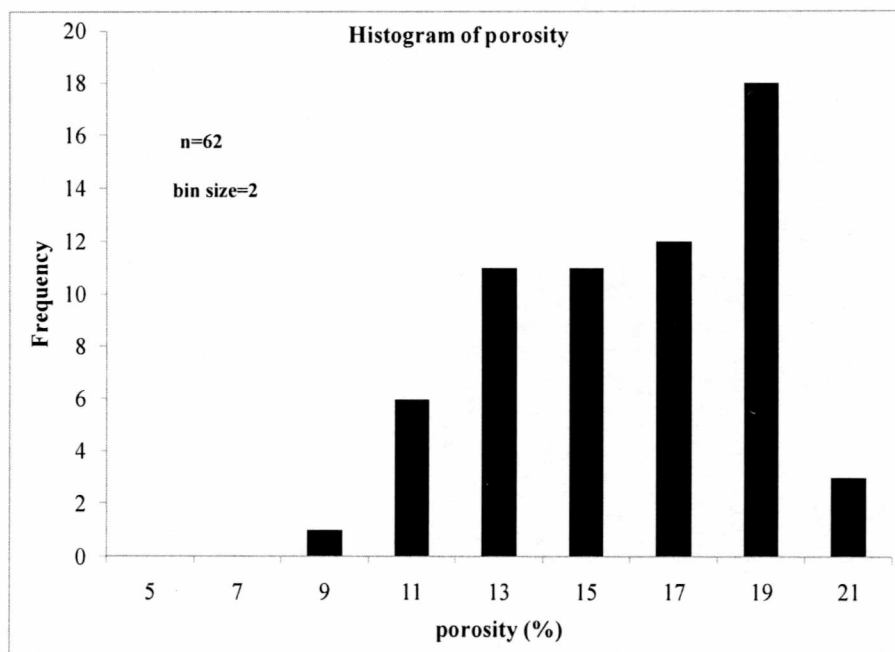


Figure 14: Histogram of Lower sand porosity

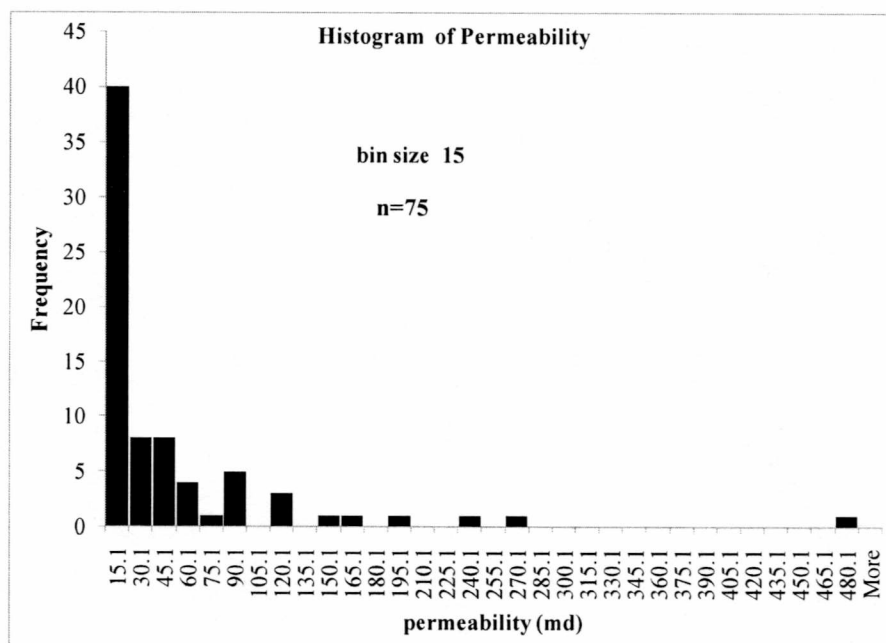


Figure 15: Histogram of Upper sand permeability

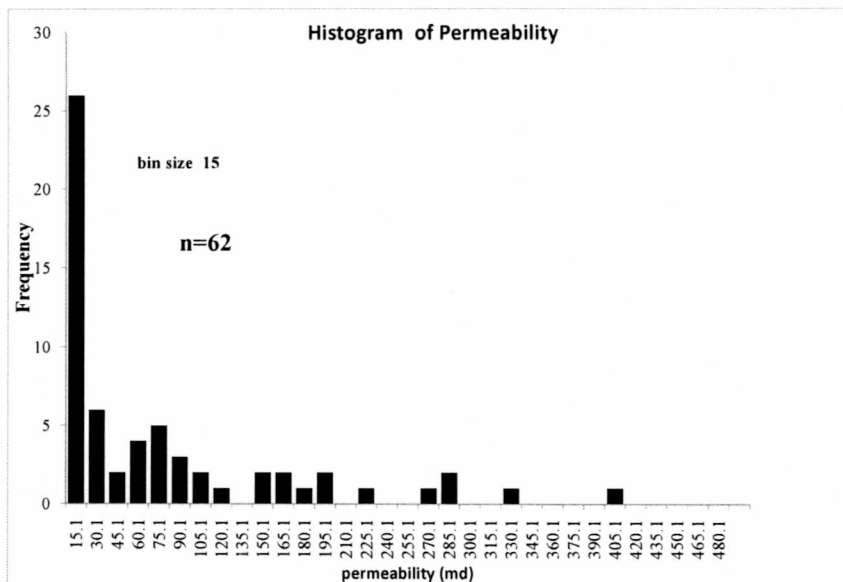


Figure 16: Histogram of Lower sand permeability

4.4 BOX PLOTS

Box plots (also known as box and whisker plots) are used to represent the fundamental parts of a distribution (Figure 17). They were introduced in 1977 by John Tukey (www.netmba.com 2002-2007). The whiskers represent the 5th and 95th percentile or, in some cases, the maximum and minimum values of the data when there are no outliers. The line in the box represents the median; the upper unit of the box stands for the 75th percentile while the lower unit indicates the 25th percentile.

The median line can be a pointer to the extent of skewness of the data depending on the position of the line from the whiskers. If the line is at the center, then the box distribution is not skewed.

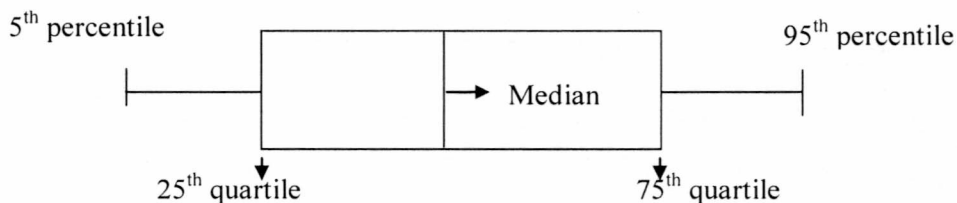


Figure 17: Generic box plot

Box plots are better than most statistical methods because they show outliers. They provide comparison of the distribution of data sets at a glance and are important in exploratory data investigation (www.netmba.com 2002-2007). The spacing between the various parts of the box is used to identify the degree of spread and skewness in the data and outliers. Box and whisker plots can be drawn either horizontally or vertically.

Box plots of porosity and permeability in the Upper and Lower sands were constructed for some of the wells (Figures 18, 19, 20 and 21) using Microsoft excel. This was done to examine the change in these petrophysical properties across Umiat field. The input data for the box plots are the summary statistics (Table 4 and 5). The represented wells are the ones with available porosity and permeability data.

Box plots of porosity and permeability in the Upper sand (Figures 18 and 19) show that Umiat #3, #2 and #11 look similar while Umiat #1 and #9 look different.

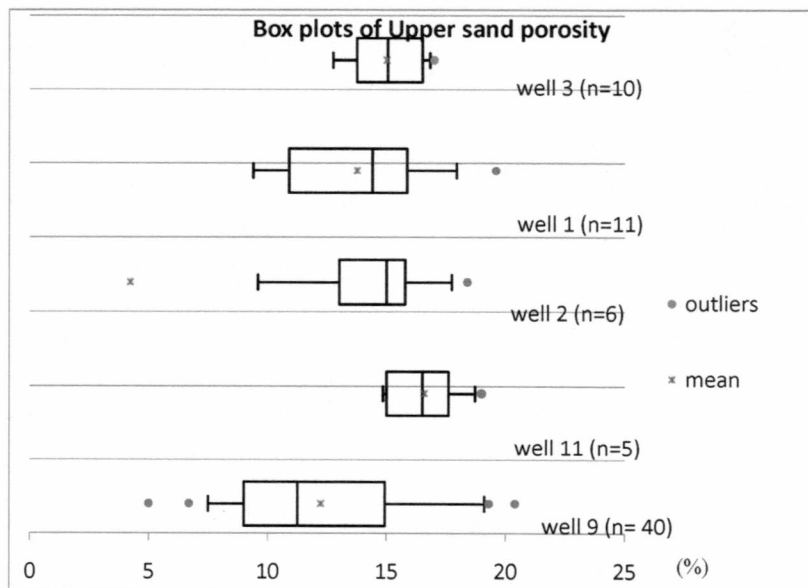


Figure 18: Box plots showing the Upper sand porosity in some Umiat wells

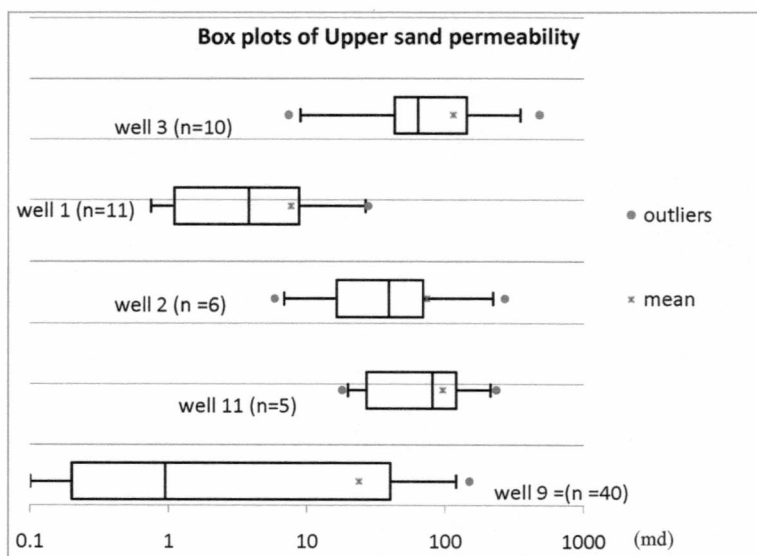


Figure 19: Box plots showing the Upper sand permeability in some Umiat wells

Box plots of porosity in the Lower sand (Figure 20) show that Umiat #2 and #9 look similar while Umiat #1 and #11 are different. In the box plots of permeability in Lower sand (Figure 21) Umiat #1, #2 and #9 look similar but Umiat #11 seems to be different.

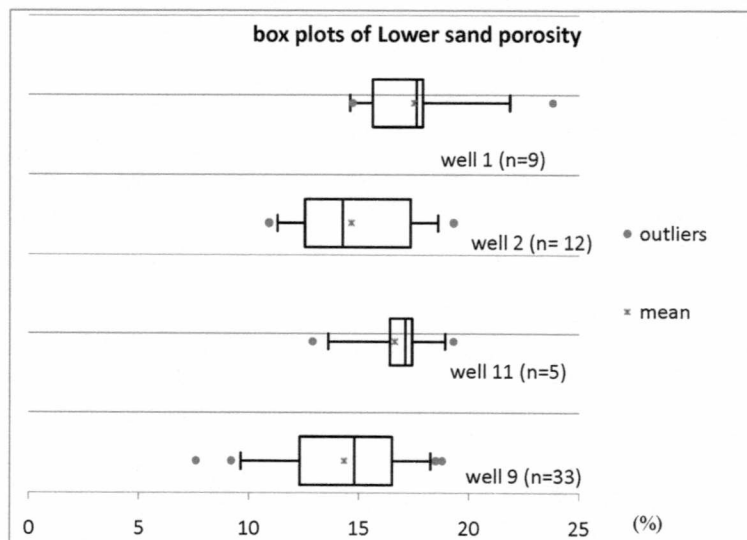


Figure 20: Box plots showing the Lower sand porosity of some Umiat wells

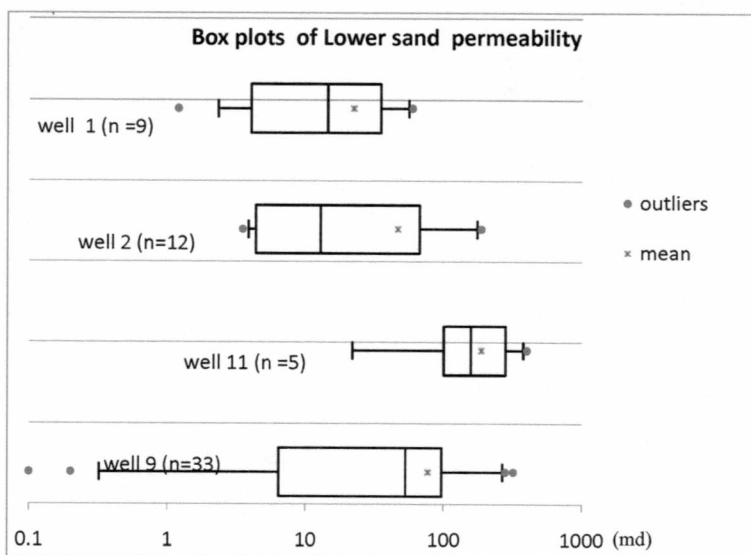


Figure 21: Box plots showing the Lower sand permeability in some Umiat wells

It can be observed that most of the wells have a narrow porosity range (Figure 18 and 20) however, the permeability range in the observed wells falls within a wider range (Figure 19 and 21). This confirms the complexity in permeability values across the Umiat anticline.

4.5 T-TESTS

T-tests are means of examining if two groups of data are statistically distinct. It is used to test the hypotheses that a parent distribution and another random distribution originate from the same population. The Upper and Lower sands were tested to observe if the two sands are from the same population using Umiat # 9 as the parent population.

A standard alpha value of 0.05 was selected and values higher than this indicate that the two groups of data tested have a high probability of coming from the same population. Values less than 0.05 signify that the two groups of data are statistically distinct and therefore may not be from the same population.

The T-test was carried out in order to confirm if the Upper and Lower sands are from the same population using all available data. There is a 0.005 probability that the Lower and Upper sands are from the same parent population (Table 6). Since this is less than the 0.05 alpha value, the sands should be treated differently.

Table 6: T-test results of the Upper and Lower sands porosity in well 9

T-Test of porosity in the Upper and Lower sands :Assuming Equal Variances		
	Upper sand	Lower sand
Mean	13.31	14.98
Variance	13.87	9.30
Observations	75	62
P(T<=t) two-tail		0.005

Table 7 represents the T-test results of porosity in the Upper sand for individual wells. This was used to verify which wells have similar porosity as Umiat #9 (the parent population). The results show that porosity values of the Upper sand in Umiat#2, Umiat #3 and Umiat #1 are likely from the same population as in Umiat#9. The Upper sand in Umiat#11 may be from a different population than Umiat #9. The T-test results conform to the observation from the box plots of porosity in the Upper sand.

Table 7: T-test results for the Upper sand in wells with available porosity data using well 9 as the parent population

T-Test of porosity(%) using upper sand well 9 as parent population Assuming Equal Variances					
	<i>Well 9</i>	<i>Well 11</i>	<i>Well 2</i>	<i>Well 1</i>	<i>Well 3</i>
Mean	12.24	16.58	14.23	13.76	15.01
Variance	17.69	3.14	11.27	10.60	2.66
Observations	40.00	5.00	6.00	11.00	10.00
P(T<=t) two-tail		0.03	0.28	0.27	0.05

Table 8 shows the T-test results of porosity in the Lower sand for individual wells using Umiat # 9 as the parent population. The Lower sand in Umiat #1 (Table 8) is from a different population as in Umiat#9 while the Lower sand in Umiat#11 and Umiat#2 are statistically from the same population as in Umiat #9. These T test results conform to the observations made from the box plots of porosity in the Lower sand with the exception of Umiat #11. This could possibly be as a result of sampling errors.

Table 8: T-test results for the Lower sand in wells with available porosity data using well 9 as the parent population

T-Test of porosity(%) using well 9 lower sand as parent population: Assuming Equal Variances				
	<i>Well 9</i>	<i>Well 11</i>	<i>Well 2</i>	<i>Well 1</i>
Mean	14.35	16.62	14.65	17.49
Variance	8.39	5.48	7.82	7.65
Observations	33.00	5.00	12.00	9.00
P(T<=t) two-tail		0.10	0.75	0.01

The results (Tables 7 and 8) are represented in Figures 21 and 22 in order to make these comparisons relative to the location of the wells on the Umiat anticline.

The blue dots represent wells with similar porosity to Umiat # 9 while the red dots are the wells which exhibit different porosity from Umiat # 9 (Figures 21 and 22). The porosity in the wells changes across the field in both the Upper and Lower sands (Figure 21 and fig 22). This could possibly be as a result of the depositional environment or the presence of thrust faults in Umiat field.

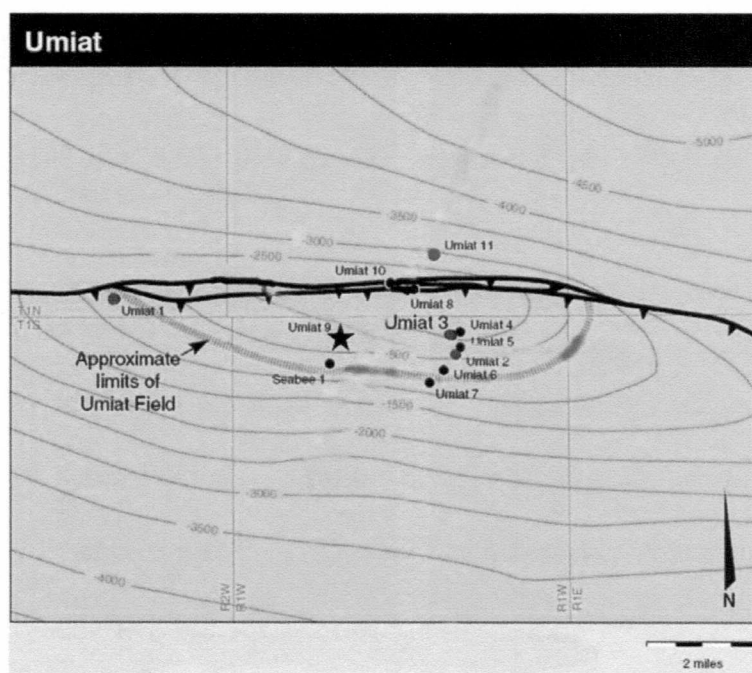


Figure 22: Map of Umiat wells showing the porosity change in the Upper sand. Modified from Kumar et al. (2002)

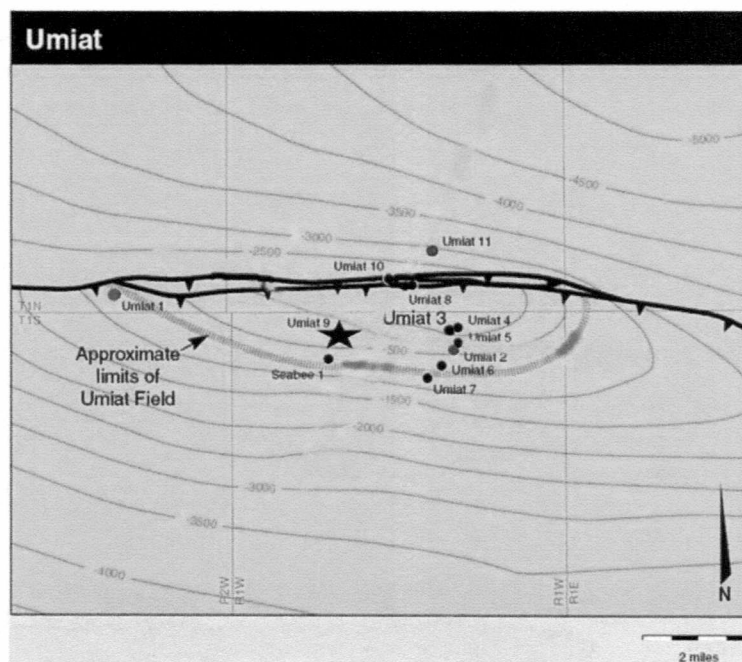


Figure 23: Map of Umiat wells showing the porosity change in the Lower sand. Modified from Kumar et al. (2002)

4.6 COMPARISON OF THE UPPER AND LOWER SANDS BASED ON POROSITY AND PERMEABILITY CUT OFFS

The Upper and Lower sands were compared using porosity and permeability cut-offs. Cut-offs define minimum porosity and permeability (storage and flow capacities) in order to eliminate those parts of the sands that do not add much to the reservoir assessment. Although physical cut-offs have been used for over 50 years there is no logical process for recognizing and applying them and this is compounded by various approaches in reservoir evaluation (Worthington and Cosentino 2005). A 5 percent porosity cut-off was used in this study because this minimum porosity value is widely acceptable for oil reservoirs (Abdus et al. 2007). Using the petrographic studies of Umiat #1 by Collins (1958) (Table 9) as a guide, the permeability cut-offs were

chosen in order to demonstrate the probability of encountering a reservoir quality rock using these assumptions.

Table 9: Permeability cut-offs based on petrographic studies of Umiat #1. Modified from Collins (1958)

Permeability value	Reservoir quality
Less than 2.55 md	Poor
Greater than 62 md	Very good

Table 10 shows the percentage of sands having porosity and permeability based on the set cut-off values for the Upper and Lower sands. 98.70 percent of the Upper sand and 100 percent of the Lower sand have probabilities of having porosities greater than or equal to 5 percent. The permeability of most of the sandstones is fair with 37.30 percent of the Upper sand and 14.52 percent of the Lower sand exhibiting permeabilities less than 2.55 millidarcies.

Table 10: Summary of probability results based on porosity and permeability cut offs

Cut-offs	Upper sand	Lower sand
≤ 2.55 md	37.30%	14.52%
≥ 62 md	20%	37%
$\geq 5\%$	98.70%	100%

Cosentino (2001) argues that cut-offs should be used when there is a good knowledge of lithological type, reservoir fluids and production mechanism in order to know where to focus in reservoir studies, well completions and stimulation studies. Cut-offs using porosity, permeability or water saturation values will be useful in studies of the Umiat field only when more information on reservoir characteristics is obtained by further development.

4.7 MODIFIED LORENZ PLOT

A modified Lorenz plot is a plot of cumulative flow capacity (permeability feet) versus cumulative storage capacity (porosity feet) (Gunter et al.1997). The profiles of the modified Lorenz plot illustrate the flow performance of the reservoir. The sections having steep slopes are linked to high percentage of reservoir flow capacity and therefore high production potential while the sections with horizontal behaviors or shallow slopes have storage capacity, but little flow capacity. If the horizontal behavior stretches over a broad area, it could inhibit successful reservoir production. Segments with neither flow capacity nor storage capacity are considered seals (Gunter et al. 1997).

Modified Lorenz plots give us an idea of the flow units and flow barriers within a zone as well as help in the forecast of drainage areas, flow capacities and storage capacities.

Modified Lorenz plots were used to define flow characteristics of the Upper and Lower sands in Umiat # 9 (Figures 24, 25 and 26). This analysis focused on Umiat #9 because it had the most cored interval in the reservoir and thus had the most porosity and permeability data. The lithologs within the plots were obtained from “Umiat test wells Alaska report” after Collins (1958). The modified Lorenz plots show the vertical distribution of heterogeneities in the Upper and Lower sands (Figures 24, 25 and 26).

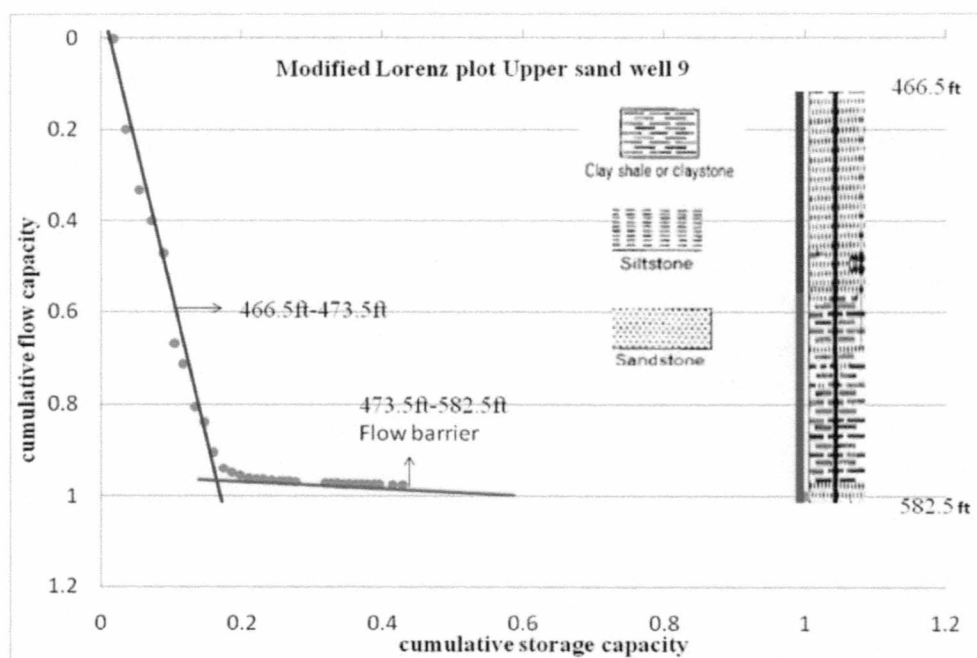


Figure 24: Modified Lorenz plot of the Upper sand in well 9

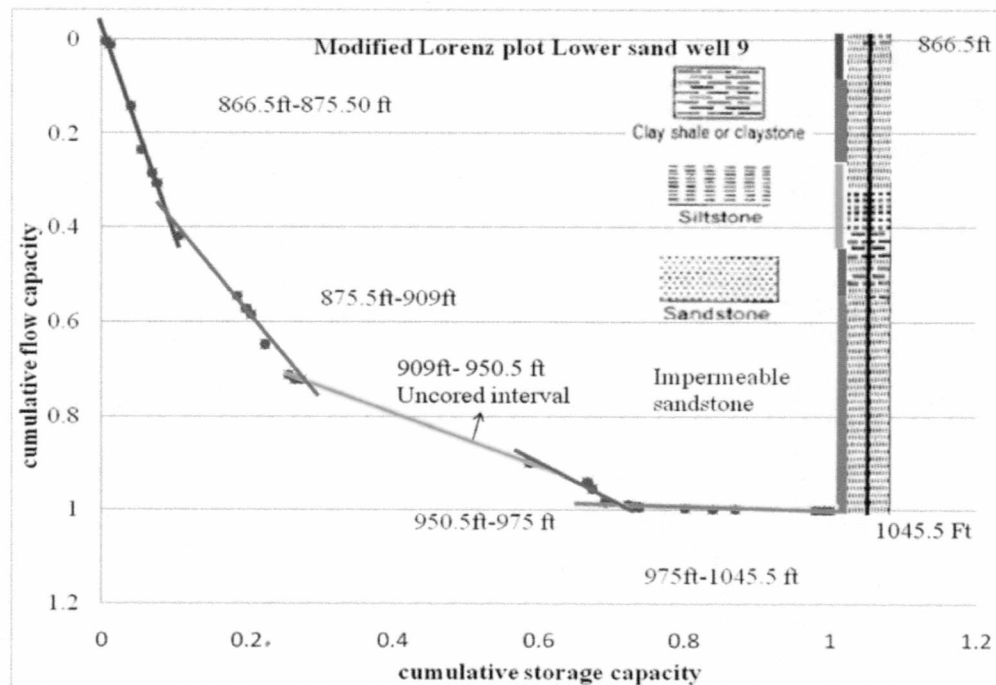


Figure 25: Modified Lorenz plot of the Lower sand in well 9 with the uncored interval

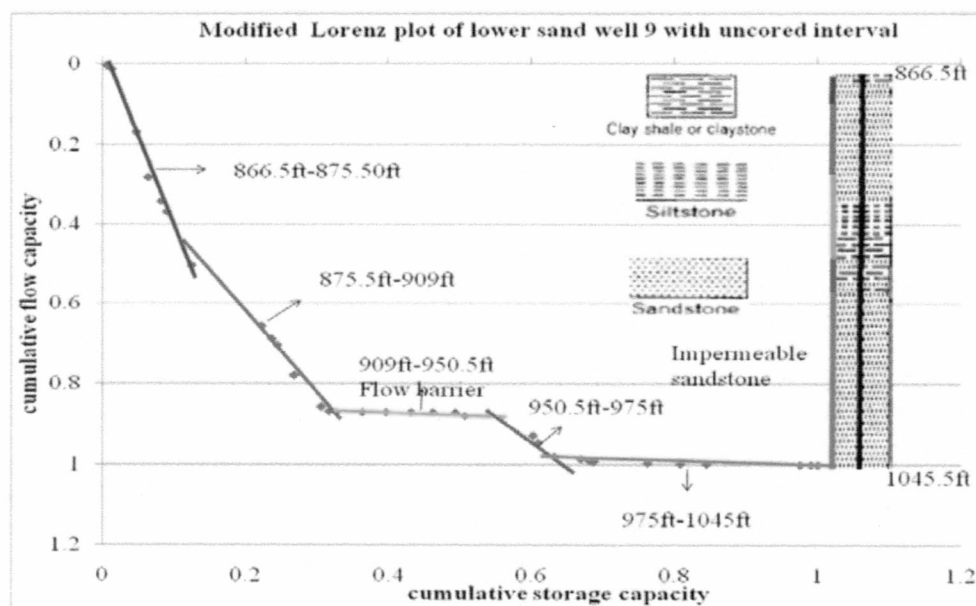


Figure 26: Modified Lorenz plot of the Lower sand in well 9 with values assigned to the uncured interval.

The yellow line (Figure 25) represents an uncured depth interval. Based on the core description of similar lithology, porosity values between 8%-9.5% and permeability values between 0.10-0.20md were assumed.

From the modified Lorenz plot of the Upper sand in Umiat #9 (Figure 24), it can be observed that the sand bodies have a good flow unit at the top of the sand but this transitions abruptly into a flow barrier with depth. All the flow capacity seems to be at the top of the Upper sand with the most significant flow unit between 466.5-473.5 feet. The flow barrier is correlated to very fine grained sandstones, silty and argillaceous materials.

There are three observed flow units within the Lower sand in Umiat#9 but the most significant lies between 875-909 feet. In the Lower sand the observed heterogeneity is attributable to the intercalations of siltstone, claystone, shale and very fine-grained sandstones with multiple distinct zones (Figure 24 and 25). The flow barriers in the Lower sand are near the bottom and will act to inhibit vertical permeability.

The difference in the porosity and permeability structure of the Upper and Lower sands is due to the inherent complexity of the depositional environment of Umiat field. The intercalations of fine grained sediments in the Lower sand are probably because it was deposited at a period of low depositional energy which did not encourage the winnowing of the sediments. However the Upper sand was probably deposited by high energy which facilitated winnowing and sorting of the sediments. The observed difference could also be as a result of the intertonguing of marine and non-marine sediments.

The inadequacy of data in the other wells made it impossible to distinguish their flow characteristics as there were significant intervals with no porosity and permeability data. Data for the modified Lorenz plots are represented in the appendices (A.3 and A.4).

The main conclusions based on the statistical analyses of the sands are

- 1) There is a wider variability in permeability than porosity in the sands across the Umiat field.
- 2) The Upper and Lower sands should be treated differently as they are statistically distinct.

CHAPTER 5

PETROPHYSICAL PROPERTY MODELING OF UMIAT FIELD

Reservoir modeling is the process of building and maintaining a reservoir model (Roxar 1994-2008). A reservoir property model is a reliable illustration of all data and information about a reservoir applicable to its management. It should include all available data from the reservoir in order to ensure success in its management. A reservoir property model includes the following parts: a description of the structural framework, the petrophysical properties of the reservoir, the initial distribution of fluids and pressures, and the dynamic fluid behavior and properties.

A forecast of hydrocarbon production can be made by using models of reservoirs and the correct illustration of the flow processes. Robinson et al. (2005) believe that geostatistical modeling technology and workflow procedures are important platforms for the incorporation of data in building valid static geologic models. A petrophysical property model for Umiat field was built using IRAP RMS geostatistical software designed and marketed by Roxar Inc. The modeling software has a workflow management which allows for the easy access to all the procedures saved in it. The workflow shows a sequence of the procedures carried out during the modeling process (Figure 27). This facilitates the adjustment of results after a modification is made to the input data thereby saving run time.

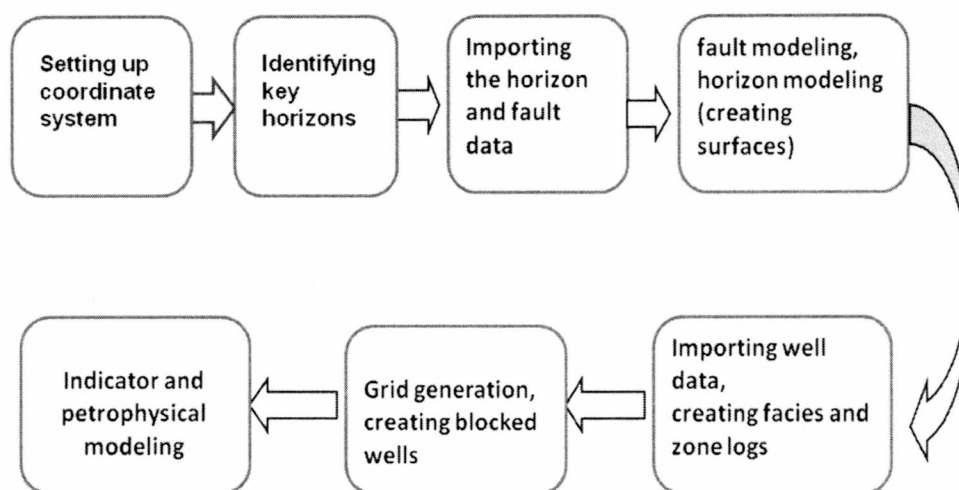


Figure 27: Flowchart of the entire modeling procedure.

It is essential that a model is built in a simple way in order to ensure that it can be easily used and modified when necessary. Input parameters in a reservoir model include the top of the structure, the depth of the key horizons as well as fault data which are usually obtained from seismic data interpretation.

The input parameters used in building the Umiat model included seismic data, well log data, and core data. The well tops and the well log data were provided by Renaissance Alaska and the lithologic description was obtained from “Test wells Umiat area Alaska” by Collins (1958). The lithologic description was used to estimate the percentage of each lithofacies as well as their interval thicknesses in the wells (A.5-A.15) These data were loaded into IRAP RMS and were used to build a petrophysical

model of Umiat field detailing porosity and permeability distribution as well as lithofacies distribution.

Since there were no well logs from which porosity and permeability could be calculated, an internal programming language (IPL) script generated by Roxar Inc. was used in loading the data from core analyses.

5.1 STEP BY STEP PROCEDURE OF BUILDING UMIAT PETROPHYSICAL PROPERTY MODEL

5.11 SETTING UP THE COORDINATE SYSTEM AND UNITS

The first task in creating the model for Umiat field was to set up the coordinate system and units. The field units were set in feet in order to ensure correct conversions while transferring the input data which were all in feet. All the X, Y axes are in UTM coordinates.

5.12 DEFINING THE STRATIGRAPHIC FRAMEWORK

The stratigraphic framework was established by identifying key horizons and arranging the horizons in their correct depth order, from the top: the Chandler sand, the Upper sand, the Shale barrier and the Lower sand (Figure 4). Depth surfaces for the Upper sand, Lower sand, and the Shale barrier in between them were used to construct internal surfaces of the Umiat reservoir. A constant thickness of 300 feet was assumed for the Shale barrier. This thickness is approximately the average thickness of the Shale barrier in all the 11 Umiat test wells. The horizons are all interpreted horizons apart from the Shale barrier which is a calculated horizon. Interpreted horizons are those with

enough data e.g. seismic data while calculated horizons do not have enough data and are usually in between interpreted horizons.

5.13 IMPORTING HORIZON AND FAULT DATA

The horizons' data were imported as points. These horizons were all interpreted horizons from seismic interpretation with the depth surface in point format. The input data was loaded and a structure surface was mapped out of it. Scalar operations were used to flip the points in sub-sea depths (negative).

The fault data was imported as polylines. The input data available had two thrust faults in the field: the main thrust fault and the secondary thrust fault (Figure 5).

5.14 FAULT MODELING

Fault modeling is one of the vital operations in the property modeling procedure since it determines structural arrangements and connectivity between different regions of the reservoir (Panda and Morahan 2008). This procedure involved creating the fault surfaces from the fault input data (Figure 28). The fault input data were treated as soft data. Soft data are used to generate the overall shape of the fault surface. If only one data type is selected (which is the case in this modeling job) it must be specified as soft. Fault sticks, midlines, or polygons are considered as soft data (Roxar 1994-2008)

After the soft data were imported, each of the faults was examined and the surface shape was edited. The tip line polygon of the fault was set as a convex hull and was shaped by a line drawn around the outermost points in such a way that every point

was enclosed. This made the resulting fault shape to be close to the input data. A polygon represents the tip line of a fault where the fault dies or dips out in XY and also in Z (Roxar 1994-2008). The gridding parameters used include the smoothing factor, algorithm and grid increment. The smoothing factor is a percentage showing the degree of smoothness of the fault surface whereas the grid increment defines the spacing between grid nodes in XY units (Roxar 1994-2008). Quality control of the surface shape and intersections was executed.

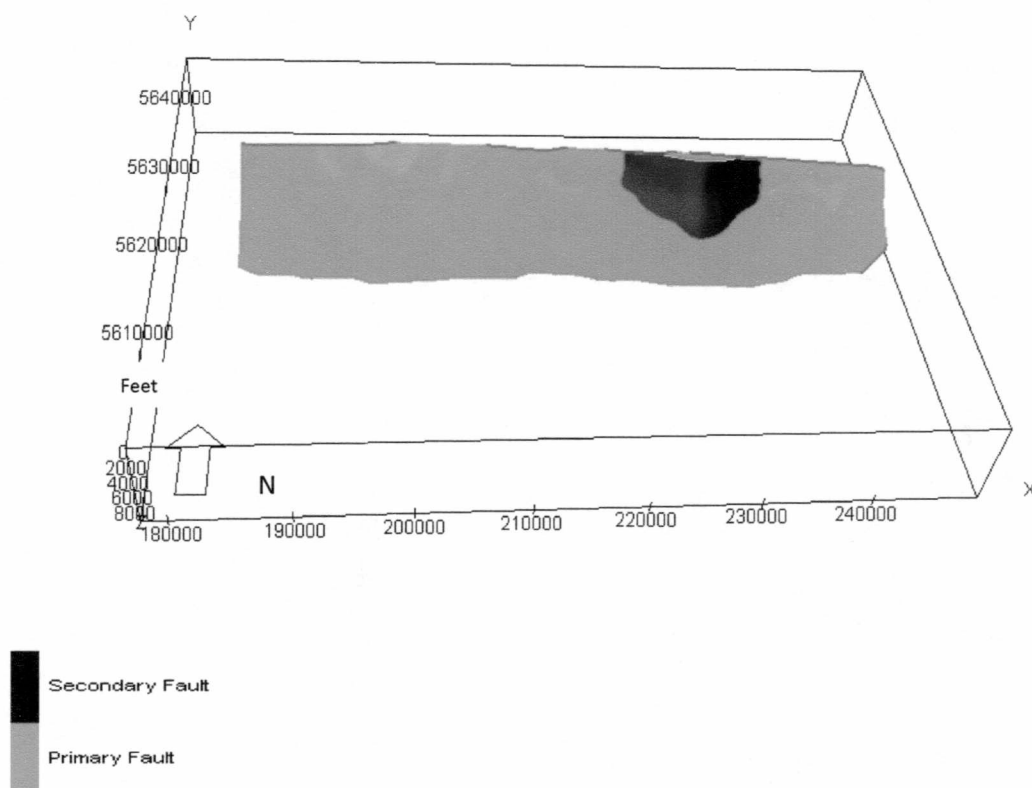


Figure 28: Fault model of Umiat field

5.15 CREATING THE MODEL BOUNDARY

The boundary for the Umiat model was generated from the converted points of the fault input data. The calculation of the fault model generated the model boundary and this enclosed the entire Umiat model structure.

5.16 HORIZON MODELING

Horizon modeling involved the creation of the full horizon surfaces and the adjustment of the depth surfaces of the selected horizons; Chandler sand, the Upper sand, the Shale barrier and the Lower sand to the fault model (Figure 29). The horizon data was filtered in order to remove the noise often present in the faults which gives a smeared look to the horizons near the fault surfaces.

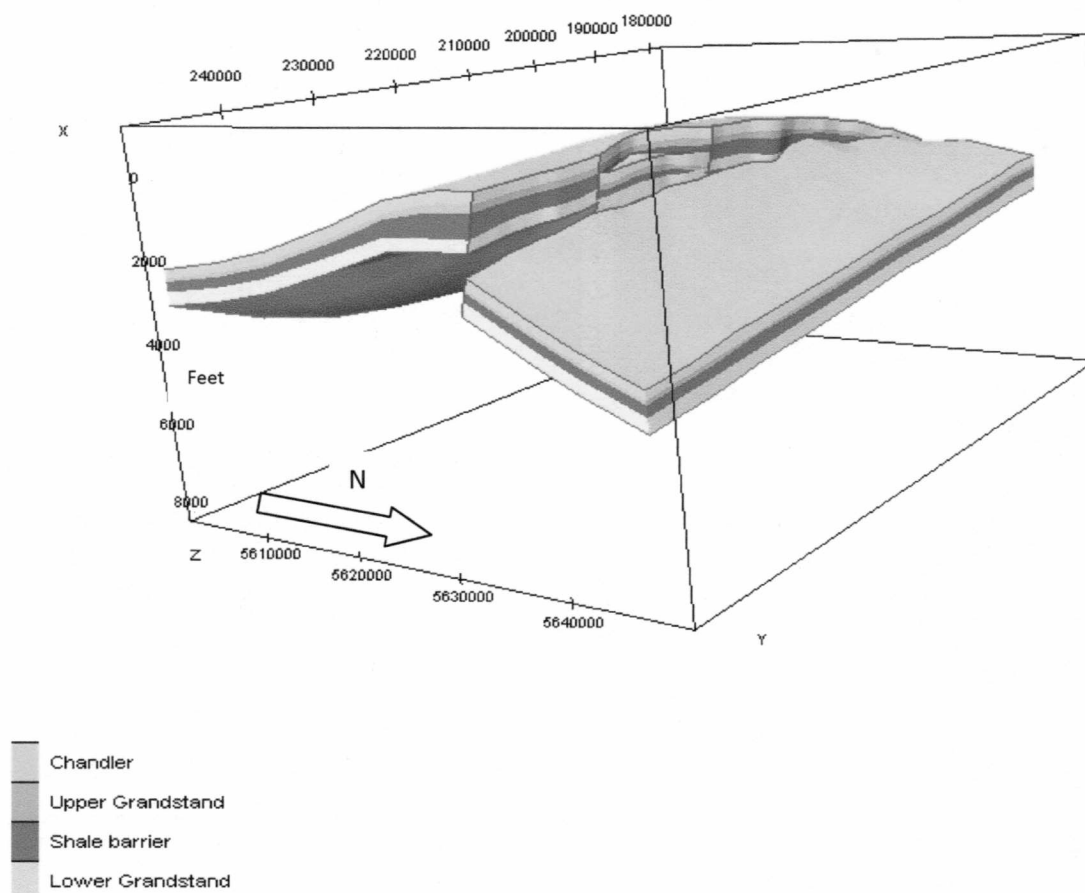


Figure 29: Horizon model of Umiat field

5.17 IMPORTING WELL DATA

The well locations of the 11 test wells were imported with the calculation type set as measured depth (MD), East, North, and total vertical depth (TVD) (Figure 30). The well header information had the well name, the X, Y locations, and the rotary kelly bushing (RKB) value.

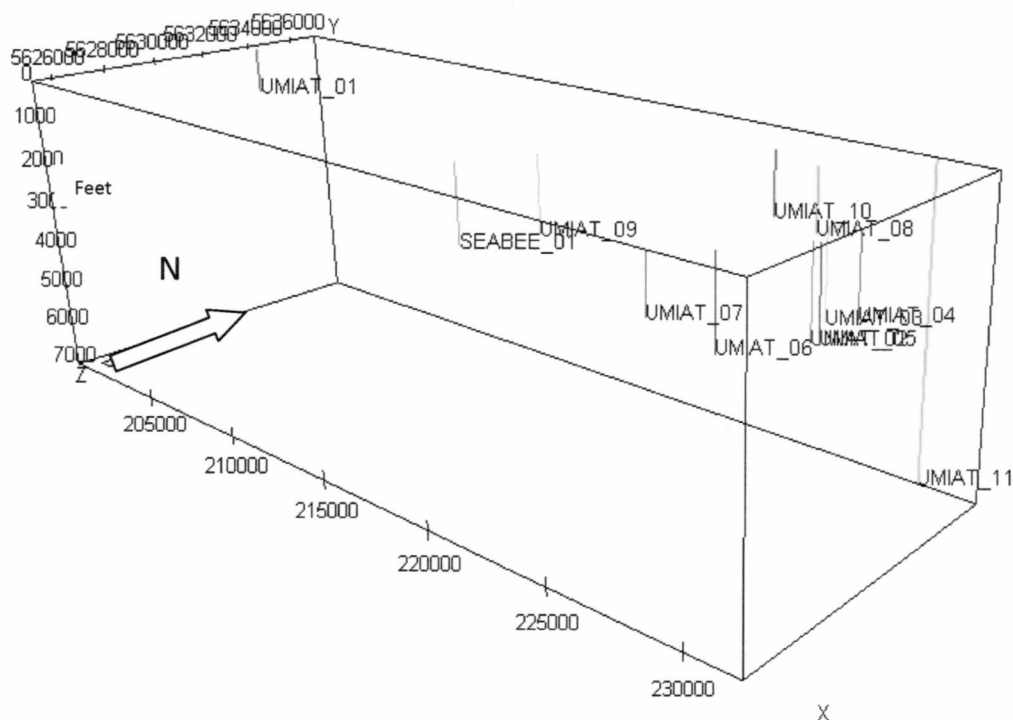


Figure 30: Umiat model box showing the location of the 11 Umiat wells

5.18 CREATING THE LITHOFACIES LOGS

A simple lithofacies log named Umiat lithofacies was designed using the log editor/calculator on IRAP RMS (Figure 31). The value of 1 was assigned to sand, while the value 0 was assigned to shale which represents the background.

5.19 CREATING THE ZONE LOGS

Zone logs were created to define the various horizons present in Umiat field; Chandler sand, the Upper sand, the Shale barrier and the Lower sand. The well picks which represent the intersections between well trajectories and horizons depth surfaces

were loaded. Information from the well picks was obtained from the well top data for the Chandler sand, the Upper sand and the Lower sand provided by Renaissance Alaska. The top of the Shale barrier was assumed to be at a height of 300 feet from the top of the Lower sand. The well picks formed the basis for creating the zone logs.

The zone log can also be any discrete log e.g. the lithofacies log. The Lithofacies log shows the lithofacies distribution in the wells while the zone log shows the various horizons in the Umiat model (Figure 31).

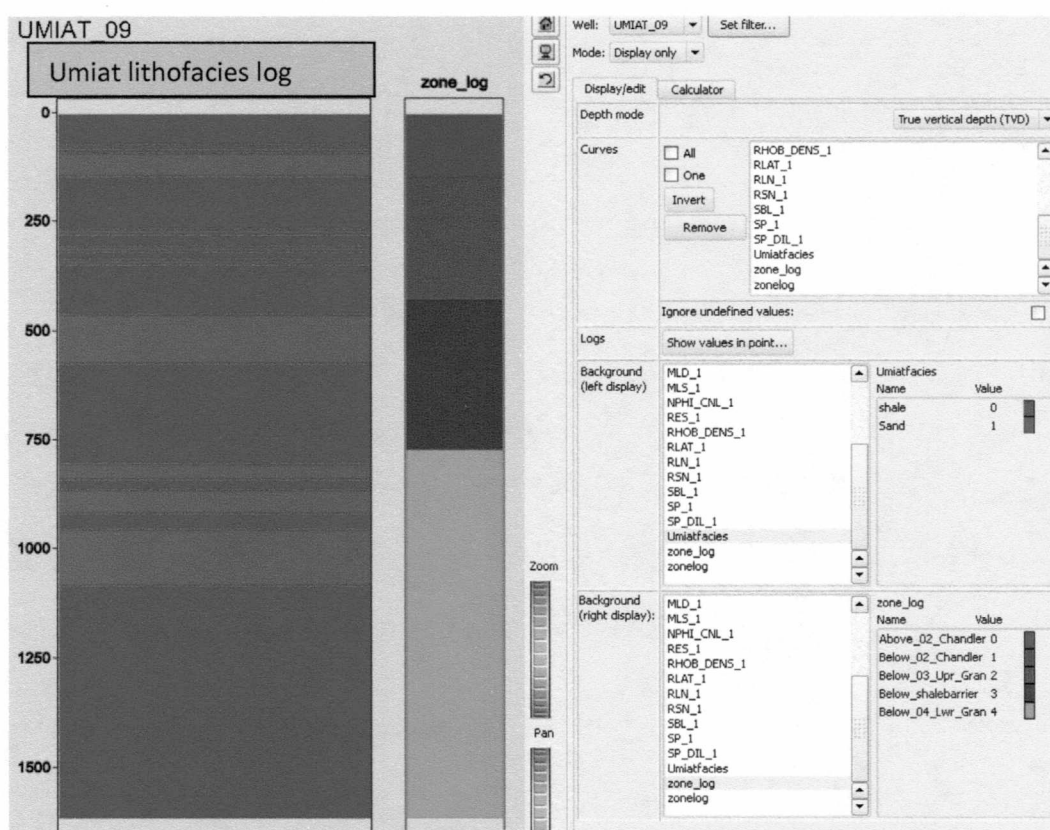


Figure 31: Umiat well #9 showing the lithofacies log and zone log in the log editor

5.2 GRID GENERATION

This involves building the grid empty framework. The grid represents cells which are part of the integrated stratigraphic framework of Umiat field. The corner point regularized grid for Umiat field was generated from the stratigraphic structure and the fault model. In the gridding parameters settings, repeat sections were allowed to account for cells which are duplicated especially due to the presence of faults. The repeat sections create parameters for use in simbox space and account for cells that have the same IJK(XYZ directions) index (Roxar 1994-2008). This is especially useful if the model has stair stepped reverse faults as is the case in Umiat field.

5.21 GRIDDING PARAMETERS

The thickness of the grid cell should capture the heterogeneities present within each modeled zone. To guarantee that this is achieved, histograms generated from the lithofacies log of the 11 Umiat test wells (Figures 32, 33, 34 and 35) were used to determine the most frequent thickness interval of the sand bodies in all the zones. The choice of varying cell thicknesses in the modeled zones was important in order to retain the vertical characteristics of Umiat field (Table 11).

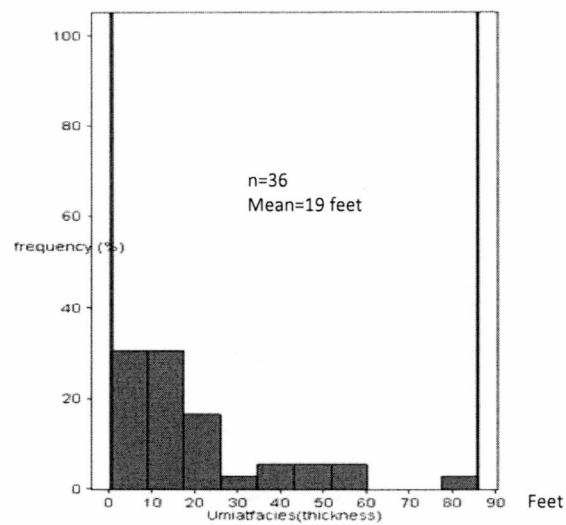


Figure 32: Histogram showing the sand thickness interval in the Chandler sand

An average cell thickness of about 12 feet was assumed for the Chandler sand. Since the most frequent sand interval from the histogram is below 20 feet, the assumed cell thickness of 12 feet will be sufficient to capture heterogeneities in this zone.

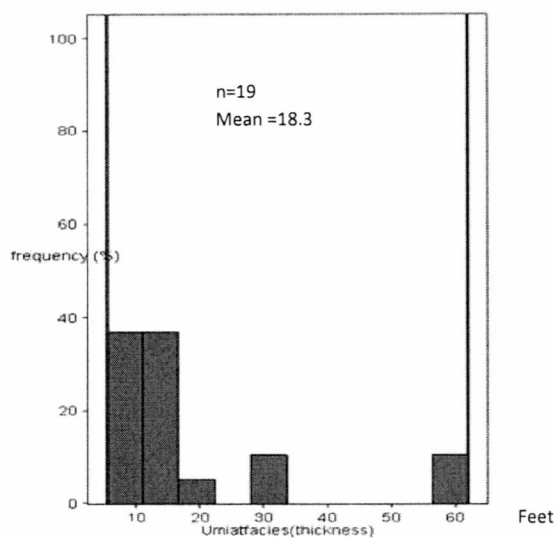


Figure 33: Histogram showing the sand thickness interval in the Upper sand

The most frequent sand thickness in the Upper sand is below 20 feet. A cell thickness of approximately 8 feet was used to grid this horizon because the smaller the cell thickness the more heterogeneities captured.

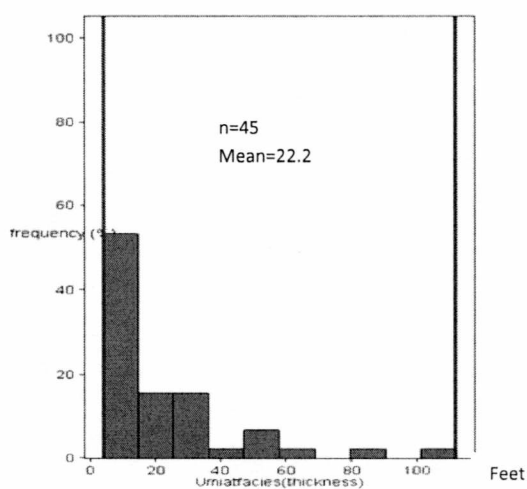


Figure 34: Histogram showing the sand thickness interval of the Shale barrier

Most of the sand bodies within the Shale barrier are less than 20 feet in thickness. An estimated cell thickness of 18 feet was used in gridding this zone.

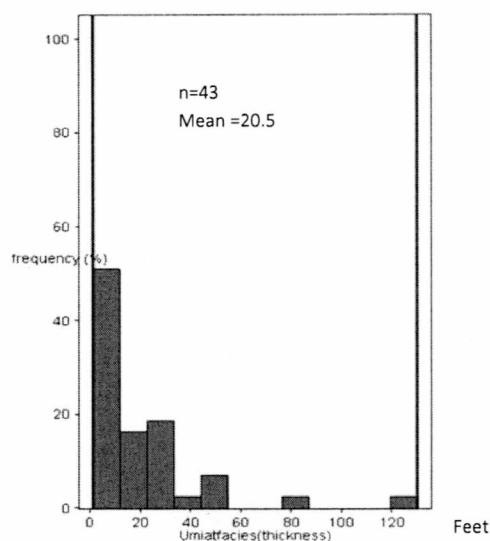


Figure 35: Histogram showing the sand thickness interval in the Lower sand

In the Lower sand most of the sand bodies had thicknesses below 15 feet, a thickness value of about 11 feet was used in gridding this horizon.

Although the bin sizes in the histograms seem large, the information obtained from them was compared with the summary lithology in the appendices (A.3- A.13) in order to ensure consistency in the sand lithofacies thicknesses in the various zones. It is better to choose a smaller thickness than a larger thickness in order to capture evident heterogeneities in the reservoir.

Table 11: Simbox thicknesses of horizons in Umiat field

ZONE	NO OF LAYERS	GRID CELL THICKNESS (Feet)	SIMBOX TOTAL THICKNESS (Feet)	ZONE THICKNESS (Feet)
CHANDLER	23	11.70	270	258
UPPER GRANDSTAND	11	7.70	85	104
SHALE BARRIER	12	18.00	215	289
LOWER GRANDSTAND	34	10.60	359	241

Simbox or simulation box represents a dual grid of the property model (lithofacies and petrophysical). The simbox total thickness of a zone is the number of layers within that zone multiplied by the average cell thickness in the zone.

In the gridding parameters, the total number of layers is 80. These layers have an associated index (K) from the first to the last layer. The number of columns NX is 100 (100 feet each) and the number of rows NY is 100 (100 feet each). The X direction runs west to east with a total coverage of 10000 feet and the column index (I) is associated with the X direction. The Y direction which runs south to north is associated with the column index (J) and covers a distance of 10000 feet. The 100 feet by 100 feet areal grid dimension will satisfactorily capture the areal changes across the reservoir. There is a total number of 800,000 grid cells.

5.3 CREATING THE BLOCKED WELLS

Blocked logs are similar to well logs but are of the grid dimension and form the foundation for geostatistical modeling. A generated IPL script was used to load the available porosity and permeability values. These values were obtained from cored intervals. An IPL script is an internal programming language which functions with any parameter and applied to define the parameter settings for external jobs (system

commands) integrated in the workflow (Roxar 1994-2008). In order to ensure accuracy, the values were compared with the original data after the script was run in the workflow. Blocked wells were created based on the loaded porosity and permeability values (Figure 36). Statistical analysis was also performed using the blocked well data to calculate parameters as mean, standard deviation and skewness of the data. Results were compared to the results from earlier work to verify its consistency.

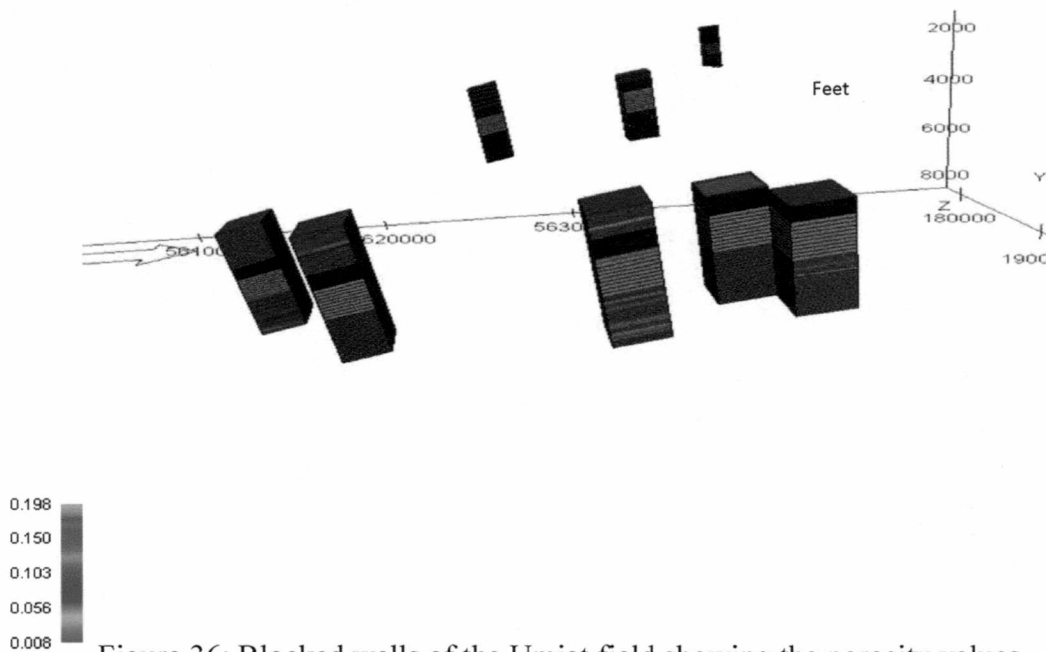


Figure 36: Blocked wells of the Umiat field showing the porosity values

5.4 INDICATOR GRID MODELING

The indicator model is a pixel based facies model showing the distribution of facies relative to their direction of deposition. It is a stochastic modeling method which generates a discrete facies parameter using the kriging method (Roxar 1994-2008). The

codes assigned to the lithofacies (Sand=1 and Shale=0) in the Umiat lithofacies log form the basis for creating this model.

The stochastic process is a statistical procedure involving the change of a value at different points. It varies from the kriging method which is an interpolation process that assigns values to unobserved locations based on known values in close proximity. The grid cells are populated based on the probabilities calculated by the well log and/or user defined parameters (Robinson et al. 2005) , the sequential indicator simulation conditioned to a vertical proportion curve created by the blocked wells populates the grid. These vertical proportion curves show the vertical variation of facies. Sequential indicator simulation works by visiting each point on the grid to be simulated and estimate the conditional distribution at that point. Roxar (1994-2008) defines conditional distribution as a probability distribution for the facies at a position given understanding of the facies at nearby well locations.

In the indicator model the percentages of sand and shale within the reservoir interval were calculated from the Umiat lithofacies log generated from the lithologic description by Collins (1958). The percentage of siltstone in the Umiat area is insignificant and not expected to be of reservoir quality.

A summary of the lithologic description of the various Umiat wells in the modeled zones (Chandler sand, Upper sand, Shale barrier and the Lower sand) within the reservoir interval are provided in the appendices (A.5-A.15). Data were derived from “Test wells Umiat Area Alaska” (Collins 1958)

The average percentages of sand in the various zones calculated from the summary of the lithologic description are: Chandler 33 percent, Upper sand 56.9 percent, Shale barrier 15.46 percent and Lower sand 58.5 percent. These values controlled the quantity of sand in the model. Sand and shale are the two most dominant lithofacies consequently siltstone was regarded as shale (background) in the indicator model.

The Umiat delta prograded northeasterly (Fox et al. 1979). This is about 45 degrees azimuth (direction of trend). This value was one of the user defined parameters utilized in building the indicator model of Umiat field. The arrow in the model box as shown in the Figures points to the true north direction. The sand lithofacies are trending in the north east direction of progradation (Figure 37, 38, 39, 40 and 41). This means that the grid cells were populated relative to the direction of trend.

Based on the indicator model (Figure 37), the sand bodies in the Chandler sand appear elongated in a north easterly direction some of which are isolated by shale.

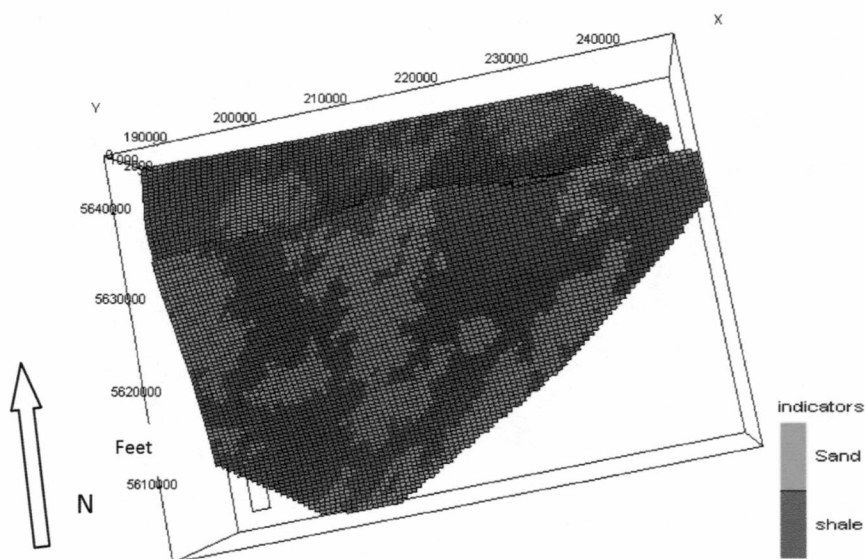


Figure 37: Indicator model after one realization showing the lithofacies distribution of the Chandler sand

The indicator model (Figure 38) shows that the sand bodies in the Upper sand occur as large sheets of continuous sand with patches of shale. This occurred in the first few layers of the sand and graded into elongated bodies of sand in the north east direction having more shale with depth (Figure 39). The high quantity of shale with depth could mean that there low energy of deposition which encouraged the deposition of these fine grained sediments.

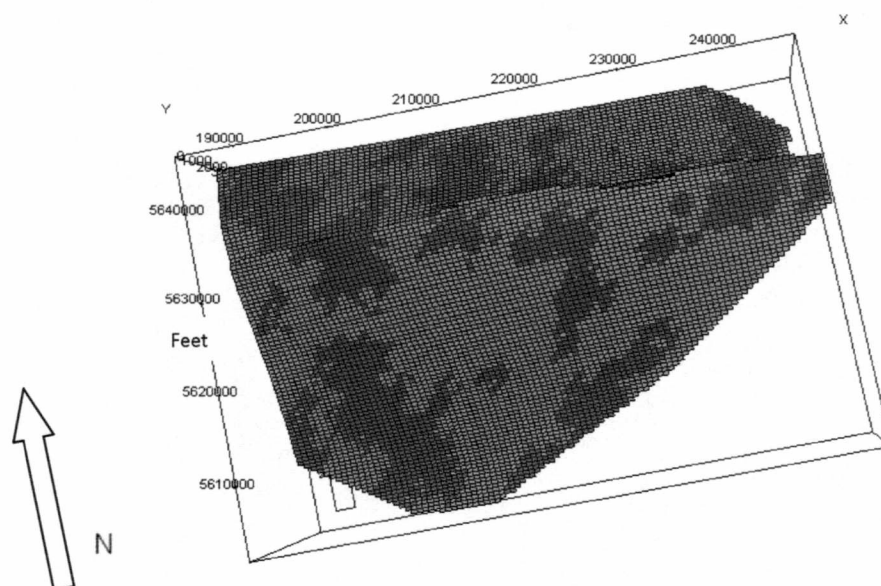


Figure 38: Indicator model after one realization showing the lithofacies distribution of the upper part of the Upper sand

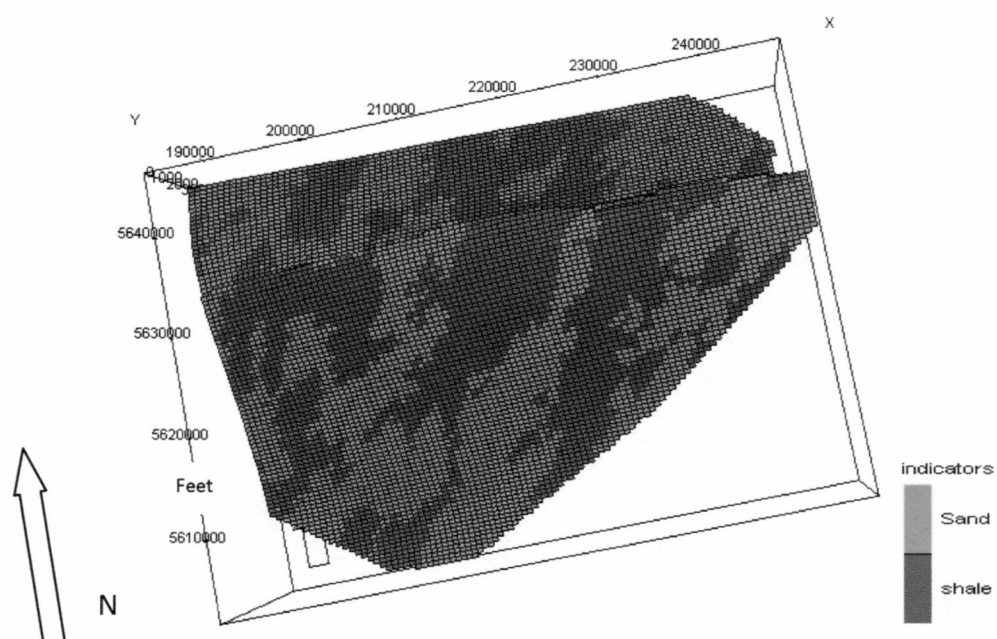


Figure 39: Indicator model after one realization showing the elongated sand bodies in the lower part of the Upper sand.

The sand bodies in the Shale barrier appear isolated and elongated. The downthrown portion of Umiat field appears to have less sand and more shale within the shale barrier (Figure 40). The Shale barrier is not composed entirely of shale but has some sand in it.

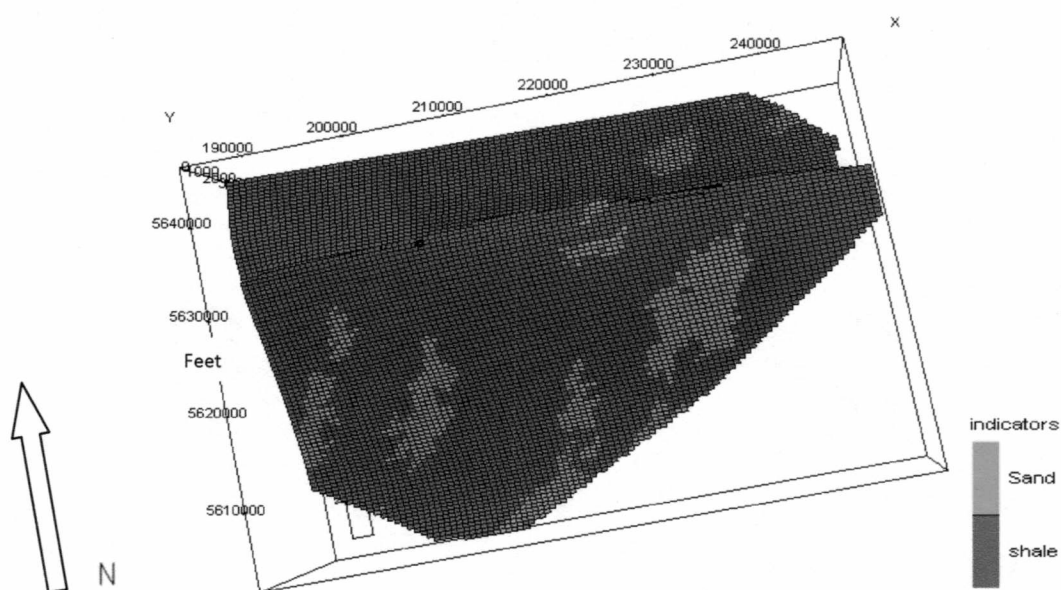


Figure 40: Indicator model after one realization of Shale barrier in Umiat field

The sand bodies in the Lower sand appear elongated and continuous over the entire field with some shale (Figure 41). There are no observed changes in the shape of the sand bodies in the Lower sand with depth.

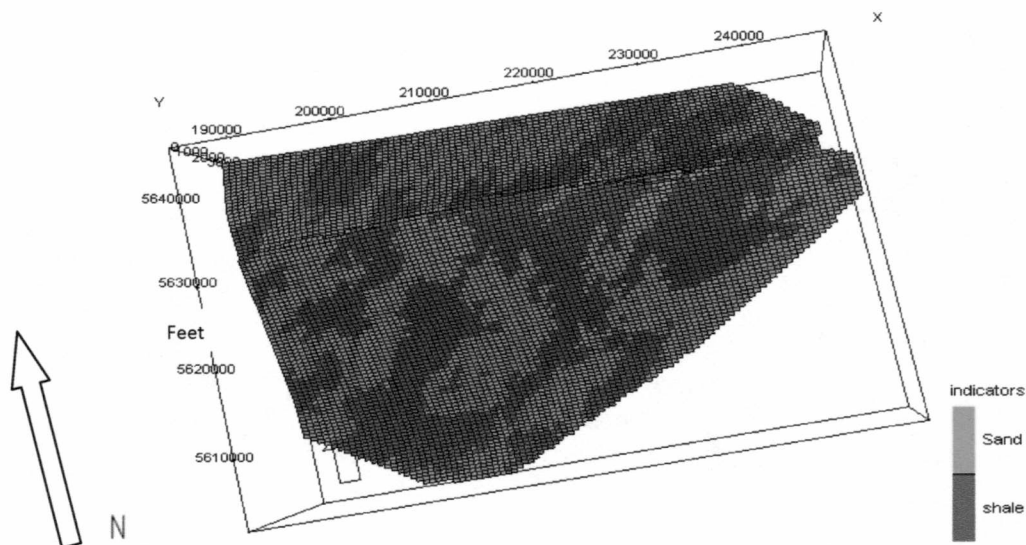


Figure 41: Indicator model after one realization of Lower sand in Umiat field

The change in the shape of the sand bodies in the various zones is dependent on the change in volume of sand as all other variables remained constant. The change in the volume of sand could be indicative of different depositional environment.

5.5 PETROPHYSICAL PROPERTY MODELING

Petrophysical modeling is a highly developed statistical method which extrapolates the observed well values within the area of the model based on the observed trends and distribution of the input data. The results take into consideration limits in the data and how rapidly values change with distance using variograms. Petrophysical modeling involves populating the grid cells with reservoir parameters such as porosity and permeability.

Figure 42 shows the various steps taken in building the petrophysical model of Umiat field using IRAP RMS. The steps are discussed below

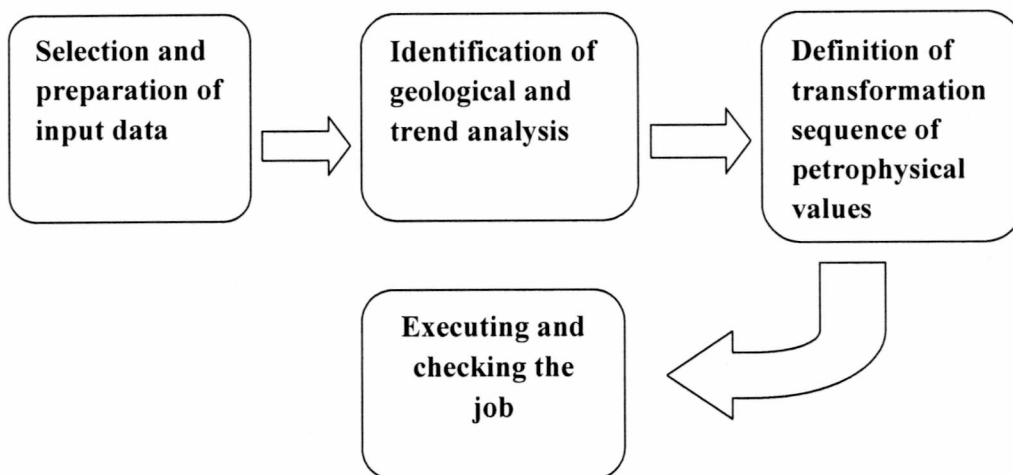


Figure 42: Flow chart showing the procedures in petrophysical property modeling

1) **SELECTING AND PREPARING THE INPUT DATA:** The input data used in the petrophysical property modeling of Umiat field is porosity and permeability values conditioned to the facies distribution. This process honors the facies distribution with respect to its corresponding porosity and permeability values. The input parameters that control the interwell property distribution are the mean, standard deviation, skewness, and variograms.

2) **IDENTIFYING GEOLOGICAL TREND AND TREND ANALYSIS:** This involves inspecting the geological trends and statistical characteristics shown by blocked porosity and permeability well logs. These characteristics were modeled for each of the

subzone separately. The statistical characteristics observed earlier as well as knowledge of geology from literature served as a good foundation in identifying possible trends and characteristics.

3) DEFINING TRANSFORMATION SEQUENCE OF PETROPHYSICAL VALUES:

Transformation definition exists just for continuous well data (porosity and permeability) from blocked well parameters. The transformation is done to make the data distribution statistically correct in order to facilitate the petrophysical property modeling procedure. The transforms defined were:

(a) TRUNCATE: The truncate transformation is used to remove undesired or incorrect data outliers (outside the specified interval). In order to have some control in the way the input data populated the grid, the truncate data transformation was activated to include values only within the range of the observed input data.

(b) MEAN: This is a specified value of the parameter and is used to transform the data values to possess a zero mean.

(c) SKEWNESS REDUCTION (NORMAL SCORE): The loaded data is assumed to be distributed according to the probability distribution function (pdf), which is either calculated from the data directly or given by a user-defined function (Roxar 1994-2008). It modifies the transformed data to have a normal (Gaussian) distribution with zero mean and unit variance and standard deviation.

(4) DEFINING THE VARIOGRAM: This involves defining the variability of the residual data based on geological knowledge and data analysis. The variogram is a statistical tool used to make approximations of data values in unsampled areas e.g. interwell areas (Krajewski and Gibbs 2001). The similarity between two observations depends on the distance between them. Inconsistency between these observations increases with increasing separation distance (increment). The variogram value according to (Krajewski and Gibbs 2001) is the calculated variance of increment. They are important because they provide information on the confidence with which the value of a cell can be predicted, based on its distance from a cell with an identified value.

Variogram terms used for the purpose of this work are:

RANGE: This is the distance within which no considerable variation is observed between samples (Table 12). It should have specified values for distance normal to azimuth, parallel to azimuth and vertical (normal to dip) (Krajewski and Gibbs 2001)

Table 12: Range values in the variogram for the sand bodies in all the zones in Umiat field

Range	Value(feet)
Parallel to Azimuth	10000
Normal to Azimuth	5000
Vertical (normal to dip)	10

These parameters (Table 12) as well as the azimuth value of 45 degrees for the direction of deposition are the variogram input data that controlled the population of the grid cells based on the observed data in the blocked wells.

SILL: Although this is not frequently present, it represents the flat area of the variogram (Figure 43, 44, 45 and 46). The higher the sill, the higher the variability and vice versa (Krajewski and Gibbs 2001).

LAG DISTANCE: This is the distance in field units within which sample differences are compared (Krajewski and Gibbs 2001) (Figure 43, 44, 45 and 46).

The generated properties for the variogram were conditioned at the wells, meaning that at these locations, the grid cell properties are in good alignment with the well data. In the interwell areas the properties were distributed according to the statistical properties (such as standard deviation, mean and variance) of the well data.

Figures 43 and 44 represent the porosity and permeability distribution in the X-Y direction in the Upper sand after the variogram analysis and Figures 45 and 46 show the permeability distribution in the X-Y direction and porosity distribution in the X-Z direction in the Lower sand after the variogram analysis.

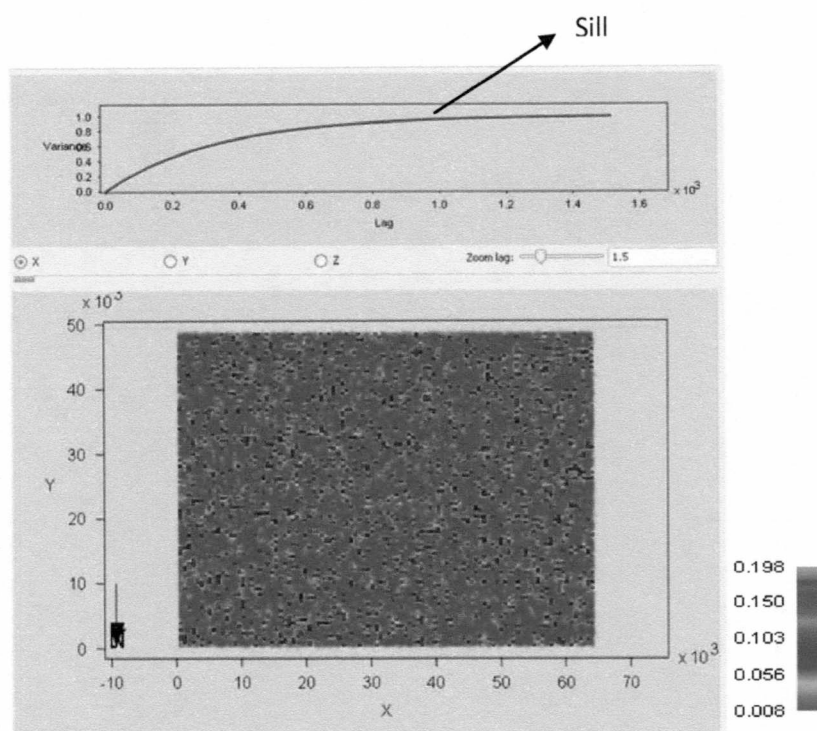


Figure 43: Porosity variogram result of shale in the Upper sand in the X-Y direction (Axes in feet)

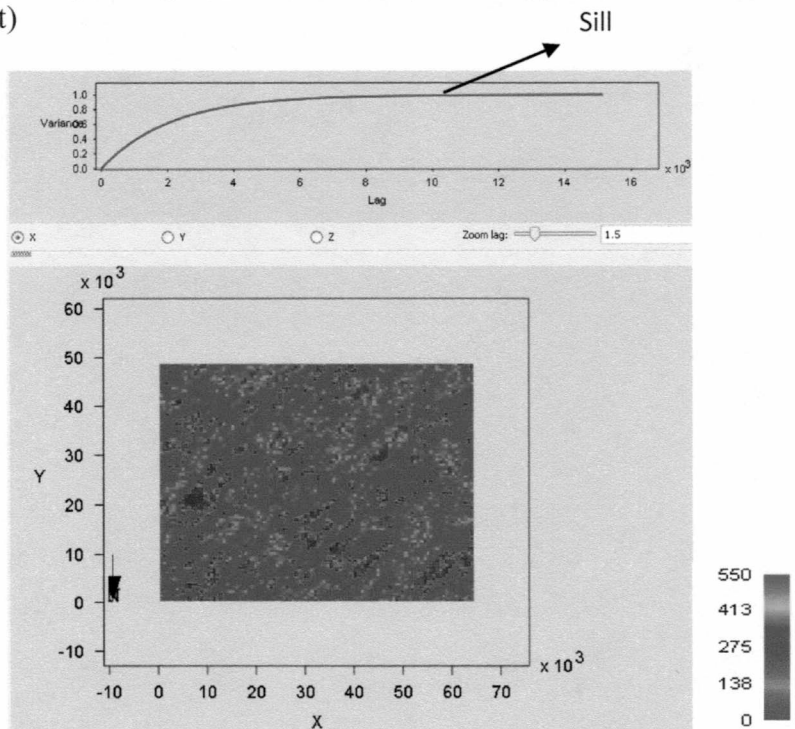


Figure 44: Permeability variogram result of sand in the Upper sand in the X-Y direction (Axes in feet)

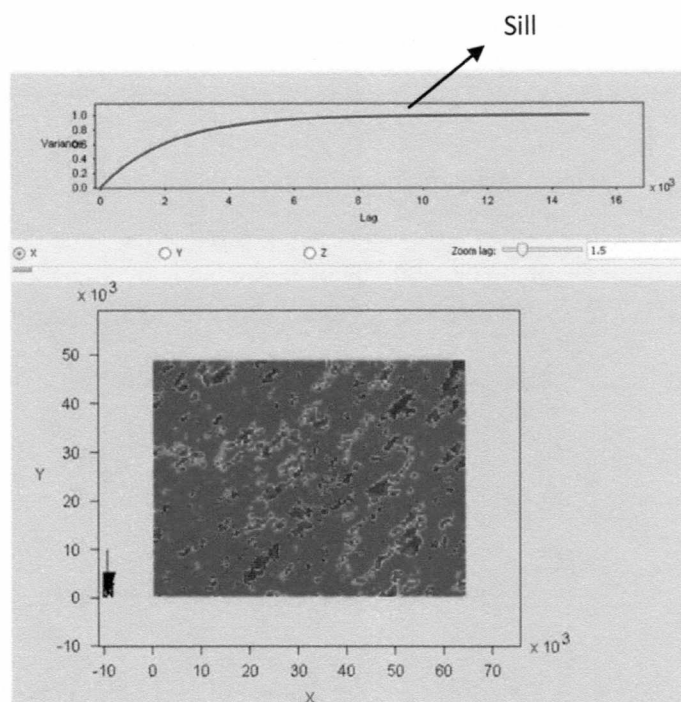


Figure 45: Permeability variogram result of sand in the Lower sand in the X-Y direction (Axes in feet)

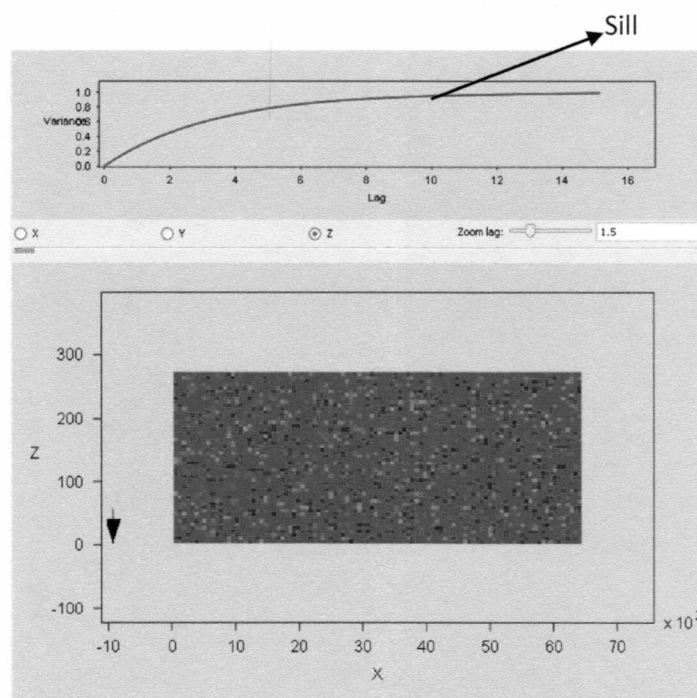


Figure 46: Porosity variogram result of shale in the Upper sand in the X-Z direction (Axes in feet)

The results of the petrophysical property modeling for the Chandler sand are shown in Figures 47 and 48.

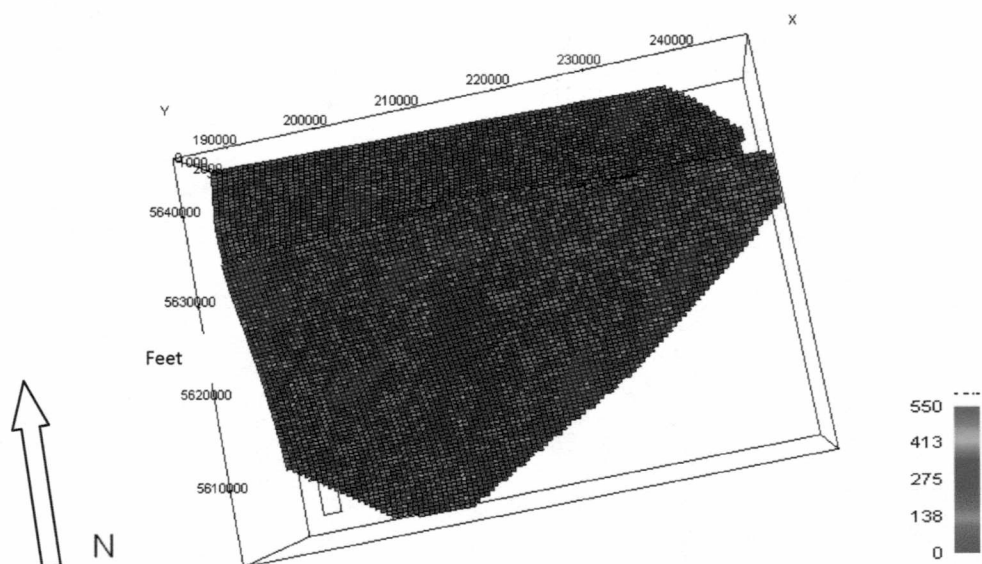


Figure 47: Chandler sand permeability distribution from the petrophysical property modeling

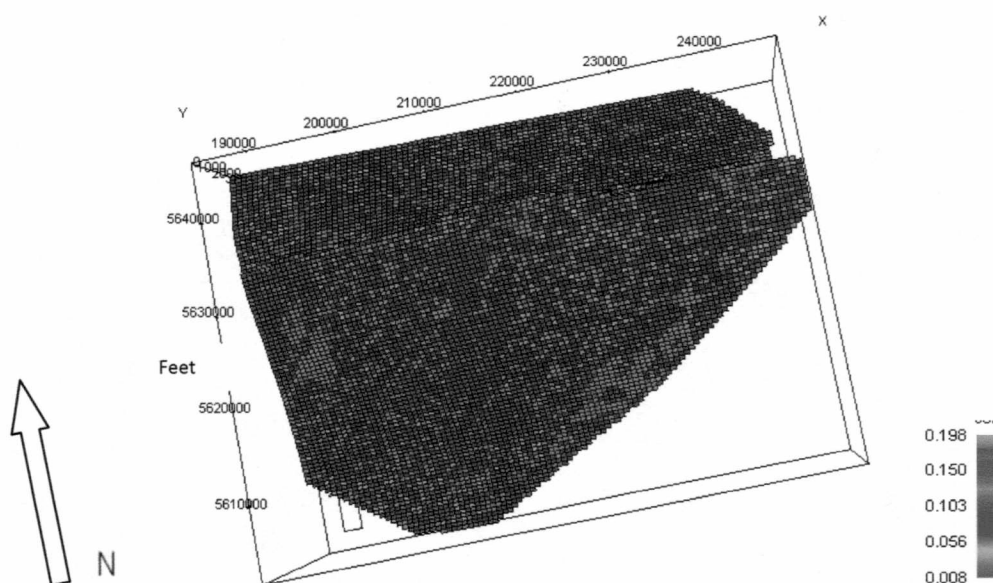


Figure 48: Chandler sand porosity distribution from the petrophysical property modeling

(4) EXECUTING AND CHECKING THE JOB: This involves comparing the petrophysical model results with the lithofacies distribution in all the zones and ensuring that there is a good match between the input data and the results.

The histograms (Figure 49, 50, 51 and 52) show the input data loaded in the blocked wells for the petrophysical job, as well as the corresponding result representing the distribution of petrophysical properties after the population of the grid cells for the porosity distribution of sand and shale in the Chandler sand. The results for the other zones are depicted in the appendices (A.16-A.43).

A careful observation of the input data histograms for all zones shows that some shale lithofacies have a greater number of observations with high permeability values (A.16-A.43). This is because the major lithofacies of interest due to its expected reservoir quality is sand therefore all the other areas outside the sand zone were treated as shale. Siltstones were also treated as shale (background) but may actually have measurable porosity and permeability. These assumptions did not affect the final volumetric estimation because the shale lithofacies is not expected to be productive as it had no reported producible hydrocarbon volume. The high permeability values observed in some shale intervals are possibly due to sampling errors as the data were collected. This makes it imperative for well log data to be available for a better analysis in future studies.

Table 13 and 14 summarize the zone by zone input and output results of the petrophysical property modeling job. The mean, median and standard deviation of both

the input and output data in the various zones have close values irrespective of the difference in the number of observations. These slight differences between the input and output results can be attributed to the truncate method in the data transformation procedure in the petrophysical property modeling. This confirms the quality of the job. In the Upper sand, the sand lithofacies permeability was not represented in log scale (A.34 and A.35) as the other permeability plots because the trend in the data distribution could not be captured in log scale. This could be because the minimum and maximum permeability values of the Upper sand fall within the same log cycle.

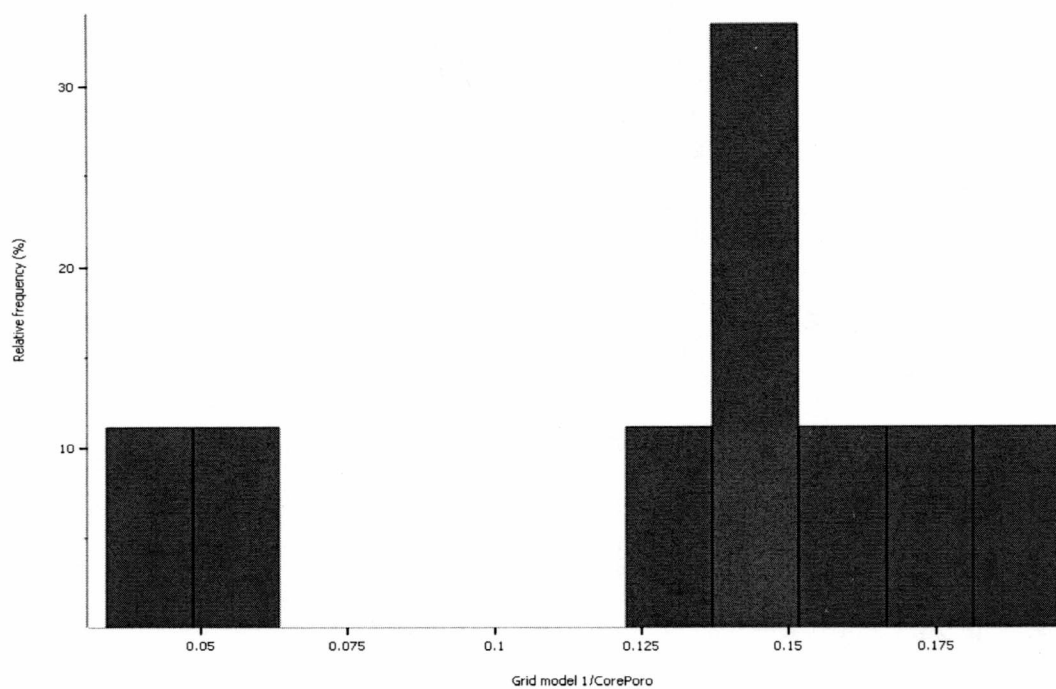


Figure 49: Histogram showing the porosity input data of shale in the Chandler sand

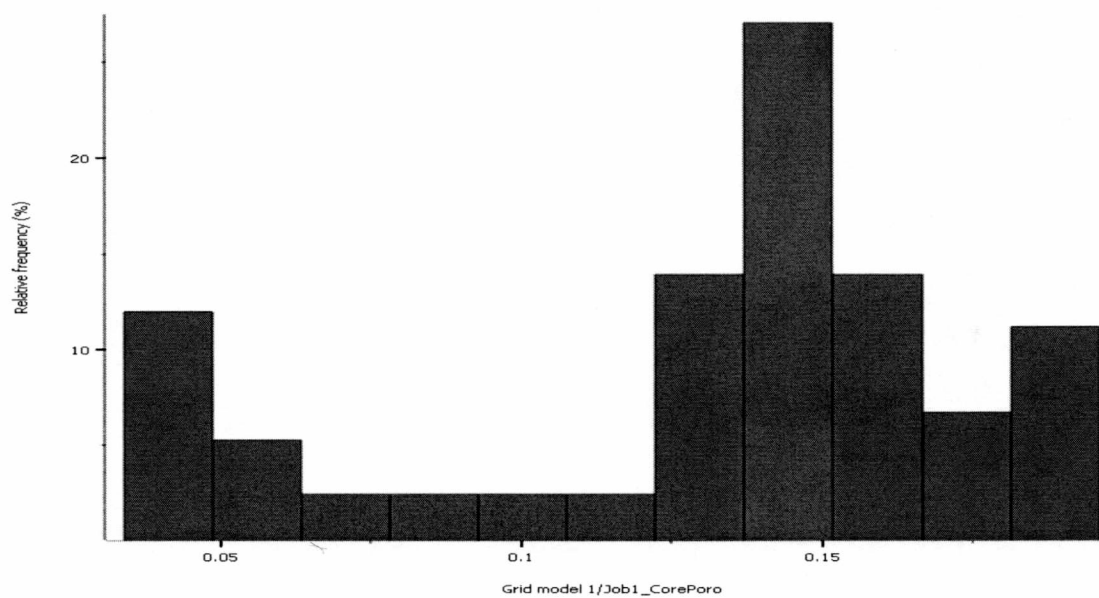


Figure 50: Histogram showing the porosity output data of shale in the Chandler sand

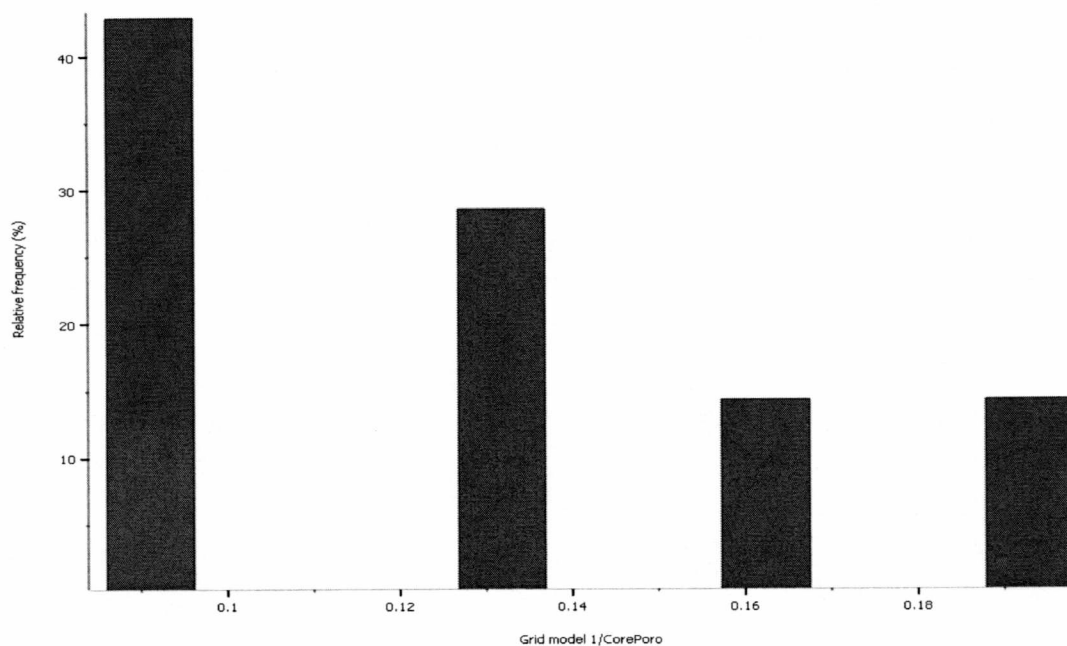


Figure 51: Histogram showing the porosity input data of sand in the Chandler sand

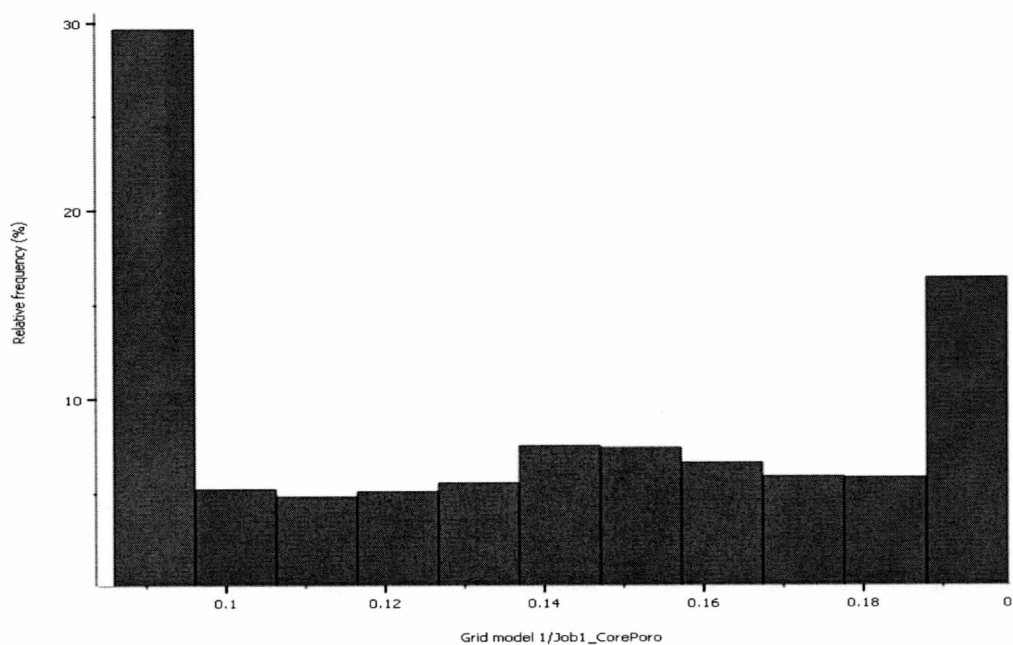


Figure 52: Histogram showing the porosity output data of sand in the Chandler sand

Table 13: Zone by zone summary results of the porosity modeling job

ZONE	FACIES	STATISTICS	INPUT DATA(POROSITY)	OUTPUT DATA(POROSITY)	
CHANDLER	SHALE	Mean	0.13	0.13	
		Median	0.14	0.14	
		Standard deviation	0.05	0.05	
		Skewness	-0.66	-0.77	
		Minimum value	0.03	0.03	
		Maximum value	0.20	0.20	
		No of Observations	9.00	119688.00	
		SAND	Mean	0.13	0.14
			Median	0.13	0.14
			Standard deviation	0.04	0.04
Skewness	0.41		0.16		
Minimum value	0.09		0.09		
Maximum value	0.20		0.20		
		No of Observations	7.00	59877.00	
UPPER SAND	SHALE	Mean	0.11	0.11	
		Median	0.11	0.10	
		Standard deviation	0.04	0.04	
		Skewness	0.23	0.23	
		Minimum value	0.03	0.03	
		Maximum value	0.19	0.19	
		No of Observations	27.00	36600.00	
		SAND	Mean	0.13	0.13
	Median		0.15	0.14	
	Standard deviation		0.04	0.03	
	Skewness		-0.40	-0.54	
	Minimum value		0.08	0.08	
	Maximum value		0.17	0.17	
			No of Observations	6.00	49282.00
SHALE BARRIER	SHALE	Mean	0.15	0.16	
		Median	0.13	0.16	
		Standard deviation	0.04	0.03	
		Skewness	0.38	0.00	
		Minimum value	0.13	0.13	
		Maximum value	0.19	0.19	
		No of Observations	3.00	79393.00	
		SAND	Mean	0.12	0.11
	Median		0.14	0.11	
	Standard deviation		0.04	0.02	
	Skewness		-0.38	0.01	
	Minimum value		0.08	0.08	
	Maximum value		0.14	0.14	
			No of Observations	3.00	14254.00
LOWER SAND	SHALE	Mean	0.13	0.13	
		Median	0.12	0.12	
		Standard deviation	0.04	0.35	
		Skewness	0.43	0.34	
		Minimum value	0.06	0.06	
		Maximum value	0.22	0.22	
		No of Observations	53.00	110193.00	
		SAND	Mean	0.13	0.13
	Median		0.14	0.14	
	Standard deviation		0.05	0.05	
	Skewness		-0.98	-1.14	
	Minimum value		0.01	0.01	
	Maximum value		0.19	0.19	
			No of Observations	12.00	155047.00

Table 14: Zone by zone summary results of the permeability modeling job

ZONE	FACIES	STATISTICS	INPUT DATA(PERMEABILITY md)	OUTPUT DATA(PERMEABILITY md)
CHANDLER	SHALE	Mean	59.43	59.62
		Median	102.00	56.72
		Standard deviation	63.26	51.03
		Skewness	0.04	0.06
		Minimum value	0.70	0.70
		Maximum value	125.00	125.00
		No of Observations	4.00	119688.00
	SAND	Mean	98.07	137.04
		Median	16.00	19.60
		Standard deviation	201.46	193.75
		Skewness	1.55	1.28
		Minimum value	2.00	2.00
		Maximum value	550.00	550.00
		No of Observations	7.00	59877.00
UPPER SAND	SHALE	Mean	63.60	80.70
		Median	44.00	51.90
		Standard deviation	96.69	99.24
		Skewness	3.06	2.53
		Minimum value	0.10	0.10
		Maximum value	480.00	480.00
		No of Observations	26.00	36538.00
	SAND	Mean	45.75	47.42
		Median	57.00	45.68
		Standard deviation	28.81	23.53
		Skewness	0.18	0.15
		Minimum value	18.00	18.00
		Maximum value	81.00	81.00
		No of Observations	4.00	49282.00
	SHALE BARRIER	Mean	84.87	122.44
		Median	9.80	122.86
		Standard deviation	130.02	90.88
		Skewness	0.38	0.00
		Minimum value	9.80	9.80
		Maximum value	235.00	235.00
		No of Observations	3.00	79143.00
	SAND	Mean	180.07	130.11
		Median	270.00	124.49
		Standard deviation	155.77	108.33
		Skewness	-0.38	0.07
		Minimum value	0.20	0.20
		Maximum value	270.00	270.00
		No of Observations	3.00	14489.00
LOWER SAND	SHALE	Mean	45.52	48.89
		Median	9.80	7.92
		Standard deviation	73.39	82.21
		Skewness	2.81	2.58
		Minimum value	0.10	0.10
		Maximum value	400.00	400.00
		No of Observations	49.00	110193.00
	SAND	Mean	130.98	154.88
		Median	56.00	96.32
		Standard deviation	160.36	144.69
		Skewness	0.70	0.49
		Minimum value	4.20	4.20
		Maximum value	400.00	400.00
		No of Observations	11.00	155047.00

From figure 53, it can be inferred that the lithofacies distribution influences the porosity values with the highly porous areas corresponding with high porosity values as

observed in the blocked wells. This further confirms the accuracy of the indicator modeling job.

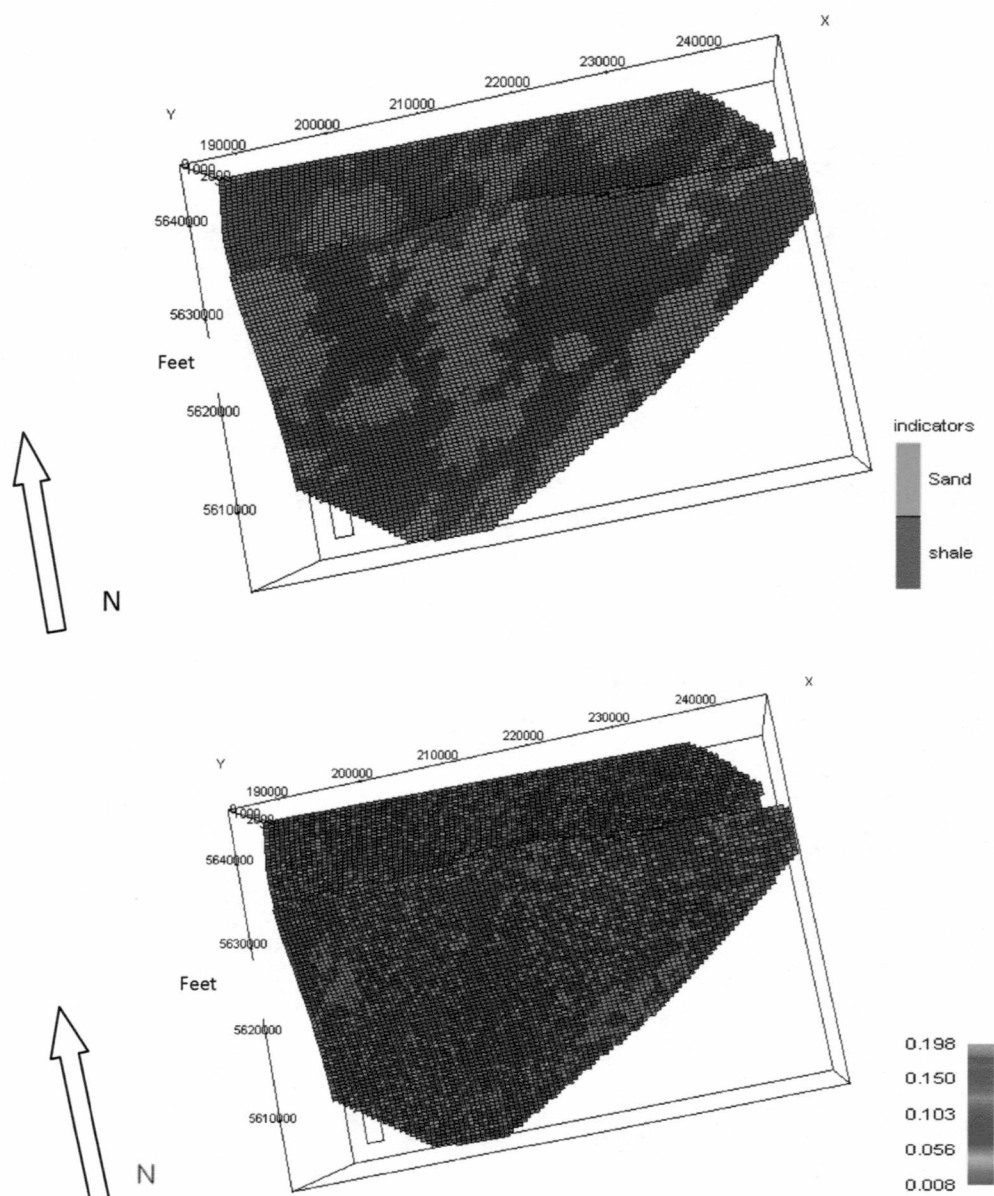


Figure 53: Comparison of the indicator and porosity models of the Chandler sand.

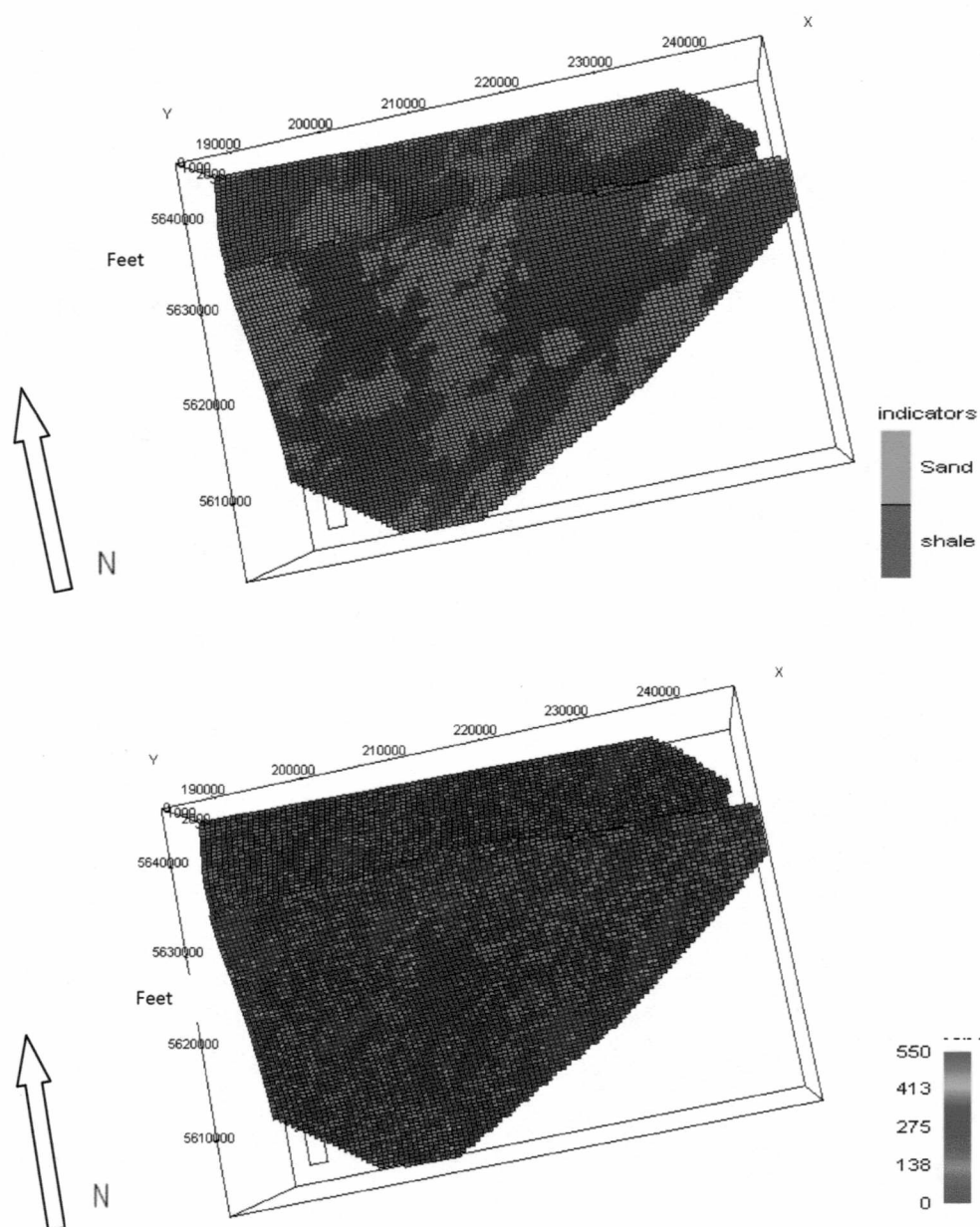


Figure 54: Comparison of indicator and permeability models of the Chandler sand

The lithofacies distribution influences the permeability values as desired. As observed, the high permeability zones in the permeability model correspond to the areas in the

indicator model with sand (Figure 54). This further confirms the accuracy of the indicator job. The porosity and permeability input data were truncated in the data transformation application so that only the data within the upper and lower limits were used in the population of the grid cells in the interwell areas.

Figures 49 and 50 show the results of the comparison in the Chandler sand the results for the other zones are shown in the appendices (A.44-A.49).

Cross checking the job confirmed that the lithofacies distribution influences the porosity and permeability distribution as desired. There is also a good match between the input data and output results in the petrophysical property modeling job.

CHAPTER 6

VOLUMETRIC CALCULATION

6.1 ESTIMATION OF STOCK TANK OIL INITIALLY IN PLACE AND ASSOCIATED GAS

Oil originally in place is the total amount of hydrocarbon in the reservoir before production and it comprises both producible and non producible oil.

6.11 PREVIOUS ESTIMATES

Molenaar (1982) estimates the OOIP in Umiat at 70 million barrels. However Espach (1951) estimates the OOIP in Umiat at 122 million barrels with an uncertain volume of gas. It is not clear from the authors the assumptions behind these estimates; however one can argue that these uncertainties can be attributable to the available technology and data at the time these estimates were made. Recent estimates show that Umiat could have an OOIP of more than 1 billion stock tank barrels (Watt et al. 2010). The assumed parameters for this estimate are listed in Table 15.

Table 15: Assumptions for OOIP estimate after Watt et al. (2010)

Parameter	Value
Productive area (acres)	7500 feet
Average porosity	14%
Average permeability	55 md
Water saturation	41%
GOR	71scf/stb

6.12 ESTIMATES FROM THIS STUDY

The Umiat grid model developed in chapter five was used to calculate the OOIP. It involved calculating the following volumes: the bulk volume (total volume of sand and shale), net volume (volume of sand), pore volume and hydrocarbon pore volume. The model was also used to calculate the area and average thickness of the zones in order to verify their consistency in feet with that from the extracted horizons. Some of the input data such as the oil water contact and water saturation were constant for all the modeled zones. The porosity input values were parameters obtained from the petrophysical job. This means that each grid block has its porosity value which was not constant across the model. The use of the parameters provided a more accurate result since the lateral and vertical variations in the field were preserved in the volumetric calculation. The calculations were done for both lithofacies (sand and shale) but only the sand lithofacies reported producible volumes since they represent the net pay zones in Umiat field.

Net pay represents a geological area of reservoir quality which contain hydrocarbon and are thus considered productive. Although net pay is a fundamental requirement in the calculation of volumes, there is no defined guideline on its computational methods, strengths and weaknesses (Caldwell and Heather 2001). Therefore defining the net pay is dependent on what one considers to be reservoir quality in a certain geological area.

Net to gross is a generic term that refers to the ratio of the reservoir quality thickness of a zone to the total thickness of that same zone in a reservoir. The net thickness in this model represents the sand thickness while the gross thickness or bulk thickness represents the total thickness of both the sand and shale lithofacies.

Since the Grandstand sands exhibit shaliness, it is imperative to introduce cut offs which help to define the net thickness of the reservoir. In this work all the sand lithofacies are to be assumed of reservoir quality. This is quite optimistic because the reservoir at Umiat is frozen and permeability could be significantly reduced due to the freezing and blocking of the pores which will in turn reduce productivity. However it is sufficient to make this assumption of eliminating shale lithofacies at this stage of study due to the limited data available since this will save run time and will not affect the overall accuracy of results.

The region index parameters represent the fault segments in the model. The thrust faults in the fault model divide this reservoir into three fault blocks. The block representing the downthrown portion of the model had no reported hydrocarbon volume based on the reported hydrocarbon pore volume of this model (Figure 55).

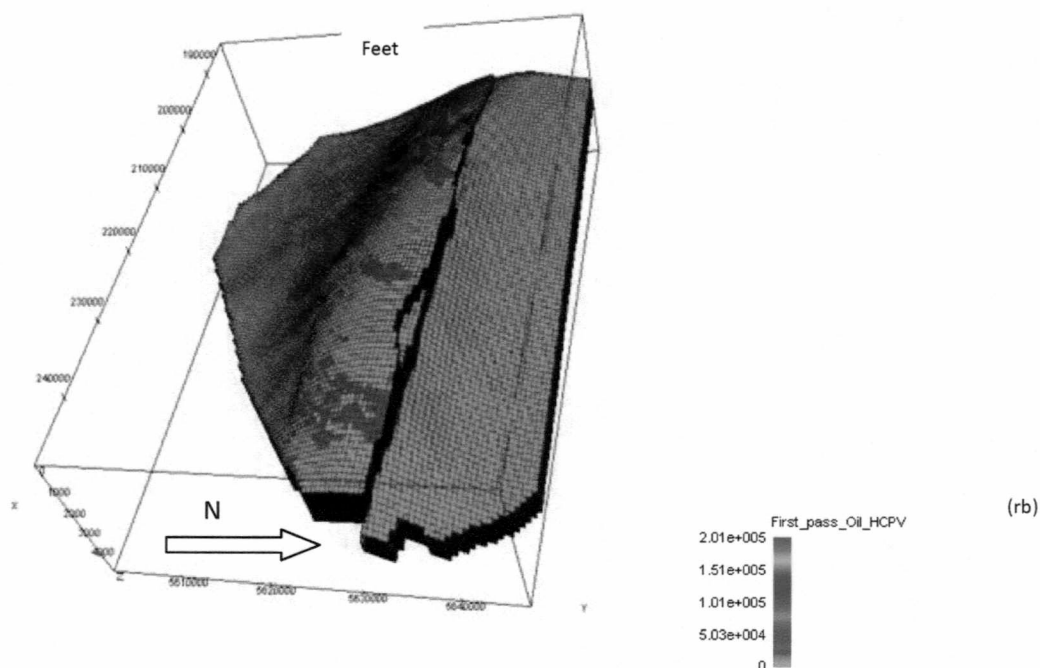


Figure 55: Umiat model showing the 3 fault blocks and their hydrocarbon pore volume
The formulae below were used to calculate the OOIP and the associated gas in Umiat field and Table 16 summarizes the input parameters.

$$\text{Stock tank original oil in place (STOOIP)} = \frac{\text{Net volume} * \text{porosity} * (1 - S_w)}{B_o} \text{ (stb)}$$

$$\text{Associated gas} = \text{STOOIP} * (\text{GOR}) \text{ (scf)}$$

Table 16: Input parameters for volumetric calculation

Parameter	Value
Porosity	Estimated from 3D porosity job
Water Saturation	41% (third party report for Renaissance Alaska)
Oil water contact	782 feet (third party report for Renaissance Alaska)
GOR	71 scf/stb (Baptist 1960)

Formation volume factor as reported by a third party for Renaissance Alaska is 1.015 rb/stb for the Upper sand and 1.01 rb/stb for the Lower sand. Since there was no

reported value for the Formation volume factor (B_o) in the Chandler Sand, the same 1.015 rb/stb value for the Upper sand was assumed.

The estimated recovery factors are 25 percent for the Upper sand and 45 percent for the Lower sand as reported for Renaissance Alaska. The assumptions for the recovery factors are:

- 1) Gas injection is the recovery mechanism.
- 2) There is an 80 acre spacing between the injection and producing well.
- 3) The injection pressure is 100 psi over the initial reservoir pressure.
- 4) The average permeability for the Upper sand is 70 millidarcies while that for the sand is 40 millidarcies.

These recovery factors were chosen because the third party report indicates that there is a three times increase in oil production while using gas injection over solution gas drive recovery mechanism.

6.2 RESULTS

Table 17 shows the summary of the hydrocarbon pore volume in all the modeled zones. The total hydrocarbon pore volume for all the modeled horizons in the Umiat area (the Chandler, the Upper sand, the Shale barrier and the Lower sand) is 1.4 billion barrels. However the volume of oil and associated gas in the Shale barrier is reported as 222 million stock tank barrels and 16 billion standard cubic feet respectively. Oil in this

zone is not expected to be producible because it might not be economical to produce from the isolated sand bodies within the Shale barrier. In addition the modeling of the Shale barrier was based on a few data points therefore much is not known about this zone. The available porosity and permeability values of the sand bodies within the Shale barrier is 2 percent -14.3 percent and 0.2-270 millidarcies respectively. These values from about 5 observations were used to populate the entire sand lithofacies within the Shale barrier and are most likely the reason for the high hydrocarbon pore volume reported in this zone. The Shale barrier volumes were therefore not included in the total volumes.

Using the Formation volume factor as reported for Renaissance Alaska by a third party: 1.015 rb/stb for the Chandler sand and Upper sand, 1.01 rb/stb for the Lower sand. The total stock tank oil in place of Umiat field was calculated. The stock tank oil in place excluding the Shale barrier is estimated to be 1.2 billion stock tank barrels and the associated gas is 84 billion standard cubic feet. This result is close to recent estimates by Watt et al. (2010). The discrepancies between this estimate and earlier estimates could be as a result of the various procedures used. It is not clear what method previous authors used for their calculation. However the calculation in this study took into account the heterogeneities present in this field. The OOIP estimate from this study improves upon previous studies because it was obtained from a model. The model is most representative of the reservoir as it captured the heterogeneities within the various zones in the reservoir. The porosity values used for the hydrocarbon calculation were obtained from the petrophysical model of the reservoir thus giving a more accurate

result than assuming a single porosity value. Previous estimates possibly were made assuming a single porosity value. The uncertainties in this calculation include the fact that most of the data used is about 50 years old and there is no known analog of Umiat field. Furthermore there are some uncertainties in the oil recovery factors. The OOIP estimate will only be more accurate when more information is obtained by further exploration of this field.

Table 17: Summary of volumetric results

ZONE	BULK (mmbbl)	NET (mmbbl)	PORE (mmbbl)	HCPV (mmbbl)	AREA (10 ⁶ ft ²)	THICKNESS (ft)	STOIIP (mmstb)	ASSOCIATED GAS
Chandler	23485.50	695235.00	965.15	569.44	1020.00	258.02	561	40mmmscf
Upper Grandstand	7776.80	403292.00	401.93	237.14	842.00	103.67	234	17mmmscf
Shale barrier	19270.90	3339.38	375.83	221.74	694.00	289.35		
Lower Grandstand	11430.00	4914.69	648.48	382.61	533.00	241.21	379	27mmmscf
Totals	61963.20	19239.33	2391.39	1410.92	3089.00	892.24	1174	84mmmscf

CHAPTER 7

RESULTS AND DISCUSSION

7.1 STATISTICAL ANALYSES

The quality of the Umiat reservoir based on petrophysical data is reasonably good. Overall the porosity of the Grandstand sands is good but the permeability is widely variable. In the study of the petrographic characteristics of the sandstones in Umiat#1 by Collins (1958), permeability values less than 2.55 millidarcies are considered poor while values above 62 millidarcies are considered very good. 37.30 percent of the Upper sand and 14.52 percent of the Lower sand have permeabilities less than 2.55 millidarcies which represents a poor quality reservoir. 20 percent of the Upper sand and 37 percent of the Lower sand has permeabilities greater than 62 millidarcies and therefore considered to have good reservoir quality. 5 percent is a porosity cut off usually used in oil reservoirs (Abdus et al. 2007). 99 percent of the Upper sand and 100 percent of the Lower sand have probabilities of having effective porosity of more than 5 percent.

From the cross plots, the R squared value for the combined plot of the Upper and Lower sands combined is 0.55, the R squared value for the Upper sand is 0.25 and the value for the Lower sand is 0.31. The scatter/cross plots indicate a weak relationship between the porosity and permeability as the R squared values are not close to the value one.

Box plots and histograms were used to analyze the distribution of data. Most of the wells had the same porosity range, but the permeability values exhibited a wider variability, especially within the Lower sand. The combined porosity histogram of the Upper and Lower sands indicates that there might be more than one population hence the decision to split the two sands. In the box plots, Umiat #3, #2 and #11 porosity and permeability show a remarkable resemblance in the Upper sand while Umiat #1, #2, #11 and #9 porosity and permeability look strikingly similar in the Lower sand. Most of the wells have a similar range of porosity values. However there is a considerable variability in the range of permeability between wells. This further validates the complexity in permeability values across the Umiat anticline.

The modified Lorenz plots of Umiat # 9 indicate that there is a difference in the flow structure in the Upper and Lower sands. The Upper sand exhibited a good flow at the top, but had a significant flow barrier with depth. The most significant flow unit in the Upper sand is between 466.5-473.5 feet. The Lower sand exhibited more complexity in Umiat#9 with several flow units exhibiting differing flow capacities. The most significant flow unit lies between 875-909 feet. There are 2 observed flow barriers within the drilled interval which could be attributed to more lithologic heterogeneity in the Lower sand. These flow barriers will act to inhibit vertical permeability.

The T-test using Umiat #9 as the parent population and the other wells indicated that for the most part, the sands are fairly consistent across the field. This is with the exception of Umiat #11 and Umiat #3 for the Upper sand and Umiat #1 for the Lower

sand. Their porosity values should therefore be treated differently from those of Umiat #9. Based on the T-test results the Upper and Lower sands were treated differently in the petrophysical model.

7.2 PETROPHYSICAL PROPERTY MODELING

A petrophysical property model of Umiat field was built based on the published geologic knowledge of the field, the horizon and fault data provided by private industry, core based porosity and permeability data and lithologs. The unavailability of gamma ray logs made it necessary to create a lithofacies log using the available lithology description. A generated internal programming language (IPL) script was used to load the available porosity and permeability values from the cored intervals into the blocked wells in the model. The statistical characteristics of the observed core porosities and permeabilities were retained in the model. In the final model, relative percentage of sand versus shale had a great influence on the porosity and permeability distribution in the field.

Volumetric calculations were made from the built model. The sand lithofacies is considered the net pay since no producible hydrocarbon volume was reported from the shale zones. The estimated stock tank oil in place is about 1.2 billion stock tank barrels and the associated gas is 84 billion standard cubic feet. The GOR is exceedingly low for a reservoir that is supposed to be produced by solution gas drive mechanism. This means that injection gas from a separate source will be required in the early life of the reservoir to enhance production from this reservoir. Using a recovery factor of 25

percent for the Upper sand and 45 percent for the Lower sand the total oil recoverable from the Grandstand sands is an estimated 232 million stock tank barrels. These recovery factors were chosen because the third party report indicates that there is a three times increase in oil production while using gas injection over solution gas drive recovery mechanism.

7.3 UNCERTAINTIES IN THE PETROPHYSICAL PROPERTY MODELING AND OOIP CALCULATION

The average 300 feet thickness assumed for the Shale barrier has some level of uncertainty because some areas will have thickness above or below this value.

The Formation volume factor, the GOR and recovery factors were obtained from third party sources therefore there was no control over the reliability of these values. Umiat field has a low GOR and solution gas drive might be limited. This means that the reservoir will require a pressure maintenance system to enhance productivity of the wells.

This model suggests that the Shale barrier could be a major contributor to the hydrocarbon volume of this field because the sand bodies within this zone have very good reservoir qualities. However they are isolated by shale and may not be producible. The Chandler sand is also a key contributor to the hydrocarbon volume in Umiat field largely because of its thickness and good reservoir qualities. This might however not be the case when more reservoir properties data become available.

CHAPTER 8

CONCLUSION AND RECOMMENDATIONS

8.1 CONCLUSION

Umiat field is a very unique field and success in its development will not only increase production from this field but will also provide vital information for the exploration of other fields in the arctic region that might share similar characteristics with Umiat field; due to its occurrence in permafrost.

The primary goal of this research was to build a reservoir petrophysical property model of Umiat field detailing porosity and permeability distribution as well as lithofacies distribution. This model was used to estimate the oil initially in place as well as the associated gas in Umiat field. The statistical analyses of the Upper and Lower sands served as a good foundation for building this model.

From this research it can be concluded that the Grandstand sands have a wide variation in permeability values. This is probably as a result of its depositional environment. No work was done in defining its structural complexity in this research. However, the literature suggests that this could also be an influential factor.

Based on the T test results, the Upper and Lower sands have to be treated differently as they change petrophysically across Umiat field.

The modified Lorenz plots illustrate that the Lower sand exhibits more heterogeneity lithologically in Umiat #9 than the Upper sand. The identification of the flow barriers and flow units within the Grandstand sands in Umiat #9 helped identify the vertical distribution of heterogeneities. Information from the modified Lorenz plots is speculated to enhance sweep patterns and recovery efficiency if augmented with more geologic knowledge and reservoir properties data.

Building the petrophysical property model was a challenging task. There were many intervals and wells without porosity and permeability values. Core data was used to populate the grids and the lithologic description used to generate the lithofacies log was obtained from well cuttings thereby reducing the level of confidence which with the grid cells were populated. The lack of verifiable GOR and recovery factors reduced the level of accuracy of the volumetric calculation.

Based on the available data at the time this model was built it is considered to be a good representation of Umiat field. This model will form a good base model for future models and can be augmented with additional information as it becomes available. The volumetric results are close to estimations in recent studies and can further be verified for accuracy by analytical methods such as decline curve analysis and material balance equations when production data becomes available.

Since the model is a static model, not much can be said with regards to the implications of the proposed drilling and production methods. This can be tested by using a simulation model to evaluate production assuming various scenarios

9.2 RECOMMENDATIONS

Umiat lies within a thrust faulted zone and it is obvious that faults and fractures play a major role in the compartmentalization of this reservoir. More accurate and up to date information on the distribution of structures in the Umiat area from outcrop studies will aid in building a more robust model.

Most of the data used for this work are old and are not compatible with modern software technologies. The availability of recent well logs will enhance accuracy in porosity and permeability estimations, through log interpretation and will in turn improve the evaluation of this reservoir.

Multiple realizations of this model should be run to determine the best model most representative of the Umiat reservoir.

This model should be upscaled into a simulation model in order to test various production strategies for Umiat field.

REFERENCES

Ahlbrandt, T. S. (1979). "Preliminary geologic, petrologic and paleontologic results of the study of Nanushuk Group rocks, North Slope, Alaska." U.S. Geological Survey Circular 794 163 p.

Baptist, O.C. (1960). "Oil Recovery and Sands Damage in Permafrost, Umiat Field, Alaska". U.S. Dept. of the Interior, Bureau of Mines.

Baptist, O. C. (1959). "Oil Production from Frozen Reservoir Rocks, Umiat Alaska". Fifth Annual Joint Meeting of the Rocky Mountain Petroleum sections. Casper Wyoming. Vol 216.

Broman, Jr., Schmohr W.H., Schnorr, D.R. (1992). "Horizontal Well Operations at Prudhoe Bay". International Meeting on Petroleum Engineering, 24-27 March 1992 Beijing China. SPE 22383-MS.

Brosge, W. P. (1966). "Geology of Umiat Maybe Creek Region Alaska." U.S. Geological Survey Vol 638.

Caldwell, R. L. and Heather, D. I. (2001). "Characterizing uncertainty in oil and gas evaluations". Society of Petroleum Engineers. Richardson Texas. SPE 68592.

Cole, F.E., Bird, K.J., Toro, J., Roure, F., Howell, D.G. (1995) "Kinematic subsidence modelling of the North-central Brooks Range and North Slope Alaska" U.S. Geological Survey Open-file report.

Collins, F. R. (1958). "Test wells, Umiat Area, Alaska". Geological survey professional paper, U.S. department of the Navy, Office of Naval Petroleum and Oil Shale Reserves. Vol 305 B.

Cosentino, L. (2001) "Integrated reservoir studies" Editions Technip.

Espach, R. H. (1951). "Recoverable petroleum reserves in the Umiat structure, Naval Petroleum Reserve No.4, Alaska." U.S. Bureau of Mines Petroleum and Natural Gas Branch Open-file report.

Fox, J. E., Lambert, P. W., Pitman, J.K., Wu, C.H. (1979). "A Study of Reservoir Characteristics of the Nanushuk and Colville Groups, Umiat Test Well 11 National Petroleum Reserve in Alaska." Geological Survey Circular 820.

Gates, G. L. and Caraway W. H. (1960). "Well Productivity related to Drilling muds National Petroleum Reserve No 4 Alaska". U.S Department of the Interior, Bureau of Mines.

Gunter, G. W., Finneran, J. M., Hartmann, D.J., and Miller, J.D. (1997). "Early determination of Reservoir flow units using an integrated petrophysical method". Society of Petroleum Engineers Annual Technical conference and Exhibition San Antonio Texas.

Houseknecht, D. W. and Schenk, C. J. (2004). "Sedimentology and Sequence Stratigraphy of the Cretaceous Nanushuk, Seabee and Tuluva Formation Exposed on Umiat mountain, North-Central Alaska". Studies by the U.S. Geological Survey in Alaska, U.S.G.S. Professional Paper 1709-B.

Kornbrath, R. C., Myers, M. D., Krouskop, D. L., Meyer, J. F., Houle, J. A., and Ryherd, T.J., Richter, K. N. (1997). "Petroleum potential of the eastern National Petroleum Reserve Alaska".

Krajewski, S. A. and Gibbs, B. L. (2001). "Understanding Contouring: A practical guide to spatial estimation using a computer and Variogram Interpretation."

Kumar, N., Nelson, P. H., Bird, K.J., Grow J.A., and Evans, K.R., (2002). "A Digital Atlas of Hydrocarbon Accumulations Within and Adjacent to the National Petroleum Reserve Alaska (NPRA)". U.S.G.S. Open-File Report 02-71.

Magoon, L.B. III (1994). "Petroleum resources in Alaska in G.Plaker and H.C. Berg, eds., The Geology of Alaska" Geological Society of America, The Geology of North America, vol. G-1, p. 905-936.

Molenaar, C. M. (1982). "Umiat field, an oil accumulation in a thrust-faulted anticline, North Slope of Alaska, in Powers, R.B., ed., Geologic studies of the Cordilleran thrust belt, Rocky Mountain Association of Geologists". p.537-548.

Mull, C. G., Houseknecht, D. W. et al. (2003). "Revised Cretaceous and Tertiary stratigraphic nomenclature in the Colville Basin, Northern Alaska". U.S. Geological Survey Professional Paper Report: P 1673.

Panda, M. and Morahan, G. T. (2008). "An Integrated Reservoir Model description for East Barrow and Walakpa Gas fields, Alaska (Topical report)". Petrotechnical Resources of Alaska LLC.

Potter, C. J. and Moore, T. E. (2003). "Brookian structural plays in the National Petroleum Reserve, Alaska". U.S.G.S. Open-File Report 03-266.

Robinson, B., Kenny, J., Hernandez-Hdez I.L., Bernal, A., and Chelak, R. (2005). "Geostatistical modeling integral to effective design and evaluation of SAGD processes of an Athabasca oil sands reservoir, a case study". Society of Petroleum Engineers International thermal operations and heavy oil symposium. Calgary Alberta, Canada. PS/CIM/CHOA 97743 PS2005-SSS.

Roxar (1994-2008). "RMS 2009 User Guide."

Satter, A., Iqbal, G. M., Buchwalter, J.L. (2007). "Practical enhanced reservoir Engineering: assisted with simulation software" Pennwell books.

Watt, J., Huckabay, A., and Landt, M.R. (2010). "Umiat: a North slope giant primed for oil development". Oil and Gas Journal (Jan 11 2010).

Worthington, P. F. and Cosentino, L. (2005). "The Role of cutoffs in integrated reservoir studies". Society of Petroleum Engineers Annual Technical Conference and Exhibition Denver. SPE 84387.

<http://www.netmba.com> (2002-2007).

APPENDIX A

A.1: Upper sand core data. Modified from Collins (1958)

Umiat Core Analysis		Upper sand		
	Depth	Effec. Porosity	Air Permeability	Interval/Sand
	ft	%	md	
Well #1	1339	9.3	1.2	Main Sd/Upper GS
	1368	11.6	27.8	Main Sd/Upper GS
	1372	9.5	1	Main Sd/Upper GS
	1374	10.2	6.5	Main Sd/Upper GS
	1379	14.4	1	Main Sd/Upper GS
	2311	15.7	3.8	UGS -Faulted Section
	2321	16.3	11	UGS -Faulted Section
	2322	19.6	25.2	UGS -Faulted Section
	2330	14.3	0.5	UGS -Faulted Section
	2335	16	5	UGS -Faulted Section
	2340	14.5	1.8	UGS -Faulted Section
Well # 2	392	18.4	78	Main Sd
	491	15.7	42	Main Sd
	493	15.8	36.4	Main Sd
	498	14.3	270	Main Sd
	517	8.6	5.85	Main Sd
	528	12.6	9.8	Main Sd
	257	16.5	165	Main Sd
	259	13.6	47	Main Sd
Well # 3	261	12.4	57	Main Sd
	344	17	480	Main Sd
	350	14.7	70	Main Sd
	352	16.6	188	Main Sd
	355	16.5	80	Main Sd
	357	14.2	7.4	Main Sd
	359	13.2	11	Main Sd
	361	15.4	42	Main Sd
Well # 6	375	12.2	13	Main Sd
	376	12.4	44	Main Sd
Well # 7	838	13.8	1	Main Sd
Well # 9	466.5	19.1	150	Main Sd
	467.5	19.3	120	Main Sd
	468.5	20.4	81	Main Sd
	469.5	18.9	41	Main Sd
	470.5	18.2	43	Main Sd
	470.5	18.2	50	Main Sd
	470.5	18.6	89	Main Sd
	471.5	16.6	120	Main Sd
	472.5	13.4	27	Main Sd
	473.5	18.1	56	Main Sd
	474.5	14.7	20	Main Sd
	475.5	13.3	40	Main Sd
	475.5	13.5	45	Main Sd
	475.5	13.9	29	Main Sd
	476.5	15.6	21	Main Sd
	477.5	12.4	5.1	Main Sd
	478.5	12.5	3.7	Main Sd
	479.5	13.8	5	Main Sd
	480.5	11	0.3	Main Sd
	481.5	10.4	0.4	Main Sd
	482.5	13.9	1	Main Sd
	483.5	11.5	0.9	Main Sd
	484.5	7.54	0.1	Main Sd
	485.5	7.8	0.2	Main Sd
	486.5	9.2	1.4	Main Sd
	492.5	7.6	0.2	Main Sd
	493.5	9.1	0.4	Main Sd
	494.5	9.1	0.23	Main Sd
	495.5	9.5	0.3	Main Sd
	495.5	8.7	0.3	Main Sd
	495.5	8.4	0.2	Main Sd
	496.5	9.2	0.5	Main Sd
	497.5	10.1	0.1	Main Sd
	498.5	9.3	0.1	Main Sd
	499.5	8.6	0.1	Main Sd
	500.5	10.1	0.1	Main Sd
	501.5	8.3	0.1	Main Sd
	504.5	6.7	0.1	Main Sd
	507.5	5	0.1	Main Sd
	582.5	8.2	0.2	Main Sd
Well # 11	2445	17.6	120	Main Sd
	2450	16.5	81	Main Sd
	2453	14.8	18	Main Sd
	2460	15	27	Main Sd
	2532	19	235	Main Sd

A.2: Lower sand core data. Modified from Collins (1958)

Umiat Core Analysis		Lower sand		
	Depth	Effec. Porosity	Air Permeability	Interval/Sand
	ft	%	md	
Well #1	1740	15.9	14.4	Lower GS
	1742	15.6	59.5	Lower GS
	1746	17.8	50	Lower GS
	1748	17.6	35	Lower GS
	1757	18.9	1.2	Lower GS
	2669	15.2	4	LGS -Faulted Section
	2690	17.9	9.5	LGS -Faulted Section
	2694	23.8	23	LGS -Faulted Section
	2698	14.7	4	LGS -Faulted Section
	796	19.3	164	Lower GS
Well #2	797	18	65	Lower GS
	802	17.7	187	Lower GS
	827	14.8	10.7	Lower GS
	833	14.7	14.9	Lower GS
	834	12.7	9.6	Lower GS
	839	12	17.9	Lower GS
	843	17.2	71.5	Lower GS
	960	11.6	4.4	Lower GS
	1011	10.9	3.5	Lower GS
	1014	13.1	4.1	Lower GS
Well #5	1016	13.8	4.2	Lower GS
	787	17.6	118	Lower GS
Well #7	1349	11.2	19.2	Lower GS
	1372	10.1	0.1	Lower GS
Well #9	866.5	13.3	25	Lower GS
	867.5	15.4	56	Lower GS
	871.5	17.8	220	Lower GS
	871.5	17.6	280	Lower GS
	871.5	17.2	260	Lower GS
	873.5	17.3	320	Lower GS
	875.5	18.5	170	Lower GS
	876.5	17.3	150	Lower GS
	880.5	18.1	190	Lower GS
	894.5	14.5	61	Lower GS
	896.5	14.8	90	Lower GS
	897.5	16.5	90	Lower GS
	900.5	16.2	140	Lower GS
	900.5	15.5	62	Lower GS
	900.5	15.8	53	Lower GS
	906	14.4	80	Lower GS
	907.5	15.1	42	Lower GS
	909	13.9	8	Lower GS
	950.5	18.8	29	Lower GS
	964.5	14.1	20	Lower GS
	965.5	15.5	97	Lower GS
	968.5	15.3	65	Lower GS
	975	11.9	5.5	Lower GS
	977	12.6	12	Lower GS
	978	12.5	9	Lower GS
	978	12.3	5	Lower GS
	978	11.8	6.4	Lower GS
	995	9.2	1.4	Lower GS
	1003	11.9	1.4	Lower GS
	1013	7.6	0.1	Lower GS
	1040.5	9.9	0.4	Lower GS
	1043.5	10.5	0.2	Lower GS
	1045.5	10.3	0.6	Lower GS
Well #11	2813	16.4	100	Lower GS
	2824	17.4	158	Lower GS
	2832	17.1	280	Lower GS
	2849	19.3	400	Lower GS
	2997	12.9	2.3	Lower GS

A.3: Upper sand modified Lorenz plot data

UPPER SAND

	Depth	Effec. Porosity	Permeability	Porosity*(H)	Permeability*(H)	Fract./(Por.)*(H)	Fract/(K)*(H)	Cumulative(Por)*(H)	Cumulative(K)*(H)
	ft	%	md					Cum storage capacity	Cum flow capacity
WELL 9									
	466.5	19.1	150	0.191	150	0.017740377	0.198457325	0.017740377	0.198457325
	467.5	19.3	120	0.193	120	0.017926141	0.15876586	0.035666518	0.357223185
	468.5	20.4	81	0.204	81	0.018947838	0.107166956	0.054614356	0.464390141
	469.5	18.9	41	0.189	41	0.017554614	0.054245002	0.07216897	0.518635143
	470.5	18.2	43	0.182	43	0.016904443	0.0568911	0.089073414	0.575526243
	470.5	18.2	50	0	0	0	0	0.089073414	0.575526243
	470.5	18.6	89	0	0	0	0	0.089073414	0.575526243
	471.5	16.6	120	0.166	120	0.015418339	0.15876586	0.104491752	0.734292103
	472.5	13.4	27	0.134	27	0.012446129	0.035722319	0.116937881	0.770014421
	473.5	18.1	56	0.181	56	0.016811562	0.074090735	0.133749443	0.844105156
	474.5	14.7	20	0.147	20	0.013653589	0.026460977	0.147403032	0.870566133
	475.5	13.3	40	0.133	40	0.012353247	0.052921953	0.159756279	0.923488086
	475.5	13.5	45	0	0	0	0	0.159756279	0.923488086
	475.5	13.9	29	0	0	0	0	0.159756279	0.923488086
	476.5	15.6	21	0.156	21	0.014489523	0.027784026	0.174245802	0.951272111
	477.5	12.4	5.1	0.124	5.1	0.011517313	0.006747549	0.185763115	0.95801966
	478.5	12.5	3.7	0.125	3.7	0.011610195	0.004895281	0.19737331	0.962914941
	479.5	13.8	5	0.138	5	0.012817655	0.006615244	0.210190964	0.969530185
	480.5	11	0.3	0.11	0.3	0.010216971	0.000396915	0.220407936	0.9699271
	481.5	10.4	0.4	0.104	0.4	0.009659682	0.00052922	0.230067618	0.970456319
	482.5	13.9	1	0.139	1	0.012910536	0.001323049	0.242978154	0.971779368
	483.5	11.5	0.9	0.115	0.9	0.010681379	0.001190744	0.253659533	0.972970112
	484.5	7.54	0.1	0.0754	0.1	0.007003269	0.000132305	0.260662803	0.973102417
	485.5	7.8	0.2	0.078	0.2	0.007244761	0.00026461	0.267907564	0.973367027
	486.5	9.2	1.4	0.092	1.4	0.008545103	0.001852268	0.276452668	0.975219295
	492.5	7.6	0.2	0.456	1.2	0.04235399	0.001587659	0.318806658	0.976806954
	493.5	9.1	0.4	0.091	0.4	0.008452222	0.00052922	0.327258879	0.977336173
	494.5	9.1	0.23	0.091	0.23	0.008452222	0.000304301	0.335711101	0.977640475
	495.5	9.5	0.3	0.095	0.3	0.008823748	0.000396915	0.344534849	0.978037389
	495.5	8.7	0.3	0	0	0	0	0.344534849	0.978037389
	495.5	8.4	0.2	0	0	0	0	0.344534849	0.978037389
	496.5	9.2	0.5	0.092	0.5	0.008545103	0.000661524	0.353079952	0.978698914
	497.5	10.1	0.1	0.101	0.1	0.009381037	0.000132305	0.36246099	0.978831219
	498.5	9.3	0.1	0.093	0.1	0.008637985	0.000132305	0.371098975	0.978963523
	499.5	8.6	0.1	0.086	0.1	0.007987814	0.000132305	0.379086789	0.979095828
	500.5	10.1	0.1	0.101	0.1	0.009381037	0.000132305	0.388467826	0.979228133
	501.5	8.3	0.1	0.083	0.1	0.007709169	0.000132305	0.396176995	0.979360438
	504.5	6.7	0.1	0.201	0.3	0.018669193	0.000396915	0.414846188	0.979757353
	507.5	5	0.1	0.15	0.3	0.013932234	0.000396915	0.428778422	0.980154267
	582.5	8.2	0.2	6.15	15	0.571221578	0.019845733	1	1
				10.7664	755.83	1	1		

A.4: Lower sand modified Lorenz plot data

LOWER SAND									
	Depth	Effec. Porosity	Permeability	Porosity*(H)	Permeability*(H)	Fract./(Por.)*(H)	Fract./(K)*(H)	Cumulative(Por)*(H)	Cumulative(K)*(H)
	ft	%	md					Cum storage capacity	Cum flow capacity
WELL 9									
	866.5	13.3	25	0.133	25	0.005346519	0.003674822	0.005346519	0.003674822
	867.5	15.4	56	0.154	56	0.006190706	0.008231602	0.011537225	0.011906424
	871.5	17.8	220	0.712	880	0.028621965	0.129353746	0.04015919	0.14126017
	871.5	17.6	280	0	0	0	0	0.04015919	0.14126017
	871.5	17.2	260	0	0	0	0	0.04015919	0.14126017
	873.5	17.3	320	0.346	640	0.013908989	0.094075451	0.054068178	0.235335622
	875.5	18.5	170	0.37	340	0.014873774	0.049977584	0.068941952	0.285313205
	876.5	17.3	150	0.173	150	0.006954494	0.022048934	0.075896446	0.307362139
	880.5	18.1	190	0.724	760	0.029104358	0.111714599	0.105000804	0.419076738
	894.5	14.5	61	2.03	854	0.08160476	0.125531931	0.186605564	0.544608668
	896.5	14.8	90	0.296	180	0.011899019	0.026458721	0.198504583	0.571067389
	897.5	16.5	90	0.165	90	0.006632899	0.01322936	0.205137482	0.584296749
	900.5	16.2	140	0.486	420	0.019536903	0.061737015	0.224674385	0.646033764
	900.5	15.5	62	0	0	0	0	0.224674385	0.646033764
	900.5	15.8	53	0	0	0	0	0.224674385	0.646033764
	906	14.4	80	0.792	440	0.031837916	0.064676873	0.256512301	0.710710637
	907.5	15.1	42	0.2265	63	0.009105162	0.009260552	0.265617463	0.719971189
	909	13.9	8	0.2085	12	0.008381573	0.001763915	0.273999035	0.721735104
	950.5	18.8	29	7.802	1203.5	0.313635633	0.176905947	0.587634668	0.898641051
	964.5	14.1	20	1.974	280	0.079353594	0.04115801	0.666988262	0.939799061
	965.5	15.5	97	0.155	97	0.006230905	0.014258311	0.673219167	0.954057371
	968.5	15.3	65	0.459	195	0.01845152	0.028663614	0.691670687	0.982720985
	975	11.9	5.5	0.7735	35.75	0.031094227	0.005254996	0.722764914	0.987975981
	977	12.6	12	0.252	24	0.010130246	0.003527829	0.73289516	0.991503811
	978	12.5	9	0.125	9	0.005024924	0.001322936	0.737920084	0.992826747
	978	12.3	5	0	0	0	0	0.737920084	0.992826747
	978	11.8	6.4	0	0	0	0	0.737920084	0.992826747
	995	9.2	1.4	1.564	23.8	0.062871844	0.003498431	0.800791928	0.996325178
	1003	11.9	1.4	0.952	11.2	0.038269818	0.00164632	0.839061746	0.997971498
	1013	7.6	0.1	0.76	1	0.030551536	0.000146993	0.869613282	0.998118491
	1040.5	9.9	0.4	2.7225	11	0.109442836	0.001616922	0.979056118	0.999735413
	1043.5	10.5	0.2	0.315	0.6	0.012662808	8.81957E-05	0.991718926	0.999823609
	1045.5	10.3	0.6	0.206	1.2	0.008281074	0.000176391	1	1
				24.876	6803.05	1	1		

A.5: Summary of the lithologic description of Umiat #1

Umiat Well 1								
Formation	Depth	Lithology	Formation	Depth	Lithology	Formation		Depth in feet
U. Grandstand	1825-1830	sh	L. Grandstand	2445-2455	slt	L. Grandstand	Chandler	Total depth = 1783
Shale Barrier	1830-1875	sst	L. Grandstand	2455-2500	slt	L. Grandstand	shale= 53%	Chandler depth = 325
Shale Barrier	1875-1885	sh	L. Grandstand	2500-2515	sh	L. Grandstand	sandstone= 37%	U. Grandstand depth = 129
Shale Barrier	1885-1910	sst	L. Grandstand	2515-2537	sst	L. Grandstand	siltstone= 5%	Shale Barrier depth = 289
Shale Barrier	1910-1920	sh	L. Grandstand	2537-2542	sst	L. Grandstand	no sample= 5%	L. Grandstand depth= 1040
Shale Barrier	1920-1970	sst	L. Grandstand	2542-2557	sst	L. Grandstand		
Shale Barrier	1970-2020	sh	L. Grandstand	2557-2563	sst	L. Grandstand	Upper Grandstand	
Shale Barrier	2020-2030	sst	Chandler	2563-2568	sst	L. Grandstand	shale= 66%	Well 1
Shale Barrier	2030-2055	sh	Chandler	2568-2573	sst	L. Grandstand	sandstone= 34%	shale= 55%
Shale Barrier	2055-2080	sh	Chandler	2573-2578	sst	L. Grandstand	siltstone= 0%	sandstone=37%
Shale Barrier	2080-2100	sh	Chandler	2578-2585	sst	L. Grandstand	no sample= 0%	siltstone= 5%
Shale Barrier	2100-2115	sh	L. Grandstand	2585-2595	sh	L. Grandstand		no sample= 3%
Shale Barrier	2115-2125	sst	L. Grandstand	2595-2600	sst	L. Grandstand	Shale Barrier	
Shale Barrier	2125-2185	sst/sh/slt	L. Grandstand	2600-2625	sh	L. Grandstand	shale= 56%	
Shale Barrier	2185-2250	sh	L. Grandstand	2625-2635	sst	L. Grandstand	sandstone= 34%	
Shale Barrier	2250-2252	slt	L. Grandstand	2635-2660	sh	L. Grandstand	siltstone= 8%	
Shale Barrier	2252-2257	sh	L. Grandstand	2660-2670	sst	L. Grandstand	no sample= 2%	
Shale Barrier	2257-2277	no sample	L. Grandstand	2670-2680	sst	L. Grandstand		
Shale Barrier	2277-2287	sh/sst	L. Grandstand	2680-2682	no sample	L. Grandstand	Lower Grandstand	
Shale Barrier	2287-2292	sh	L. Grandstand	2682-2688	sst	L. Grandstand	shale= 43%	
Shale Barrier	2292-2297	sh	L. Grandstand	2688-2695	sst	L. Grandstand	sandstone= 46%	
Shale Barrier	2297-2302	sst	L. Grandstand	2695-2715	sst	L. Grandstand	siltstone= 7%	
Shale Barrier	2302-2307	sh/sst	L. Grandstand	2715-2718	sst	L. Grandstand	no sample= 4%	
Shale Barrier	2307-2309	sst	L. Grandstand	2718-2728	no sample	L. Grandstand		
Shale Barrier	2309-2314	sst	L. Grandstand	2728-2733	sst	L. Grandstand		
L. Grandstand	2314-2318	sst	L. Grandstand	2733-2743	sst	L. Grandstand		
L. Grandstand	2318-2327	sst	L. Grandstand	2743-2748	slt	L. Grandstand		
L. Grandstand	2327-2337	sst	L. Grandstand	2748-2758	sh	L. Grandstand		
L. Grandstand	2337-2347	sst	L. Grandstand	2758-2759	sh	L. Grandstand		
L. Grandstand	2347-2357	sst/sh	L. Grandstand	2759-2765	sh	L. Grandstand		
L. Grandstand	2357-2365	sh	L. Grandstand	2765-2775	slt	L. Grandstand		
L. Grandstand	2365-2370	sh	L. Grandstand	2775-2795	sh	L. Grandstand		
L. Grandstand	2370-2390	sh	L. Grandstand	2785-2800	no sample	L. Grandstand		
L. Grandstand	2390-2425	sh	L. Grandstand	2800-2810	sh	L. Grandstand		
L. Grandstand	2425-2430	sh	L. Grandstand	2810-2820	sst	L. Grandstand		
L. Grandstand	2430-2435	no sample	L. Grandstand	2820-2825	sst	L. Grandstand		
L. Grandstand	2435-2440	sst	L. Grandstand	2825-2833	sst/slt	L. Grandstand		
L. Grandstand	2440-2445	slt	L. Grandstand	2833-2843	sst/slt	L. Grandstand		

A.6: Summary of the lithologic description of Umiat #2

Umiat Well 2							
Formation	Depth	Lithology	Formation	Depth	Lithology	Formation	Depth in feet
U. Grandstand	523-524	no sample	Shale Barrier	824-834	sst	L. Grandstand	Chandler
U. Grandstand	524-525	sh	Shale Barrier	834-843	sst	L. Grandstand	shale= 64%
U. Grandstand	525-526	sh	Shale Barrier	843-875	sst	L. Grandstand	sandstone= 33%
U. Grandstand	526-527	sh	Shale Barrier	875-880	sst	L. Grandstand	siltstone= 3%
U. Grandstand	527-528	sh	Shale Barrier	880-885	sst	L. Grandstand	no sample= 0%
U. Grandstand	528-529	no sample	Shale Barrier	885-900	slt	L. Grandstand	
U. Grandstand	529-530	sh	Shale Barrier	900-910	sst	L. Grandstand	U. Grandstand
U. Grandstand	530-531	sh	Shale Barrier	910-938	sst	L. Grandstand	shale= 11%
U. Grandstand	531-532	sh	Shale Barrier	938-948	sst	L. Grandstand	sandstone= 75%
U. Grandstand	532-533	no sample	Shale Barrier	948-956	sst	L. Grandstand	siltstone= 0%
U. Grandstand	533-534	sst	Shale Barrier	956-966	sst	L. Grandstand	no sample= 14%
U. Grandstand	534-535	sh	Shale Barrier	966-969	sst	L. Grandstand	
U. Grandstand	535-536	sh	Shale Barrier	969-979	sst	L. Grandstand	Shale Barrier
U. Grandstand	536-537	sh	Shale Barrier	979-980	sst	L. Grandstand	shale= 88%
U. Grandstand	750-760	sh/slt	L. Grandstand	986-996	sst/sh	L. Grandstand	sandstone= 5%
U. Grandstand	760-770	no sample	L. Grandstand	996-998	sst	L. Grandstand	siltstone= 0%
U. Grandstand	770-780	sst/sh	L. Grandstand	998-1000	sst	L. Grandstand	no sample= 7%
Shale Barrier	780-790	no sample	L. Grandstand	1000-1005	sst	L. Grandstand	
Shale Barrier	790-800	sst/sh	L. Grandstand	1005-1015	sst	L. Grandstand	L. Grandstand
Shale Barrier	800-810	sh/sst	L. Grandstand	1015-1025	sst	L. Grandstand	shale= 18%
Shale Barrier	810-820	sst	L. Grandstand	1025-1034	sst	L. Grandstand	sandstone= 70%
Shale Barrier	820-822	sst	L. Grandstand	1034-1044	sst	L. Grandstand	siltstone= 5%
Shale Barrier	822-824	no sample	L. Grandstand	1044-1045	sst	L. Grandstand	no sample= 7%
				1045-1055	sst	L. Grandstand	note: 537-750 another Fm

A.7: Summary of the lithologic description of Umiat #3

Umiat Well 3							
Lithology	Formation	Depth	Lithology	Formation	Depth	Lithology	Formation
sh	Chandler	294-303	sst/sh	U. Grandstand	429-439	sh	Shale Barrier
sst	Chandler	303-312	sst	U. Grandstand	439-445	sh	Shale Barrier
sh	Chandler	312-320	sst	Shale Barrier	445-454	sh	Shale Barrier
sh	Chandler	320-328	slt	Shale Barrier	454-463	sst/sh	Shale Barrier
sh	Chandler	328-335	sh/sst	Shale Barrier	463-472	sh/slt	Shale Barrier
sst	Chandler	335-344	sh	Shale Barrier	472-478	sh	Shale Barrier
sst	Chandler	344-352	sst/sh	Shale Barrier	478-481	no sample	Shale Barrier
sh	Chandler	352-359	sst	Shale Barrier	481-490	sh	Shale Barrier
sst	Chandler	359-368	sst/sh	Shale Barrier	490-498	sh	Shale Barrier
sst	Chandler	368-377	sh	Shale Barrier	498-507	sst	Shale Barrier
sst	U. Grandstand	377-385	sst/sh	Shale Barrier	407-514	slt	Shale Barrier
sst	U. Grandstand	385-393	sst/sh	Shale Barrier	514-520	sh	Shale Barrier
sst	U. Grandstand	393-402	sst/slt	Shale Barrier	520-529	sh	Shale Barrier
sst	U. Grandstand	402-411	sst/slt	Shale Barrier	529-538	sh	Shale Barrier
sst	U. Grandstand	411-419	slt/sh	Shale Barrier	538-547	sh	Shale Barrier
sst	U. Grandstand	419-429	sh	Shale Barrier	547-563	sh	Shale Barrier
					563-572	sh	Shale Barrier

A.8: Summary of the lithologic description of Umiat #4

Umiat Well 4									
Depth	Lithology	Formation	Depth	Lithology	Formation	Depth	Lithology	Formation	Depth in feet
90-100	sh	Chandler	325-335	sh	Chandler	545-550	sh	Shale Barrier	Chandler
100-110	sst	Chandler	335-343	slt	Chandler	550-560	sh	Shale Barrier	shale= 40%
110-120	sh	Chandler	343-345	sh	Chandler	560-565	slt	Shale Barrier	sandstone= 50%
120-130	sh	Chandler	345-350	sh	Chandler	565-570	sh	Shale Barrier	siltstone= 15%
130-140	sst	Chandler	350-353	sh	U. Grandsand	570-590	sh	Shale Barrier	no sample= 0%
140-150	slt	Chandler	353-357	no sample	U. Grandsand	590-595	sh	Shale Barrier	
150-160	sh	Chandler	357-360	sst	U. Grandsand	595-600	slt	Shale Barrier	U. Grandstand
160-170	sst	Chandler	360-375	sst	U. Grandsand	600-610	slt	Shale Barrier	shale= 48%
170-195	sh	Chandler	375-385	sh	U. Grandsand	610-630	sh	Shale Barrier	sandstone= 41%
195-235	sst	Chandler	385-395	no sample	U. Grandsand	630-640	slt	Shale Barrier	siltstone= 0%
235-240	sst	Chandler	395-427	sst	U. Grandsand	640-715	sh	Shale Barrier	no sample= 11%
240-245	sh	Chandler	427-445	sh	U. Grandsand	715-720	sst	L. Grandstand	
245-255	sh	Chandler	445-450	sh	Shale Barrier	720-725	sst	L. Grandstand	Shale Barrier
255-260	sh	Chandler	450-475	sst	Shale Barrier	725-735	slt	L. Grandstand	shale= 72%
260-265	sst	Chandler	475-485	sh	Shale Barrier	745-760	sst	L. Grandstand	sandstone= 15%
280-298	sst	Chandler	485-490	sst	Shale Barrier	760-764	no sample	L. Grandstand	siltstone= 0%
298-299	slt	Chandler	490-495	sst	Shale Barrier	764-767	no sample	L. Grandstand	no sample= 13%
299-300	slt	Chandler	495-500	sh	Shale Barrier	767-768	sst	L. Grandstand	
300-305	slt	Chandler	500-505	sh	Shale Barrier	768-775	sst	L. Grandstand	L. Grandstand
305-310	sh	Chandler	505-510	sh	Shale Barrier	775-820	sst	L. Grandstand	shale= 0%
310-315	sst	Chandler	510-515	slt	Shale Barrier	820-821	no sample	L. Grandstand	sandstone= 84%
315-320	sst	Chandler	515-520	sst	Shale Barrier	821-826	sst	L. Grandstand	siltstone= 9%
320-325	slt	Chandler	520-545	sh	Shale Barrier	826-831	sst	L. Grandstand	no sample= 7%

A.11: Summary of the lithologic description of Umiat #7

Umiat Well 7									
Depth	Lithology	Formation	Depth	Lithology	Formation	Depth	Lithology	Formation	Depth in feet
545-550	sst	Chandler	790-795	sst	Chandler	1060-1070	sh	Shale Barrier	Chandler
550-555	sh	Chandler	795-820	sh	Chandler	1070-1120	sh	Shale Barrier	shale= 70%
555-560	sh	Chandler	820-825	sst	U. Grandstand	1120-1125	slt	Shale Barrier	sandstone= 25%
560-570	sst	Chandler	825-830	sst	U. Grandstand	1125-1160	sh	Shale Barrier	siltstone= 5%
570-575	sh	Chandler	830-834	sst	U. Grandstand	1160-1165	slt	L. Grandstand	no sample= 0%
575-580	sh	Chandler	834-838	sst	U. Grandstand	1165-1170	sst	L. Grandstand	
580-585	sh	Chandler	838-845	sst	U. Grandstand	1170-1175	sh	L. Grandstand	U. Grandstand
585-595	sh	Chandler	845-862	sst	U. Grandstand	1175-1180	sh	L. Grandstand	shale= 15%
595-600	slt	Chandler	862-867	sst	U. Grandstand	1180-1195	sh	L. Grandstand	sandstone= 80%
600-610	sst	Chandler	867-870	no sample	Shale Barrier	1195-1200	sh	L. Grandstand	siltstone= 0%
610-635	sh	Chandler	870-879	sh	Shale Barrier	1200-1211	sst	L. Grandstand	no sample= 5%
635-640	slt	Chandler	879-880	sst	Shale Barrier	1211-1215	sst	L. Grandstand	no sample= 2%
640-645	sh	Chandler	880-890	sh	Shale Barrier	1215-1295	sst	L. Grandstand	Shale Barrier
645-650	slt	Chandler	890-895	sh	Shale Barrier	1295-1300	sh	L. Grandstand	shale= 57%
650-660	sh	Chandler	895-910	slt	Shale Barrier	1300-1310	slt	L. Grandstand	sandstone= 17%
660-695	sst	Chandler	910-915	sh	Shale Barrier	1310-1315	sst	L. Grandstand	siltstone= 26%
695-720	sh	Chandler	915-930	sst	Shale Barrier	1315-1325	no sample	L. Grandstand	no sample= 0%
720-725	sh	Chandler	930-935	sh	Shale Barrier	1325-1327	sst	L. Grandstand	
725-730	sst	Chandler	935-945	sh	Shale Barrier	1327-1349	sst	L. Grandstand	L. Grandstand
730-755	sh	Chandler	945-950	sst	Shale Barrier	1349-1352	sst	L. Grandstand	shale= 41%
755-760	sst	Chandler	950-995	sh	Shale Barrier	1352-1370	sst	L. Grandstand	sandstone= 45%
760-775	sh	Chandler	995-1025	slt	Shale Barrier	1370-1372	sst	L. Grandstand	siltstone= 8%
775-780	sh	Chandler	1025-1057	sh	Shale Barrier	1372-1384	sst	L. Grandstand	no sample= 5%
780-790	sh	Chandler	1057-1060	sh	Shale Barrier				

A.12: Summary of the lithologic description of Umiat #8

Umiat Well 8									
Depth	Lithology	Formation	Depth	Lithology	Formation	Depth	Lithology	Formation	Depth in feet
220-225	sst	Chandler	745-805	sh	Chandler	1078-1080	sh	Shale Barrier	Chandler
225-230	sh	Chandler	805-810	sst	Chandler	1080-1090	sh	Shale Barrier	shale= 67%
230-235	sh	Chandler	810-815	sh	Chandler	1090-1100	slt	Shale Barrier	sandstone= 28%
235-240	sh	Chandler	815-818	no sample	Chandler	1100-1120	sh	Shale Barrier	siltstone= 3%
240-250	sst	Chandler	818-820	sh	Chandler	1120-1125	sh	Shale Barrier	no sample= 2%
250-290	sh	Chandler	820-830	sh	Chandler	1125-1130	slt	Shale Barrier	L. Grandstand depth = 81
290-300	sst	Chandler	830-840	sh	Chandler	1130-1133	slt	Shale Barrier	U. Grandstand
300-320	sh	Chandler	840-855	sh	Chandler	1133-1145	sh	Shale Barrier	shale= 23%
320-325	no sample	Chandler	855-865	sh	Chandler	1145-1180	sh	Shale Barrier	sandstone= 62%
325-330	slt	Chandler	865-885	sst	U. Grandstand	1180-1183	no sample	Shale Barrier	siltstone= 15%
330-375	sh	Chandler	885-890	sst	U. Grandstand	1183-1188	sh	Shale Barrier	no sample= 0%
375-380	sst	Chandler	890-895	sst	U. Grandstand	1188-1209	sh	Shale Barrier	
380-400	sh	Chandler	895-900	sh	U. Grandstand	1209-1215	sh	Shale Barrier	Shale Barrier
400-405	sh	Chandler	900-910	sst	U. Grandstand	1215-1216	no sample	Shale Barrier	shale= 90%
405-445	sh	Chandler	910-920	sh	U. Grandstand	1216-1230	sh	Shale Barrier	sandstone= 2%
605-620	sst	Chandler	920-930	slt	U. Grandstand	1230-1240	sh	Shale Barrier	siltstone= 4%
620-635	sh	Chandler	930-1005	sh	Shale Barrier	1240-1243	sh	Shale Barrier	no sample= 4%
635-640	sst	Chandler	1005-1010	slt	Shale Barrier	1243-1246	sst	Shale Barrier	
640-645	sh	Chandler	1010-1015	sh	Shale Barrier	1246-1250	sst	L. Grandstand	L. Grandstand
645-650	no sample	Chandler	1015-1018	sh	Shale Barrier	1250-1260	sst	L. Grandstand	shale= 43%
650-711	sst	Chandler	1018-1038	sh	Shale Barrier	1260-1265	sh	L. Grandstand	sandstone= 53%
711-716	sst	Chandler	1038-1041	sh	Shale Barrier	1265-1295	sh	L. Grandstand	siltstone= 0%
716-722	sst	Chandler	1041-1061	sh	Shale Barrier	1295-1296	no sample	L. Grandstand	no sample= 4%
722-730	sst	Chandler	1061-1063	sh	Shale Barrier	1296-1300	sst	L. Grandstand	
730-745	sh	Chandler	1063-1078	sh	Shale Barrier	1300-1325	sst	L. Grandstand	
						1325-1327	no sample	L. Grandstand	

A.13: Summary of the lithologic description of Umiat #9

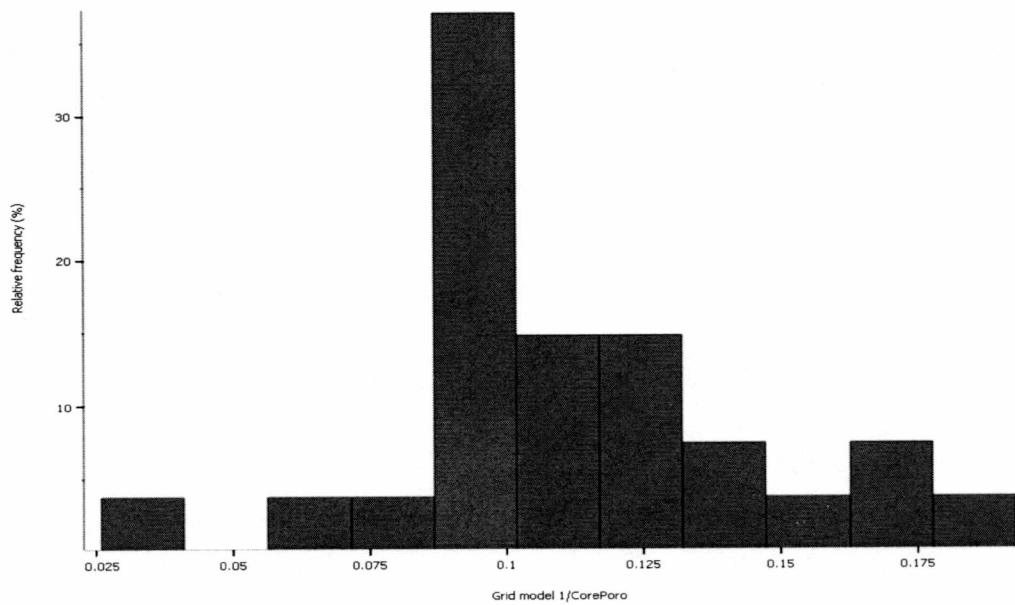
Umiat Well 9									
Depth	Lithology	Formation	Depth	Lithology	Formation	Depth	Lithology	Formation	Depth in feet
190-200	sh	Chandler	525-533	sst	U. Grandstand	949-959	sh	Shale Barrier	
200-210	sh	Chandler	533-543	sst	U. Grandstand	959-969	sst	Shale Barrier	Chandler
210-230	no sample	Chandler	543-553	sst	U. Grandstand	969-979	sst	Shale Barrier	shale= 69%
230-270	sh	Chandler	553-563	sst	U. Grandstand	979-989	sst	Shale Barrier	sandstone= 12%
270-280	sst	Chandler	563-573	sst	U. Grandstand	989-1000	sst	Shale Barrier	siltstone= 3%
280-290	slt	Chandler	583-593	sst	U. Grandstand	1000-1010	sst	Shale Barrier	no sample= 16%
290-300	sh	Chandler	593-603	sh	U. Grandstand	1010-1017	sst	Shale Barrier	U. Grandstand
300-310	sh	Chandler	603-611	sh	U. Grandstand	1017-1027	sst	Shale Barrier	Well 9
310-320	sst	Chandler	611-640	sh	U. Grandstand	1027-1037	sst	Shale Barrier	shale= 67%
320-340	no sample	Chandler	640-649	slt	U. Grandstand	1037-1047	sst	Shale Barrier	sandstone= 27%
340-350	sst	Chandler	649-659	sh	U. Grandstand	1047-1057	sst	Shale Barrier	siltstone= 5%
350-360	sh	Chandler	659-669	sh	U. Grandstand	1057-1067	sst	Shale Barrier	no sample= 1%
360-370	sh	Chandler	669-678	sh	U. Grandstand	1067-1076	sst	Shale Barrier	
370-380	sh	Chandler	678-687	sh	U. Grandstand	1076-1086	sst	Shale Barrier	Shale Barrier
380-385	no sample	Chandler	687-697	sh	U. Grandstand	1086-1096	sh	Shale Barrier	shale= 26%
385-394	sh	Chandler	697-707	sh	U. Grandstand	1096-1106	sh	Shale Barrier	sandstone= 59%
394-403	sh	Chandler	707-710	no sample	U. Grandstand	1106-1117	sh	Shale Barrier	siltstone= 15%
403-413	sh	Chandler	710-720	slt	U. Grandstand	1117-1127	slt	Shale Barrier	no sample= 0%
413-423	sh	Chandler	720-809	sh	U. Grandstand	1127-1137	slt	Shale Barrier	
423-433	sh	Chandler	809-819	sst	Shale Barrier	1137-1147	slt	Shale Barrier	L. Grandstand
433-434	sh	U. Grandstand	829-839	sst	Shale Barrier	1147-1157	sh	Shale Barrier	shale= 71%
434-443	sh	U. Grandstand	839-848	sh	Shale Barrier	1157-1167	sh	L. Grandstand	sandstone= 0%
443-454	sh	U. Grandstand	848-858	sh	Shale Barrier	1167-1177	sh	L. Grandstand	siltstone= 29%
454-464	sh	U. Grandstand	858-868	sh	Shale Barrier	1177-1187	sh	L. Grandstand	no sample= 0%
464-474	sst	U. Grandstand	868-878	sst	Shale Barrier	1187-1197	sh	L. Grandstand	
474-484	sst	U. Grandstand	878-888	sst	Shale Barrier	1197-1206	sh	L. Grandstand	
484-494	sst	U. Grandstand	888-898	sst	Shale Barrier	1206-1208	sh	L. Grandstand	
494-499	sst	U. Grandstand	898-901	sst	Shale Barrier	1208-1218	sh	L. Grandstand	
499-500	sst	U. Grandstand	901-911	sst	Shale Barrier	1218-1228	slt	L. Grandstand	
500-502	sst	U. Grandstand	911-919	sst	Shale Barrier	1228-1236	slt	L. Grandstand	
502-512	sst	U. Grandstand	919-929	slt	Shale Barrier	1236-1247	slt	L. Grandstand	
512-514	sst	U. Grandstand	929-939	slt	Shale Barrier	1247-1257	sh	L. Grandstand	
514-525	sst	U. Grandstand	939-949	sh	Shale Barrier				

A.14: Summary of the lithologic description of Umiat #10

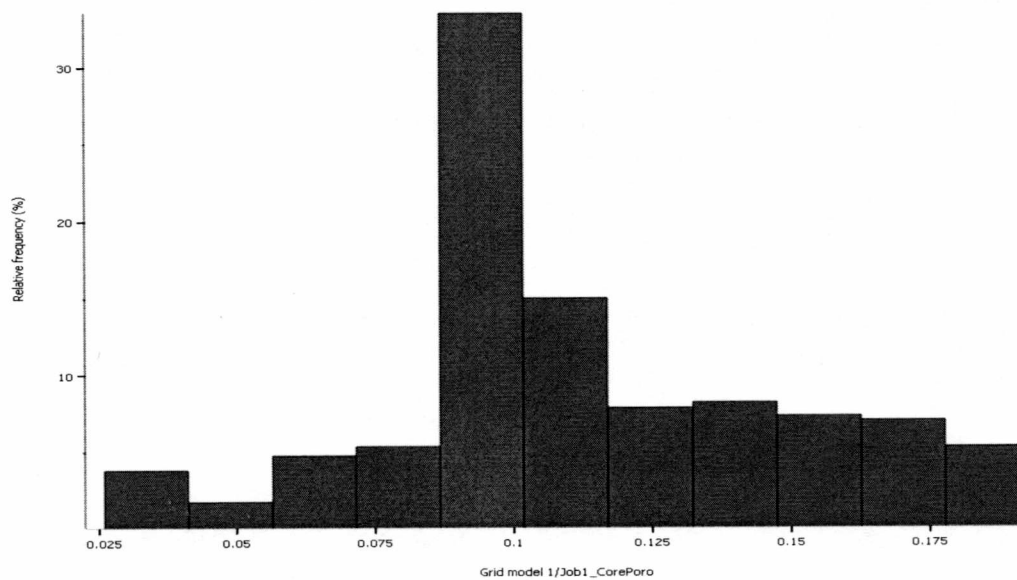
Umiat Well 10									
Depth	Lithology	Formation	Depth	Lithology	Formation	Depth	Lithology	Formation	Depth in feet
810-815	sst	Chandler	995-1000	sh	Chandler	1134-1150	slt	U. Grandstand	Chandler
815-830	sst	Chandler	1000-1010	sst	Chandler	1150-1155	slt	U. Grandstand	shale= 57%
830-832	sst	Chandler	1010-1015	slt	Chandler	1155-1195	sh	U. Grandstand	sandstone= 28%
832-835	sst	Chandler	1015-1020	sh	Chandler	1195-1210	sh	Shale Barrier	siltstone= 10%
835-840	sh	Chandler	1020-1025	sst	Chandler	1210-1215	sh	Shale Barrier	no sample= 5%
840-850	sh	Chandler	1025-1050	sh	Chandler	1215-1235	sh	Shale Barrier	L. Grandstand
850-855	no sample	Chandler	1050-1055	slt	Chandler	1235-1250	sh	Shale Barrier	U. Grandstand
855-900	sh	Chandler	1055-1065	sst	U. Grandstand	1250-1255	no sample	Shale Barrier	shale= 43%
900-905	sh	Chandler	1065-1070	sh	U. Grandstand	1255-1275	sh	Shale Barrier	sandstone= 35%
905-915	sst	Chandler	1070-1075	sst	U. Grandstand	1275-1330	sh	Shale Barrier	siltstone= 18%
915-920	sh	Chandler	1070-1080	sst	U. Grandstand	1330-1340	sh	Shale Barrier	no sample= 4%
920-924	sst	Chandler	1080-1090	sst	U. Grandstand	1340-1350	sh	Shale Barrier	no sample= 5%
924-930	slt	Chandler	1090-1100	sst	U. Grandstand	1350-1530	sh	Shale Barrier	Shale Barrier
930-935	sh	Chandler	1100-1108	sst	U. Grandstand	1530-1540	sh	Shale Barrier	shale= 96%
935-940	sst	Chandler	1108-1111	no sample	U. Grandstand	1540-1542	slt	Shale Barrier	sandstone= 0%
940-944	slt	Chandler	1111-1120	sst	U. Grandstand	1542-1545	sh	Shale Barrier	siltstone= 4%
944-970	sh	Chandler	1120-1124	slt	U. Grandstand	1545-1570	sh	Shale Barrier	no sample= 0%
970-975	slt	Chandler	1124-1131	sst	U. Grandstand	1570-1573	no sample	Shale Barrier	
975-995	sh	Chandler	1131-1134	sh	U. Grandstand				

A.15: Summary of the lithologic description of Umiat #11

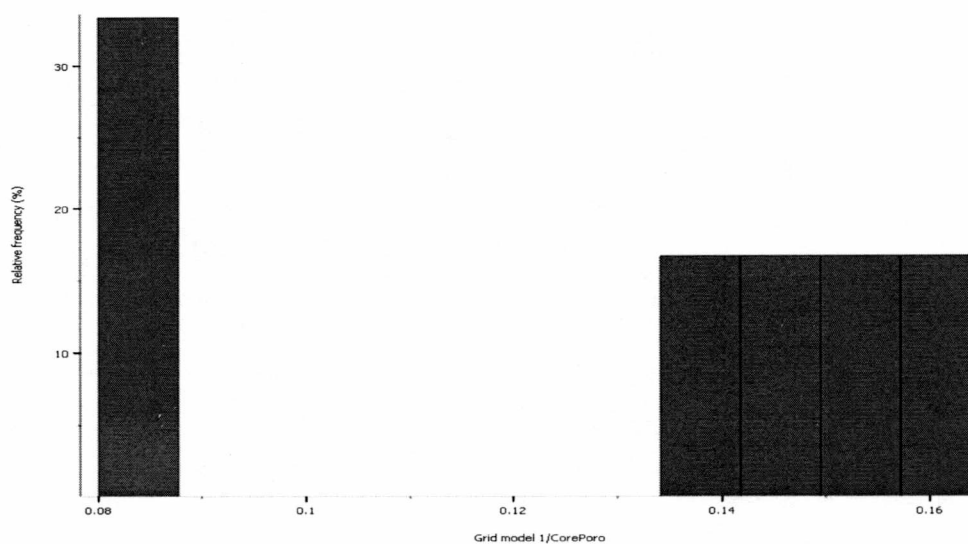
Umiat Well 11									
Depth	Lithology	Formation	Depth	Lithology	Formation	Depth	Lithology	Formation	Depth in feet
2192-2203	sst	Chandler	2435-2444	sst	Chandler	2680-2700	sh	Shale Barrier	Chandler Total depth = 888
2203-2221	sst	Chandler	2444-2448	sst	U. Grandstand	2700-2701	no sample	Shale Barrier	shale= 52% Chandler depth = 243
2221-2239	sh	Chandler	2448-2461	sst	U. Grandstand	2701-2721	sh	Shale Barrier	sandstone= 32% U. Grandstand depth = 90
2239-2259	sh	Chandler	2461-2485	sst	U. Grandstand	2721-2750	sh	Shale Barrier	siltstone= 16% Shale Barrier depth = 280
2259-2270	sh	Chandler	2485-2495	sh	U. Grandstand	2750-2805	sh	Shale Barrier	no sample= 0% L. Grandstand depth = 275
2270-2277	slt	Chandler	2495-2505	sh	U. Grandstand	2805-2810	sst	L. Grandstand	
2277-2285	slt	Chandler	2505-2510	sh	Shale Barrier	2810-2830	sst	L. Grandstand	U. Grandstand Well 11
2285-2295	sh	Chandler	2510-2520	sh	Shale Barrier	2830-2837	sst	L. Grandstand	shale= 25% shale= 41
2295-2315	sst	Chandler	2520-2529	sst	Shale Barrier	2837-2850	sst	L. Grandstand	sandstone= 75% sandstone= 51
2315-2335	sh	Chandler	2529-2545	sst	Shale Barrier	2850-2870	sst	L. Grandstand	siltstone= 0% siltstone= 6
2335-2344	sh	Chandler	2545-2595	sh	Shale Barrier	2870-2920	sst	L. Grandstand	no sample= 0% no sample= 2
2344-2350	sst	Chandler	2595-2605	slt	Shale Barrier	2920-2940	sst	L. Grandstand	
2350-2373	sh	Chandler	2605-2615	sh	Shale Barrier	2940-2960	slt	L. Grandstand	Shale Barrier L. Grandstand
2373-2374	sst	Chandler	2615-2625	sst	Shale Barrier	2960-2970	sst	L. Grandstand	shale= 82% shale= 4%
2374-2394	sst	Chandler	2625-2635	no sample	Shale Barrier	2970-2989	sst	L. Grandstand	sandstone= 6% sandstone= 89%
2394-2405	slt	Chandler	2635-2665	sst	Shale Barrier	2989-3009	sst	L. Grandstand	siltstone= 4% siltstone= 7%
2405-2411	sh	Chandler	2665-2670	no sample	Shale Barrier	3009-3020	sst	L. Grandstand	no sample= 11% no sample= 0%
2411-2417	slt	Chandler	2670-2675	sh	Shale Barrier	3020-3030	sh	L. Grandstand	
2417-2435	sh	Chandler	2675-2680	no sample	Shale Barrier	3030-3080	sst	L. Grandstand	



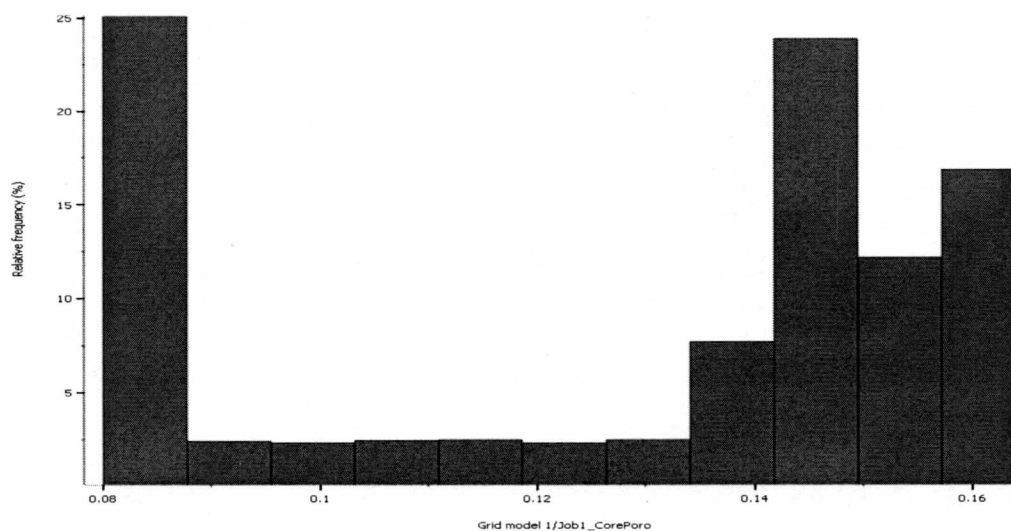
A.16: Histogram showing the porosity input data of shale in the Upper sand



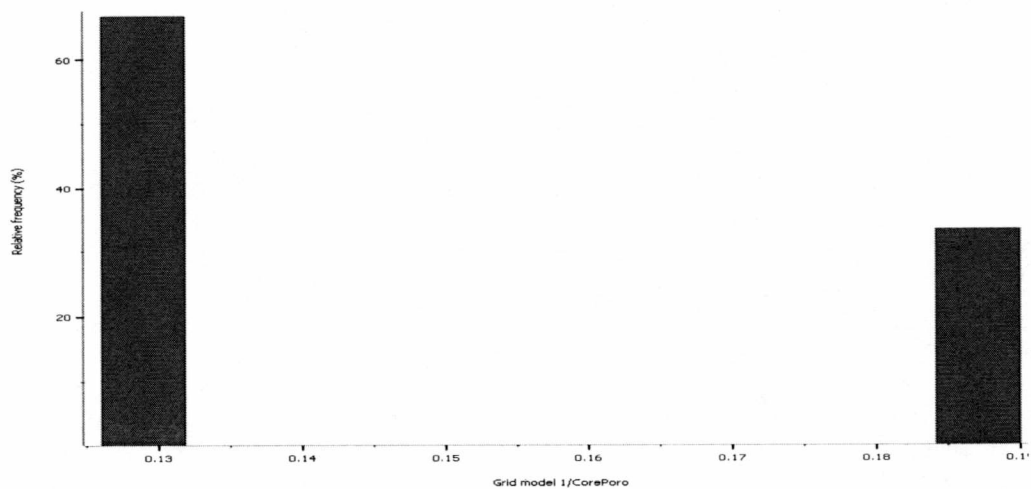
A.17: Histogram showing the porosity output data of shale in the Upper sand



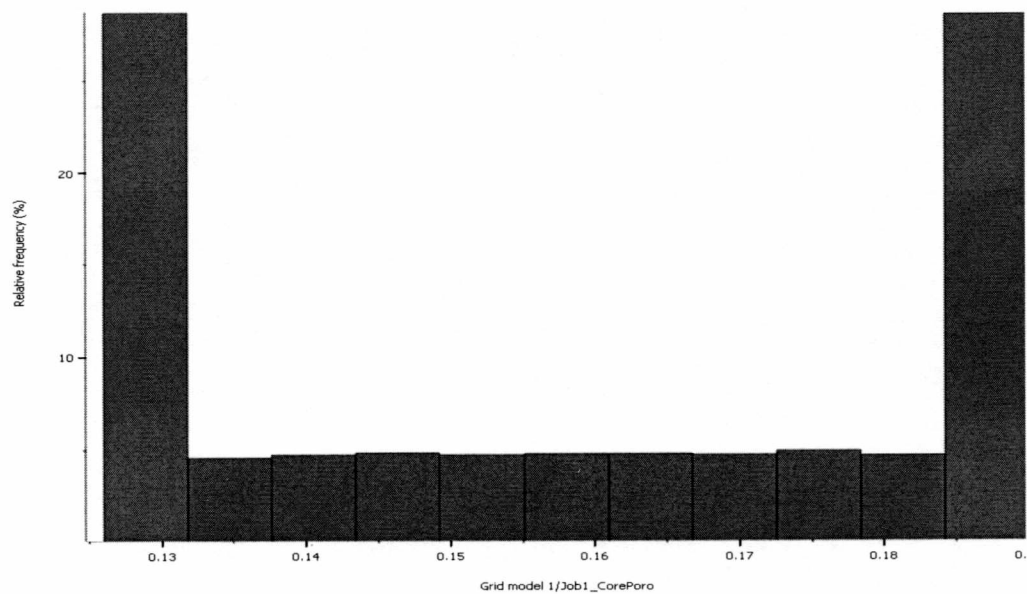
A.18: Histogram showing the porosity input data of sand in the Upper sand



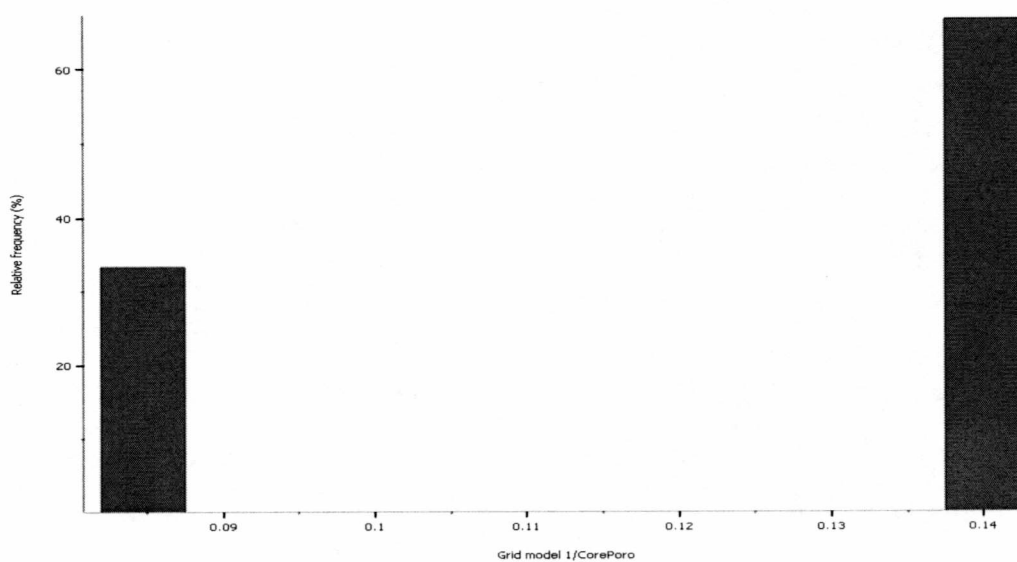
A.19: Histogram showing the porosity output data of sand in the Upper



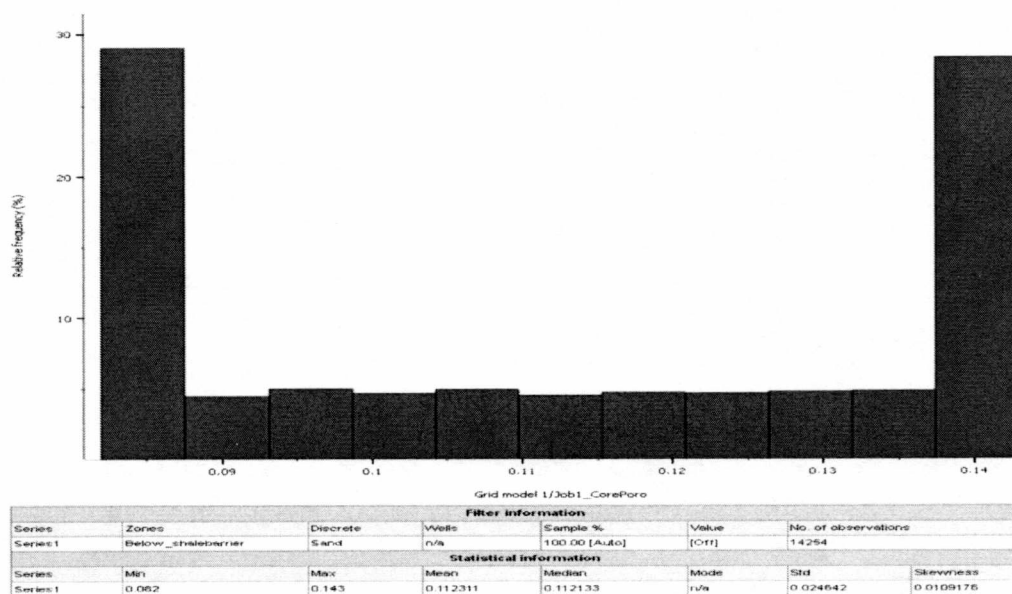
A.20: Histogram showing the porosity input data of shale in the Shale barrier



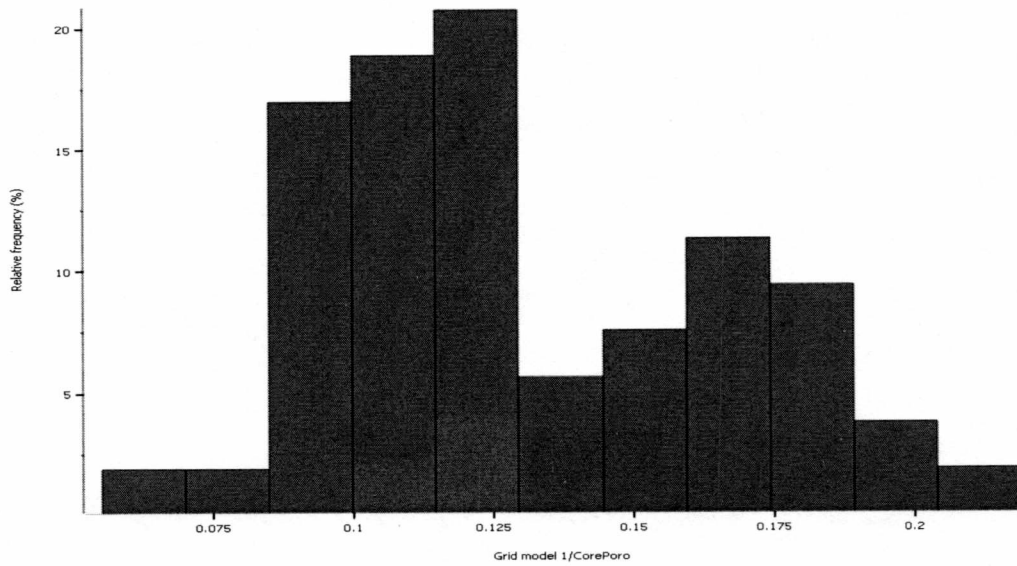
A.21: Histogram showing the porosity output data of sand in the Shale barrier



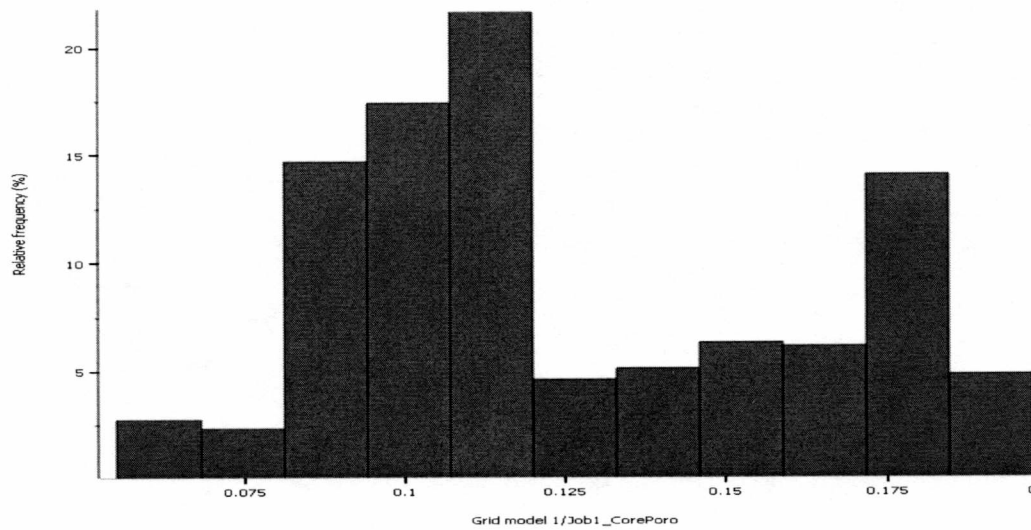
A.22: Histogram showing the porosity input data of sand in the Shale barrier



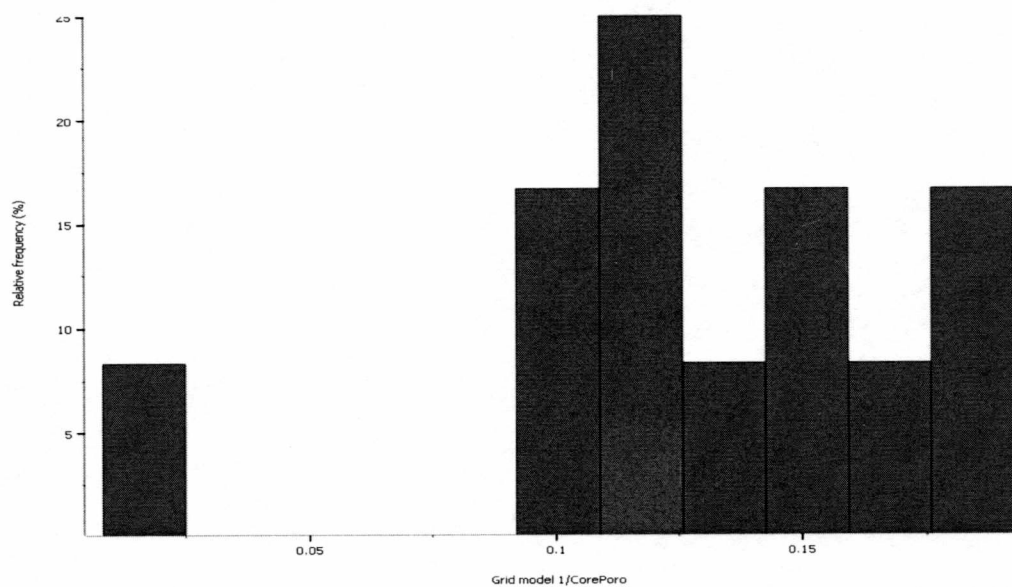
A.23: Histogram showing the porosity output data of sand in the Shale barrier



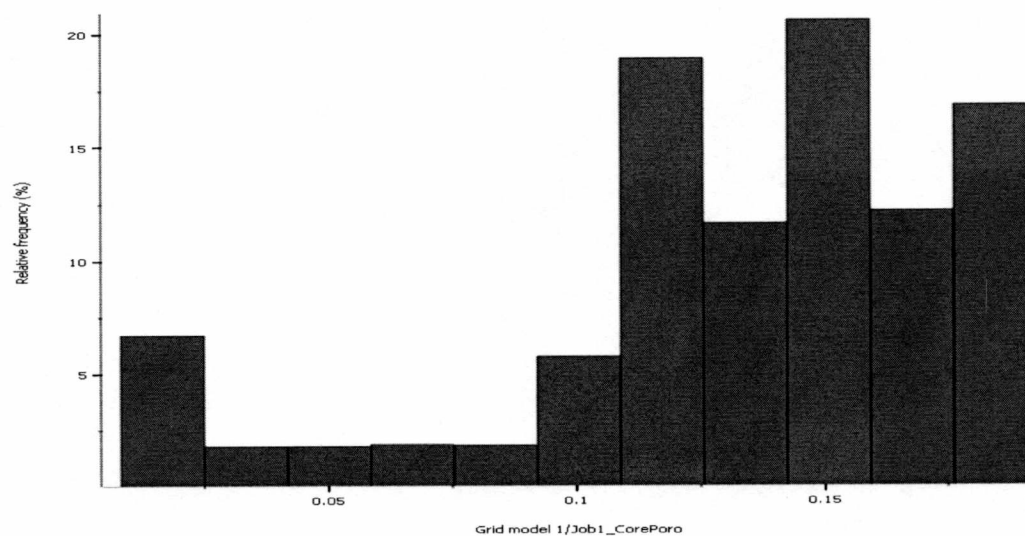
A.24: Histogram showing the porosity input data of shale in the Lower sand



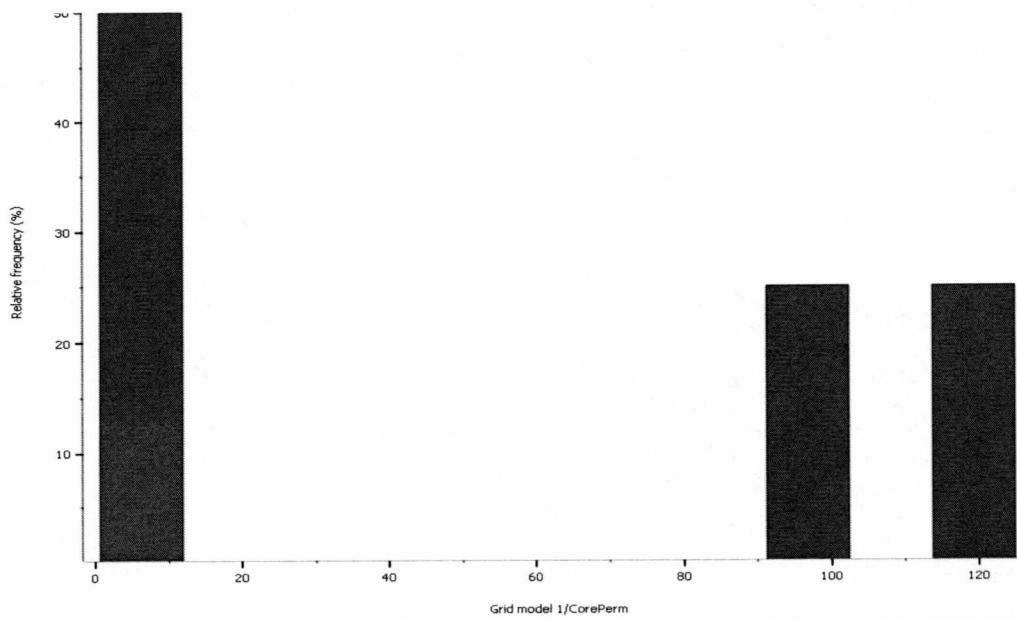
A.25: Histogram showing the porosity output data of shale in the Lower sand



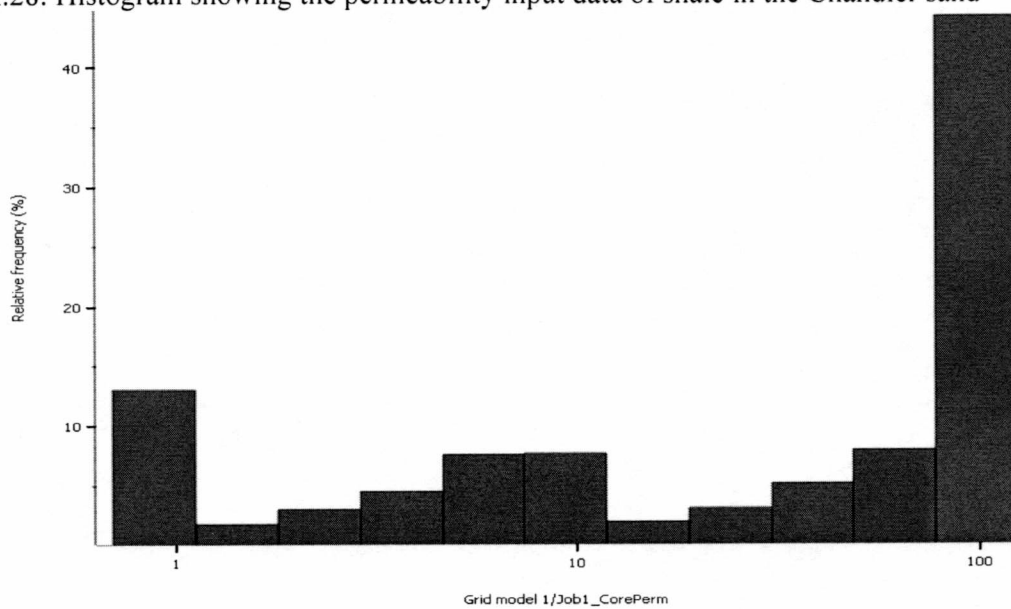
A.26: Histogram showing the porosity input data of sand in the Lower sand



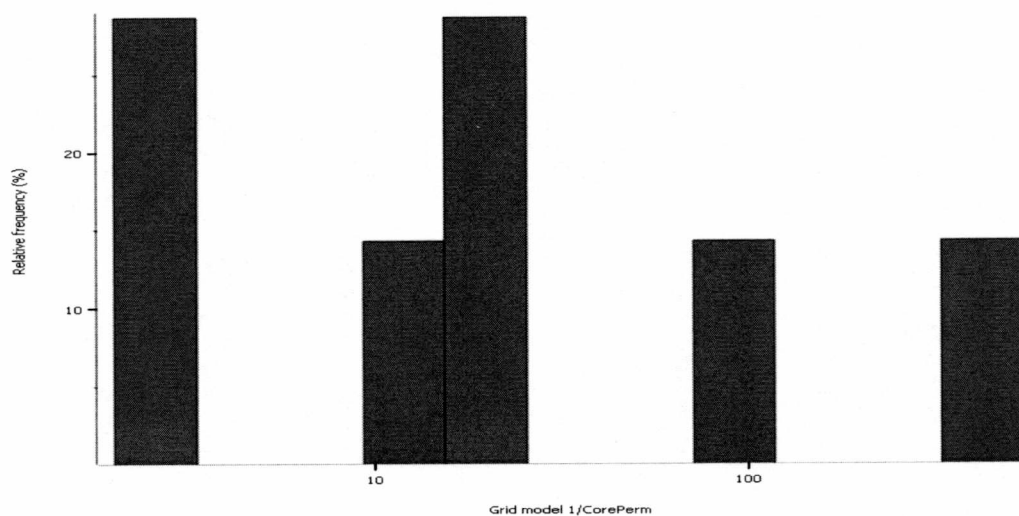
A.27: Histogram showing the porosity output data of shale in the Lower sand



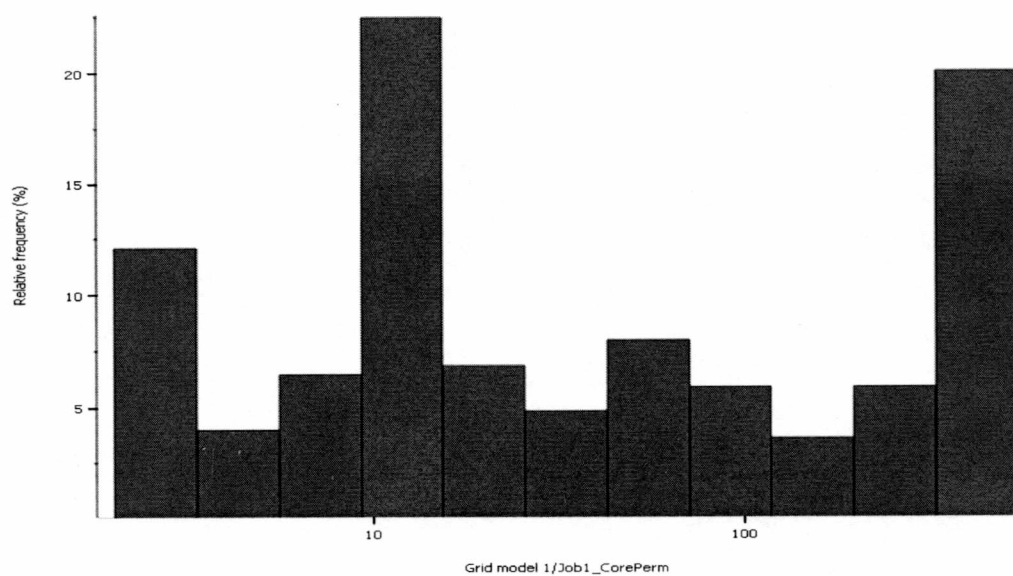
A.28: Histogram showing the permeability input data of shale in the Chandler sand



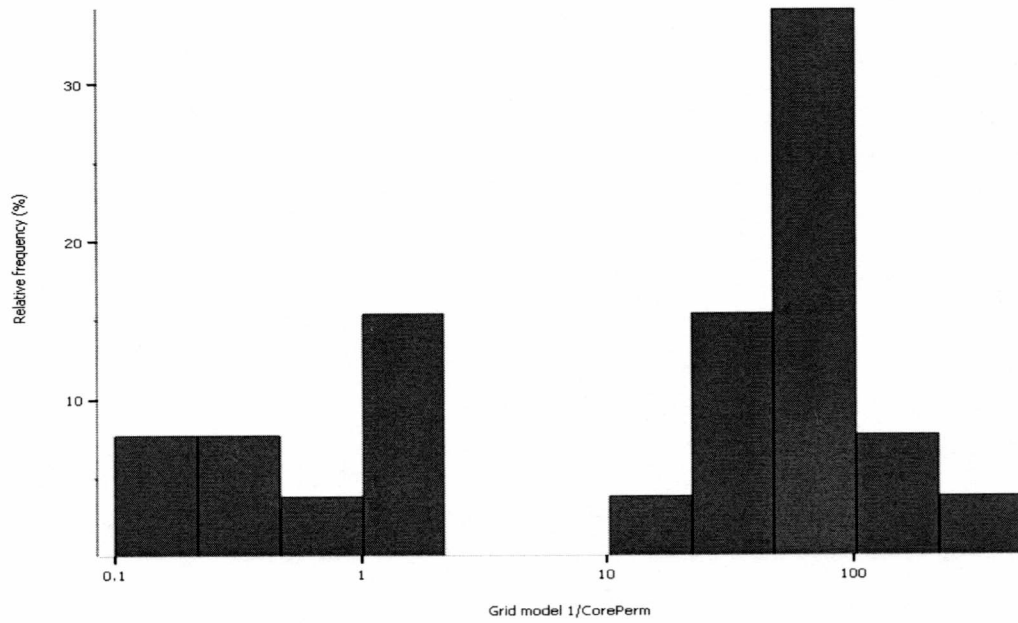
A.29: Histogram showing the permeability output data of shale in the Chandler sand



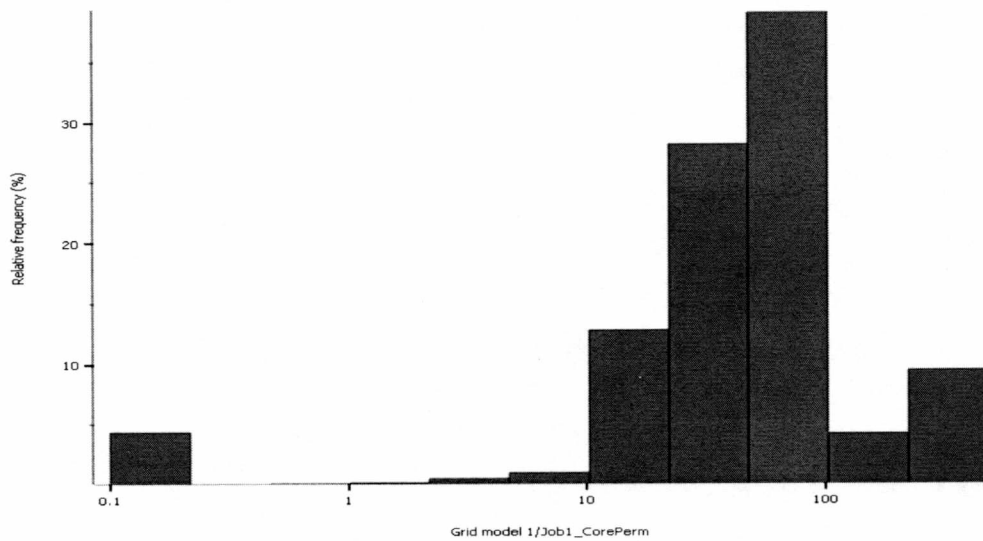
A.30: Histogram showing the permeability input data of sand in the Chandler sand



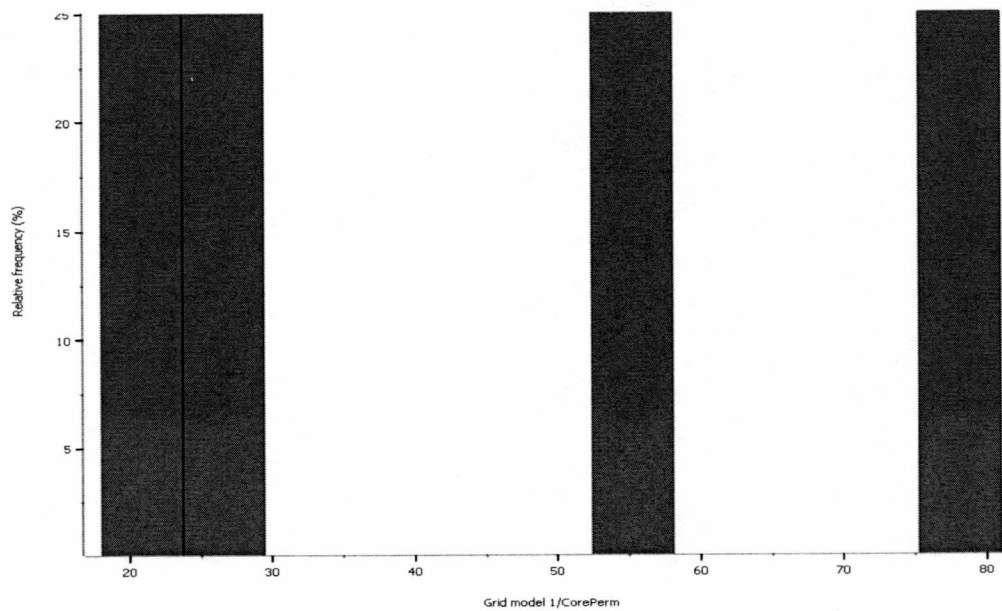
A.31: Histogram showing the permeability output data of shale in the Chandler sand



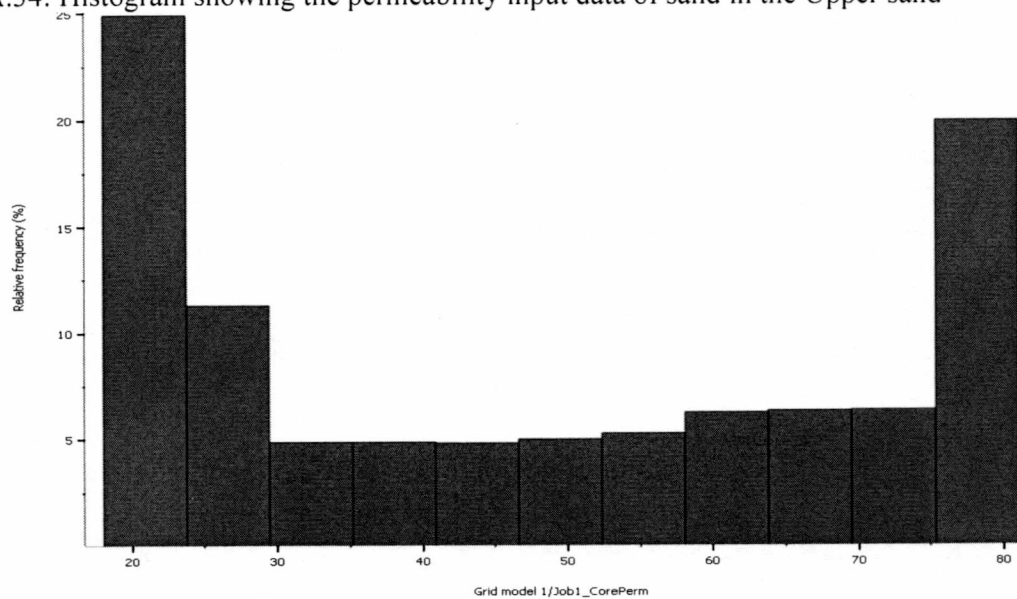
A.32: Histogram showing the permeability input data of shale in the Upper sand



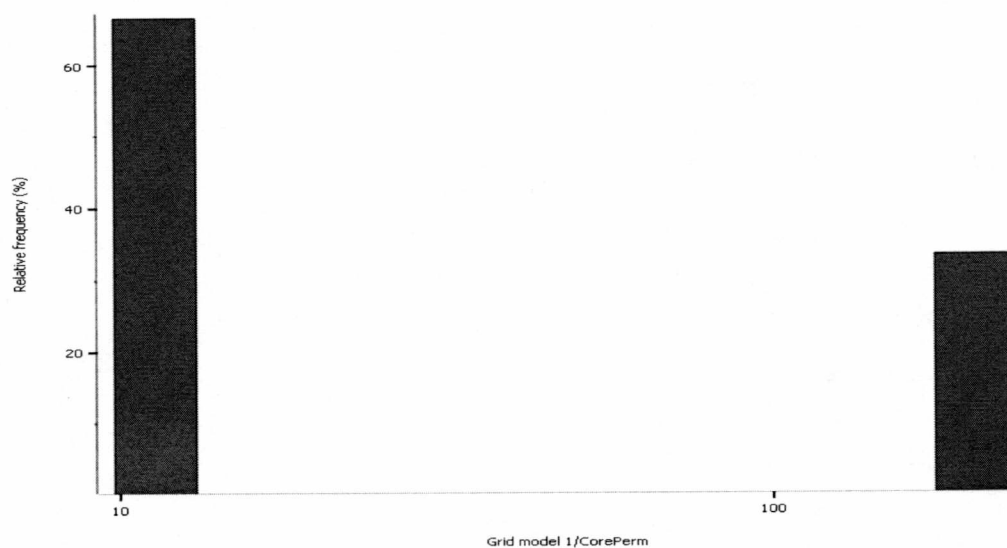
A.33: Histogram showing the permeability output data of shale in the Upper sand



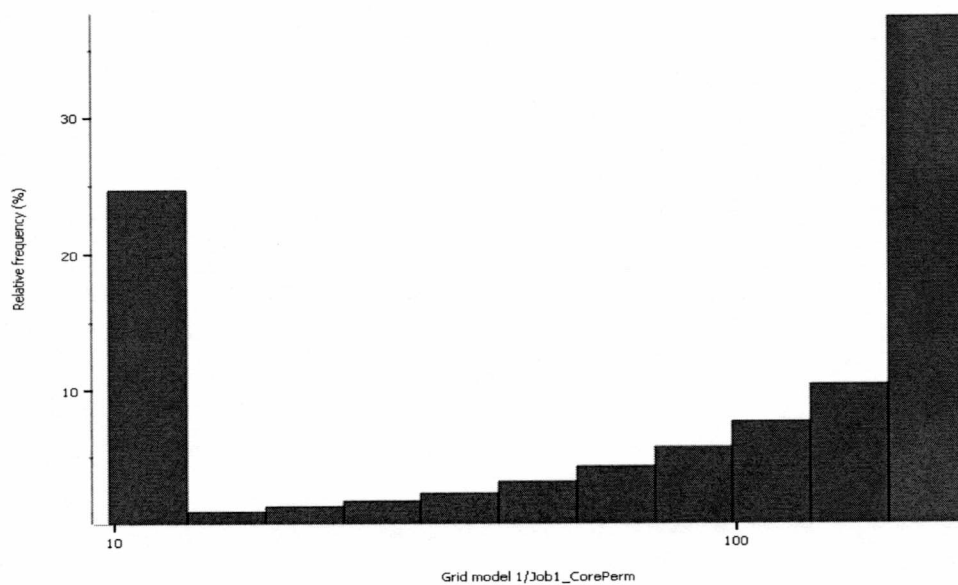
A.34: Histogram showing the permeability input data of sand in the Upper sand



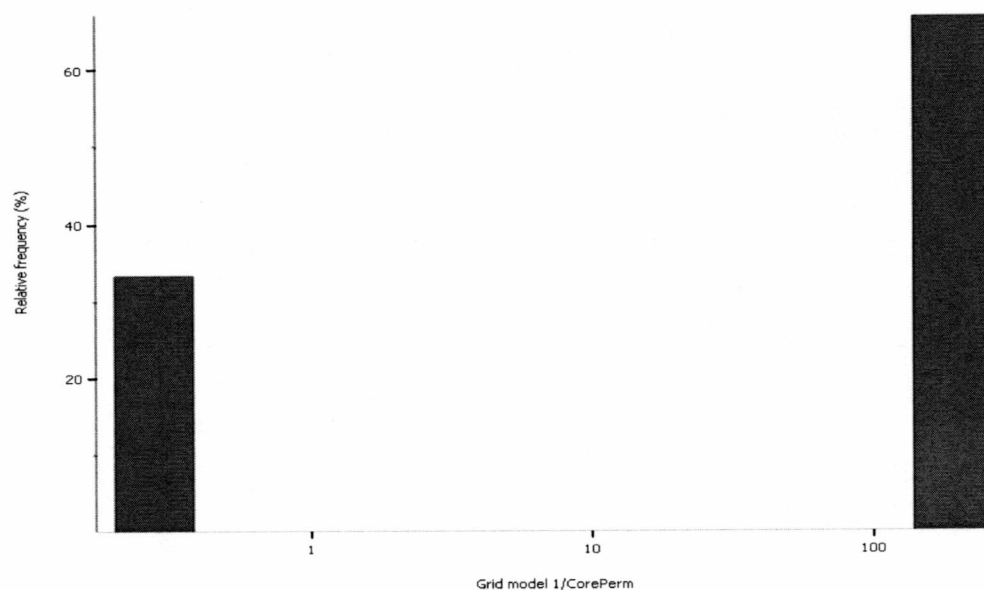
A.35: Histogram showing the permeability output data of sand in the Upper sand



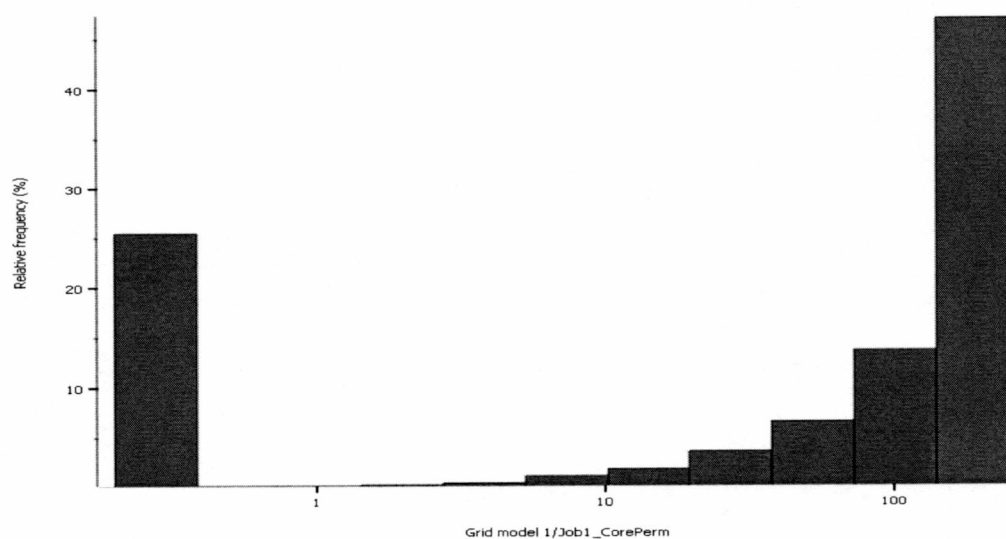
A.36: Histogram showing the permeability input data of shale in the Shale barrier



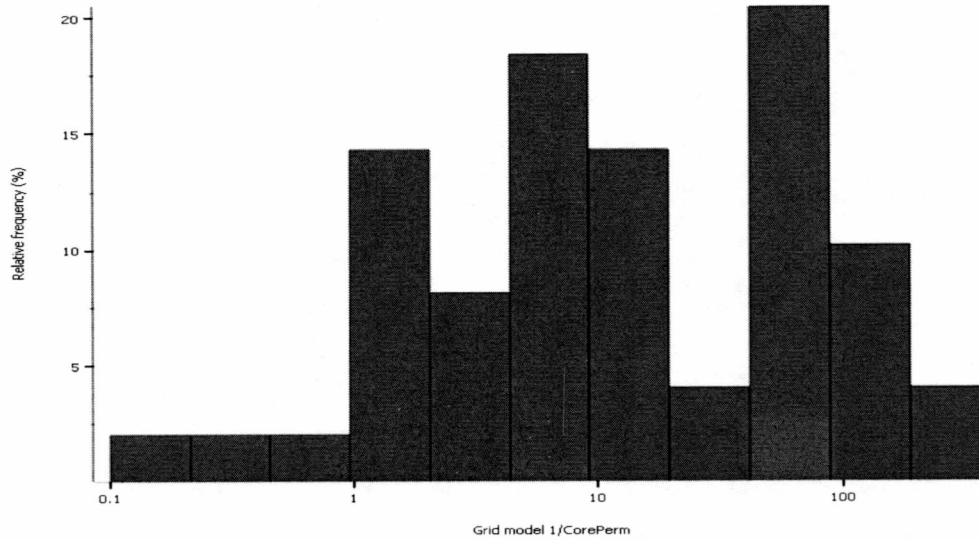
A.37: Histogram showing the permeability output data of shale in the Shale barrier



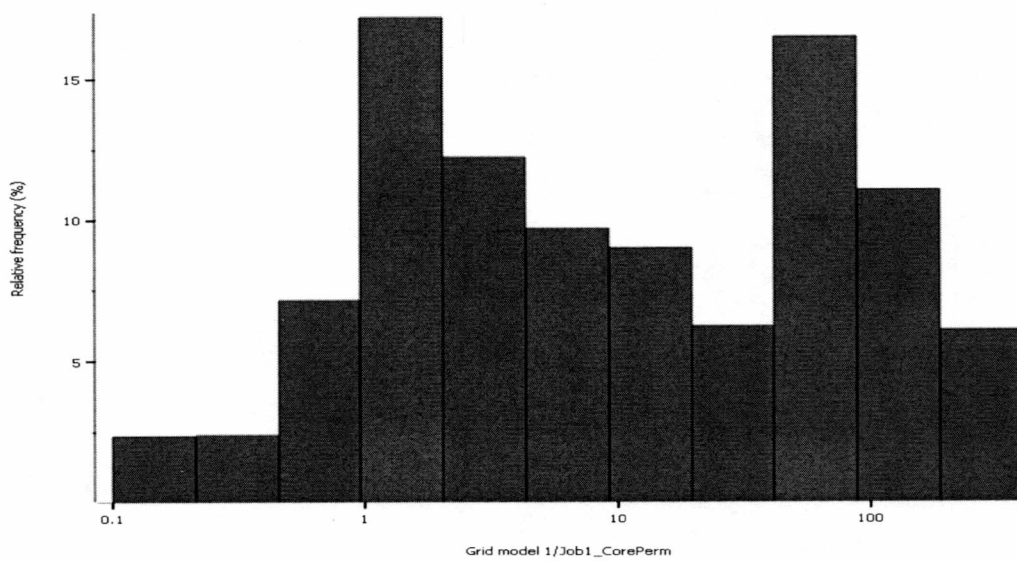
A.38: Histogram showing the permeability input data of sand in the Shale barrier



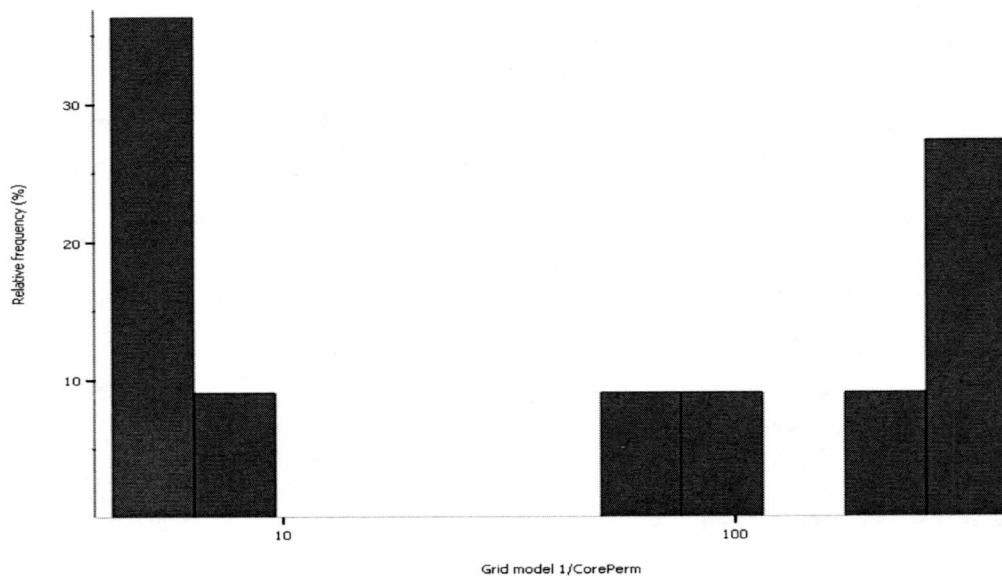
A.39: Histogram showing the permeability output data of sand in the Shale barrier



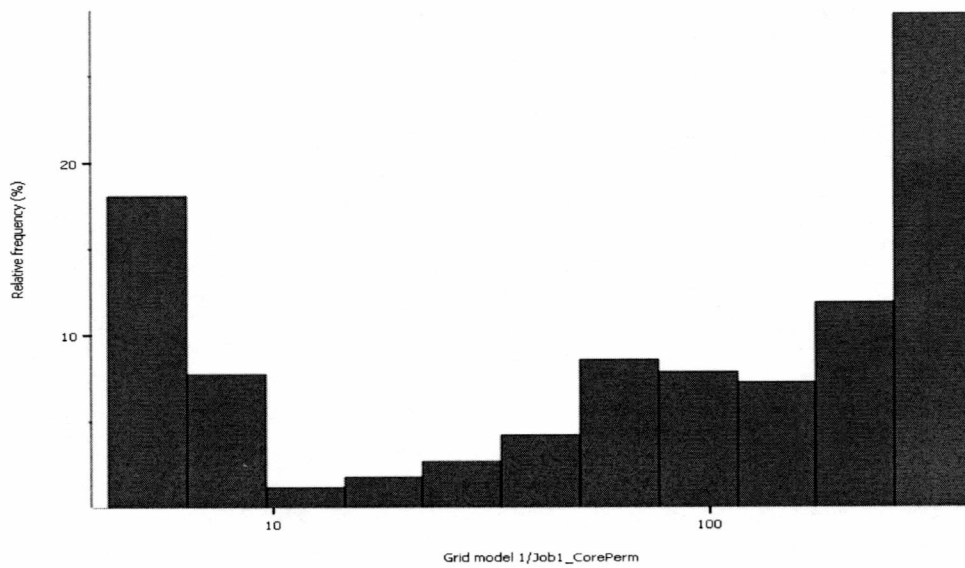
A.40: Histogram showing the permeability input data of shale in the Lower sand



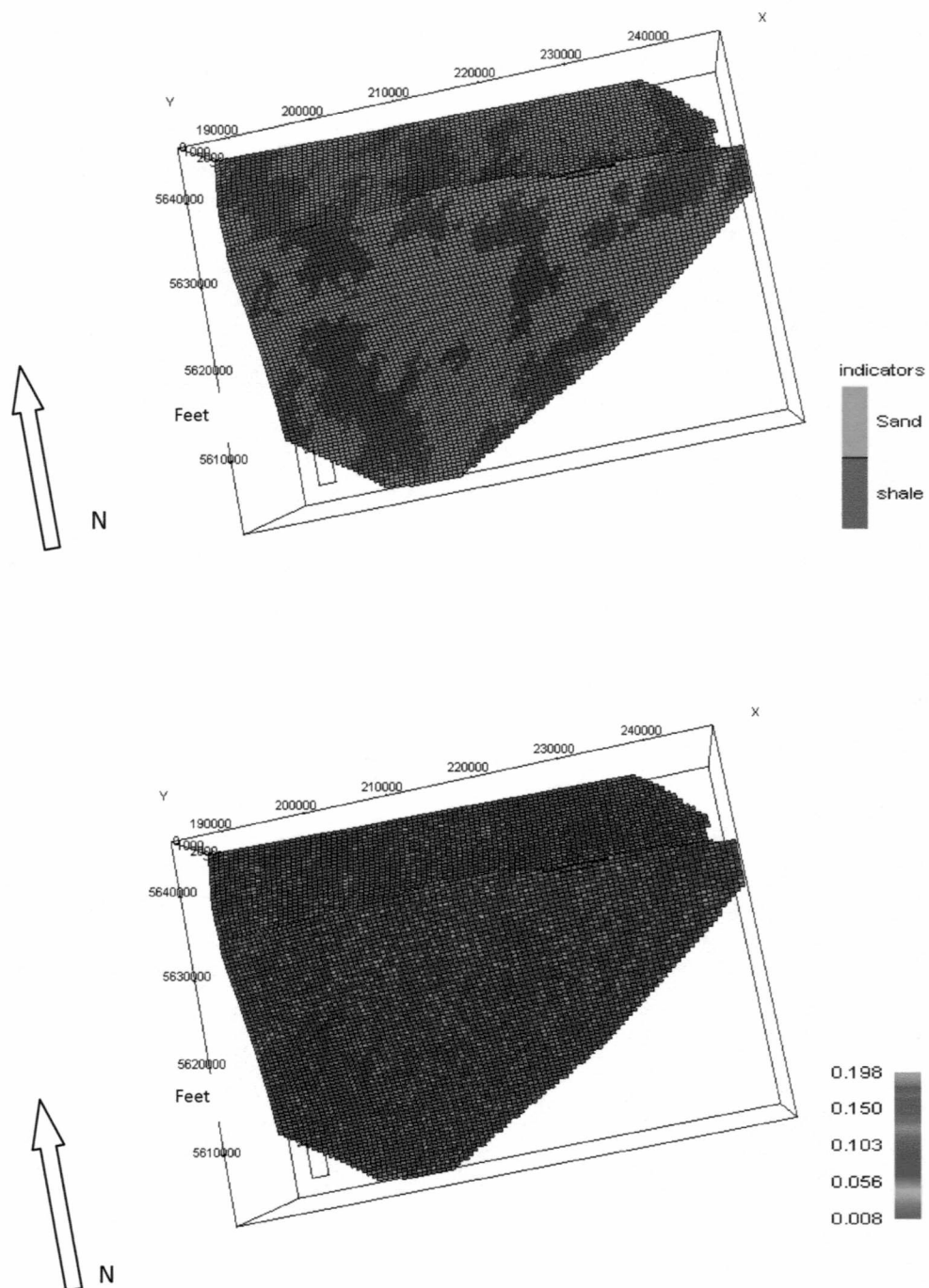
A.41: Histogram showing the permeability output data of shale in the Lower sand



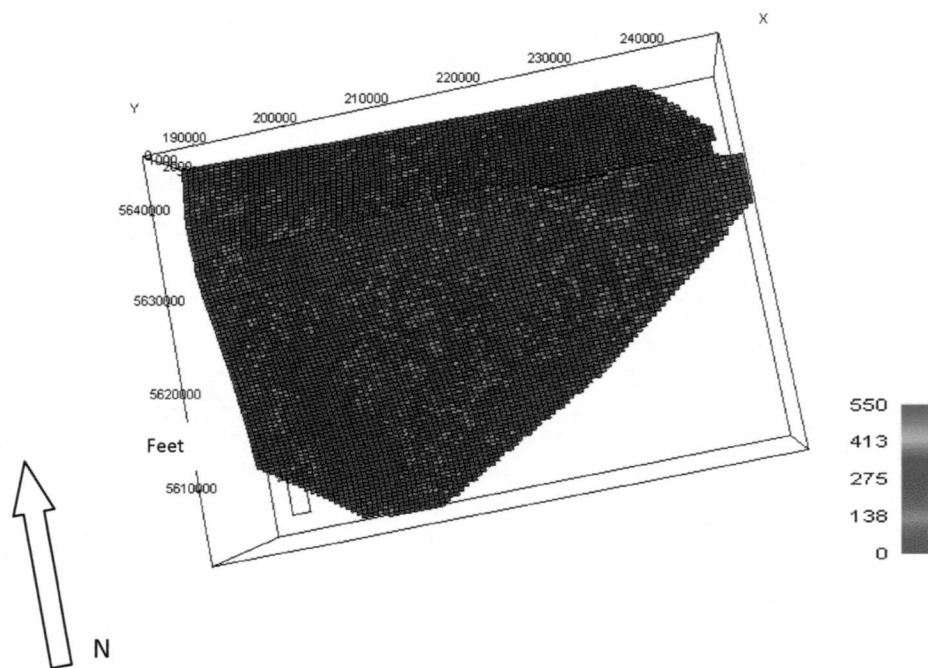
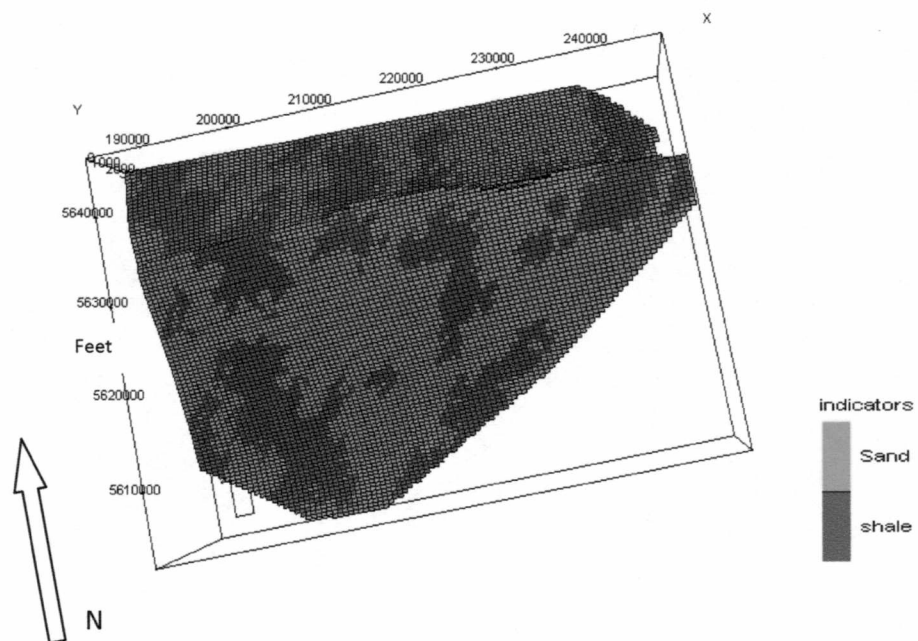
A.42: Histogram showing the permeability input data of sand in the Lower sand



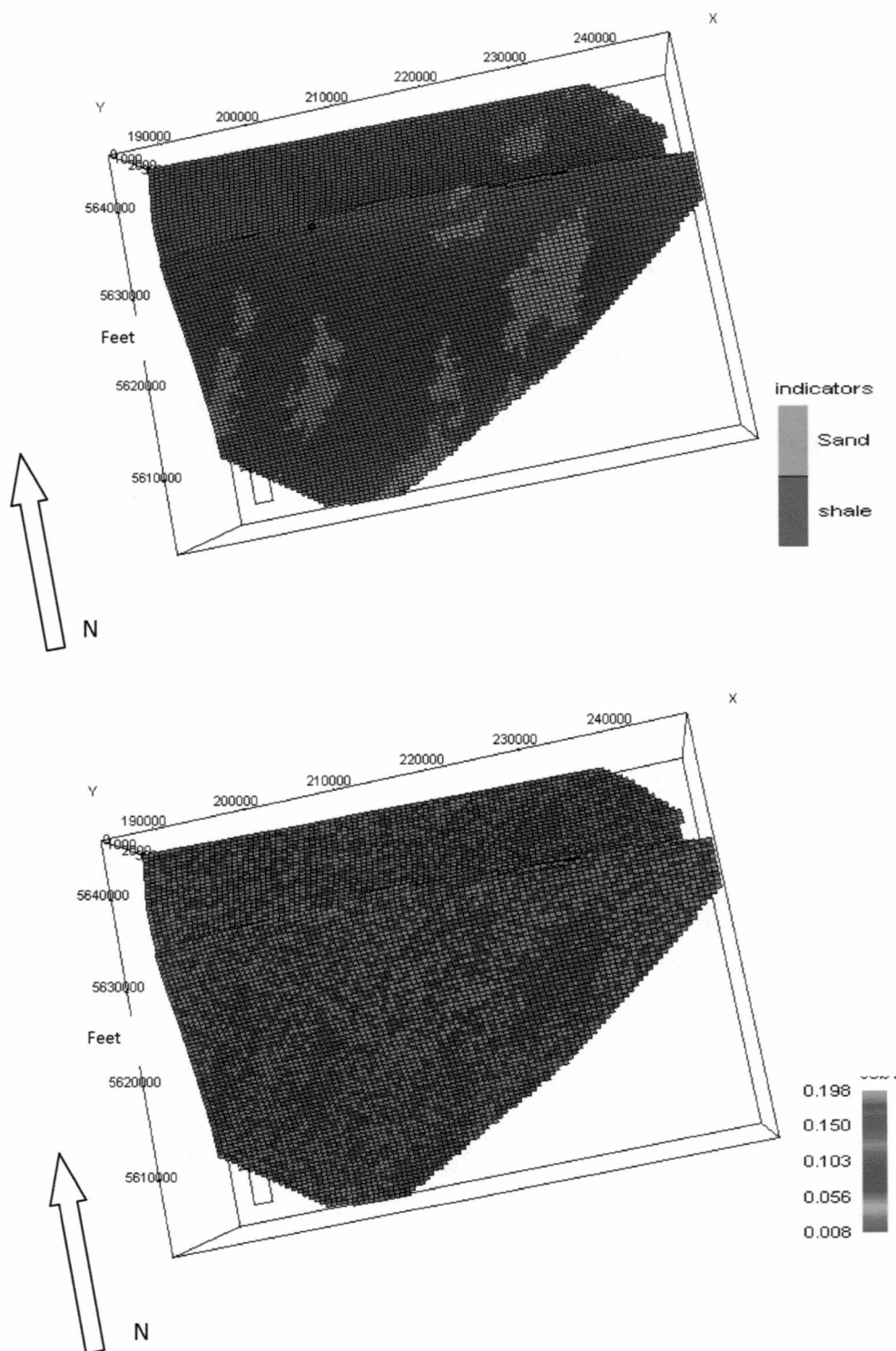
A.43: Histogram showing the permeability output data of sand in the Lower sand



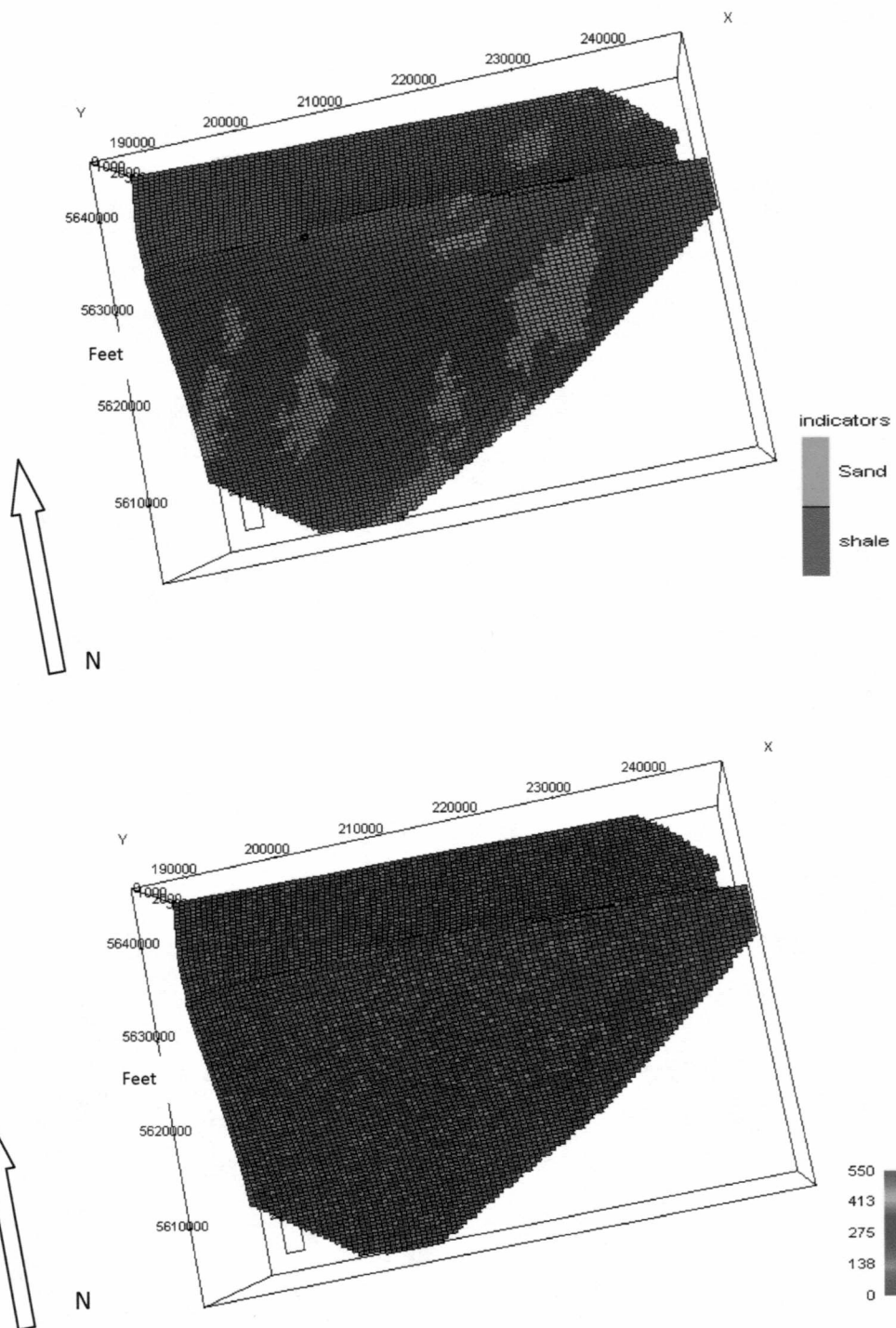
A.44 Comparison of the indicator and porosity models of the Upper sand



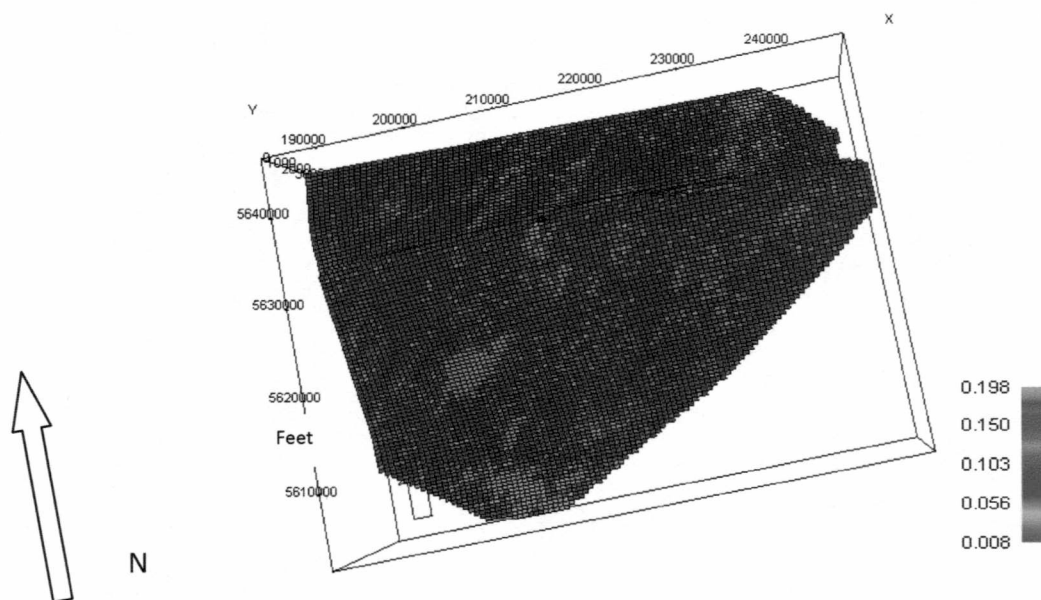
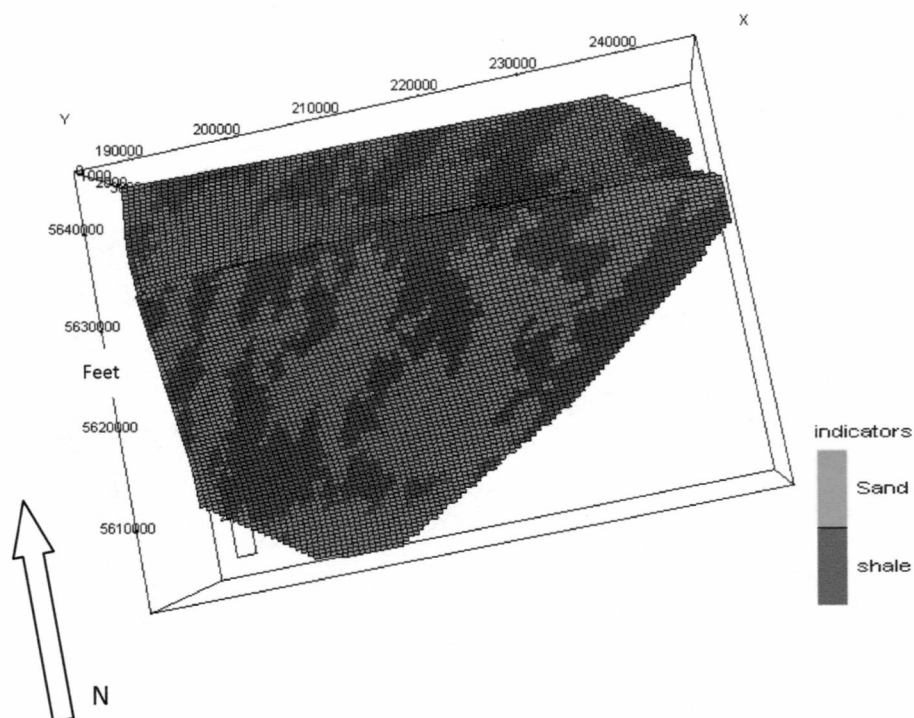
A.45 Comparison of the indicator and permeability models of the Upper sand



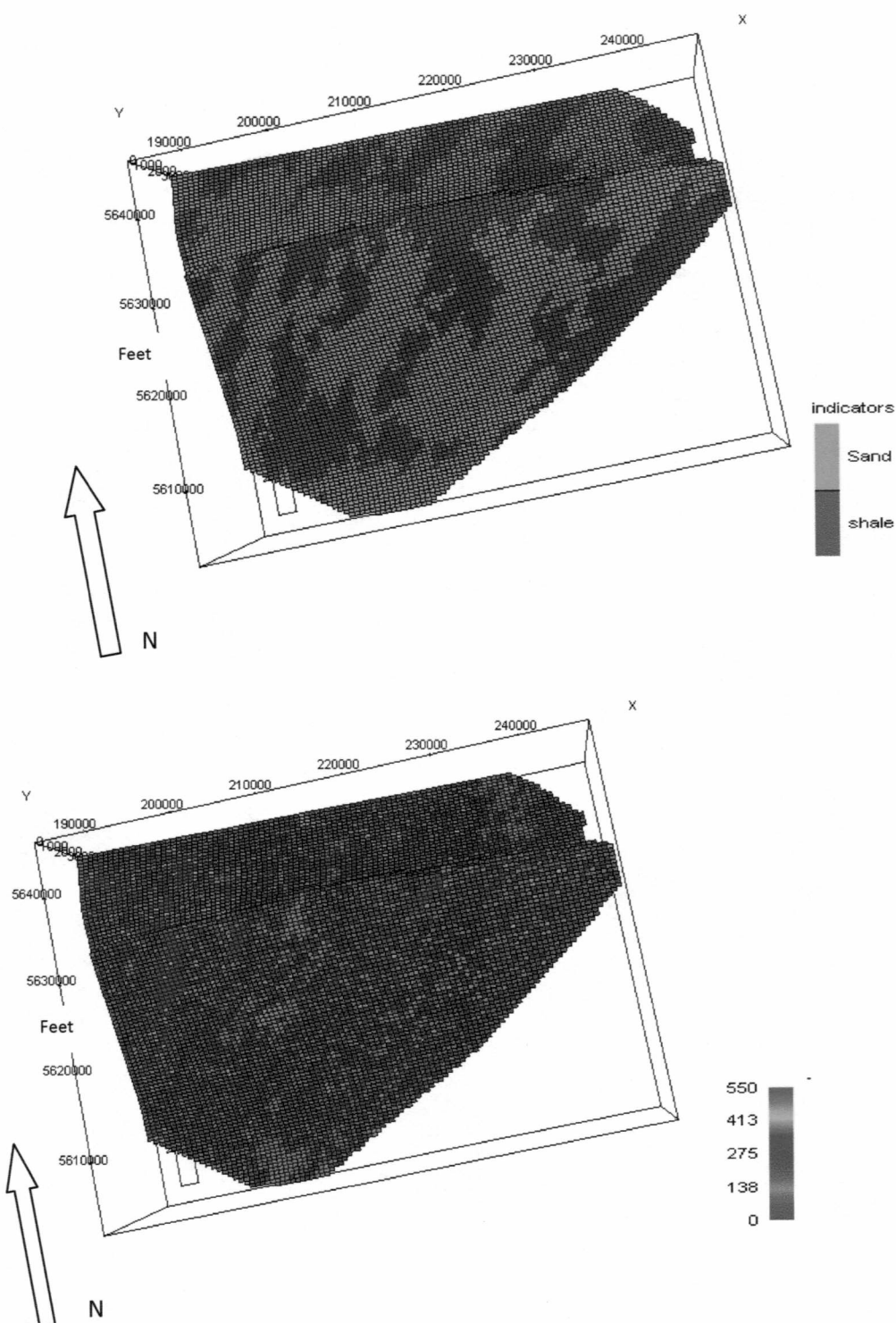
A.46 Comparison of the indicator and porosity models of the Shale barrier



A.47 Comparison of the indicator and permeability models of the Shale barrier



A.48 Comparison of the indicator and porosity models of the Lower sand



A.49 Comparison of the indicator and permeability models of the Lower sand

APPENDIX B

B.1: Digital project archive

The Input data and property petrophysical model for this research are archived on the attached CD. The included data provide all the required files to run the Umiat property petrophysical model in IRAP-RMS.